AD-A172 434 CORROSIVE-WEAR OF BUOY CHAIN(U) COAST GUARD RESEARCH AND DEVELOPMENT CENTER GROTON CT C A KOHLER ET AL. JUL 86 CGR/DC-05/86 USCG-D-21-86 1/2

UNCLASSIFIED F/G 11/6 NL

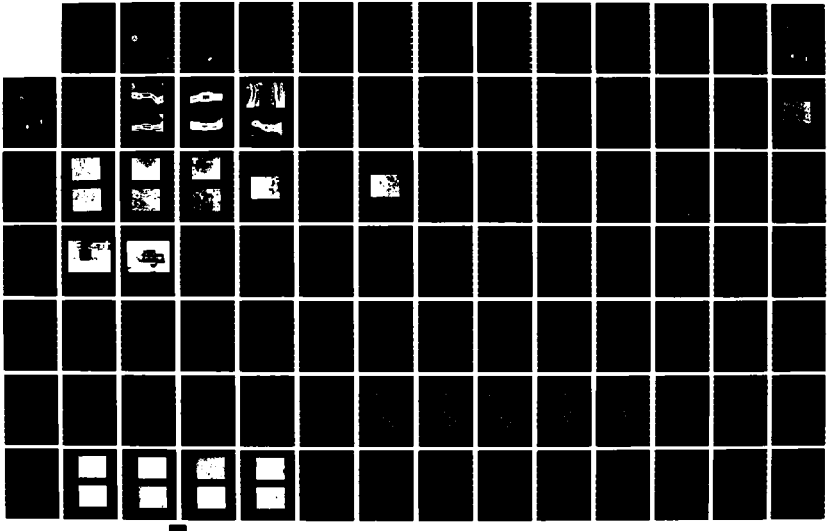

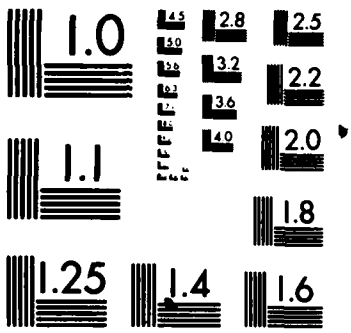

MICROCOPY RESOLUTION TEST CHART
NATIONAL BUREAU OF STANDARDS-1963-A

Report No. CG-D-21-86

CORROSIVE-WEAR OF BUOY CHAIN

Craig A. Kohler, Daniel R. May,
Thomas H. Briggs, Richard Brown

U.S. COAST GUARD RESEARCH AND DEVELOPMENT CENTER
AVERY POINT, GROTON, CONNECTICUT 06340-6096

INTERIM REPORT
July 1986

Prepared for:

U.S. Department Of Transportation
United States Coast Guard
Office of Research and Development
Washington, DC 20593

NOTICE

This document is disseminated under the sponsorship of the Department of Transportation in the interest of information exchange. The United States Government assumes no liability for its contents or use thereof.

The United States Government does not endorse products or manufacturers. Trade or manufacturers' names appear herein solely because they are considered essential to the object of this report.

The contents of this report reflect the views of the Coast Guard Research and Development Center, which is responsible for the facts and accuracy of data presented. This report does not constitute a standard, specification, or regulation.

SAMUEL F. POWELL, III
Technical Director
U.S. Coast Guard Research and Development Center
Avery Point, Groton, Connecticut 06340-6096

Technical Report Documentation Page

1. Report No.	2. Government Accession No.	3. Recipient's Catalog No.
CG-D-21-86		

4. Title and Subtitle	5. Report Date
CORROSIVE-WEAR OF BUOY CHAIN	JULY 1986
	6. Performing Organization Code
7. Author(s)	8. Performing Organization Report No.
Craig A. Kohler, Daniel R. May, Thomas H. Briggs, Richard Brown	CGR&DC 05/86
9. Performing Organization Name and Address U.S. Coast Guard Research and Development Center Avery Point Groton, Connecticut 06340-6096	10. Work Unit No. (TRAIS)
	11. Contract or Grant No.
12. Sponsoring Agency Name and Address Department of Transportation U.S. Coast Guard Office of Research and Development Washington, D.C. 20593	13. Type of Report and Period Covered INTERIM
	14. Sponsoring Agency Code

15. Supplementary Notes

16. Abstract

Corrosive-wear, which is responsible for the majority of buoy chain degradation, was investigated in two laboratory studies. The objective of the first study was to isolate the two components, corrosion and wear, in order to determine each of their influences on the corrosive-wear process on steels. The second study was designed to produce uniform wear on the steel's surface, providing more accurate data on the steel's wear resistance and to determine the effects of alloy additions. The steel presently being used for buoy chain, which is similar in composition to ASTM 1022 steel, was compared to ASTM 4140, 4340, 8740, and a heat-treated 4140 steel in order to identify a material which would provide a longer life buoy chain.

The results of the experiments showed that the wear component contributed material losses of one to two orders of magnitude greater than the corrosion process. It was also determined that the 4340 steel would be the most suitable material for longer life buoy chain. This alloy's high nickel content would reduce the potential for pitting attack, which can be extremely damaging to a mooring. The microstructure of the 4340, with a low ferrite to pearlite ratio and fine grain size, would provide an increased wear resistance of up to four times greater than the 1022 steel. Keywords: Corrosion resistance, Microstructure.

17. Key Words	18. Distribution Statement
CORROSION ABRASION WEAR BUOY STEEL CHAIN	Document is available to the U.S. public through the National Technical Information Service, Springfield, Virginia 22161

19. Security Classif. (of this report)	20. SECURITY CLASSIF. (of this page)	21. No. of Pages	22. Price
UNCLASSIFIED	UNCLASSIFIED		

Form DOT F 1700.7 (8/72) Reproduction of form and completed page is authorized

METRIC CONVERSION FACTORS

Approximate Conversions to Metric Measures

Symbol	When You Know	Multiply By	To Find	Symbol
		LENGTH		
in	inches	* 2.5	centimeters	cm
ft	feet	30	centimeters	cm
yd	yards	0.9	meters	m
mi	miles	1.6	kilometers	km
		AREA		
in^2	square inches	6.5	square centimeters	cm^2
ft^2	square feet	0.09	square meters	m^2
yd^2	square yards	0.8	square meters	m^2
mi^2	square miles	2.6	square kilometers	km^2
	acres	0.4	hectares	ha
		MASS (WEIGHT)		
oz	ounces	28	grams	g
lb	pounds	0.45	kilograms	kg
	short tons (2000 lb)	0.9	tonnes	t
		VOLUME		
tsp	teaspoons	5	milliliters	ml
tbsp	tablespoons	15	milliliters	ml
fl oz	fluid ounces	30	milliliters	ml
c	cups	0.24	liters	l
pt	pints	0.47	liters	l
qt	quarts	0.95	liters	l
gal	gallons	3.8	liters	l
ft^3	cubic feet	0.03	cubic meters	m^3
yd^3	cubic yards	0.76	cubic meters	m^3
		TEMPERATURE (EXACT)		
°F	Fahrenheit temperature	5/9 (after subtracting 32)	Celsius temperature	°C

* 1 in = 2.54 (exactly). For other exact conversions and more detailed tables, see NBS Misc. Publ. 286, Units of Weights and Measures. Price $2.25. SD Catalog No. C13.10:286.

Approximate Conversions from Metric Measures

Symbol	When You Know	Multiply By	To Find	Symbol
		LENGTH		
mm	millimeters	0.04	inches	in
cm	centimeters	0.4	inches	in
m	meters	3.3	feet	ft
m	meters	1.1	yards	yd
km	kilometers	0.6	miles	mi
		AREA		
cm^2	square centimeters	0.16	square inches	in^2
m^2	square meters	1.2	square yards	yd^2
km^2	square kilometers	0.4	square miles	mi^2
ha	hectares (10,000 m^2)	2.5	acres	
		MASS (WEIGHT)		
g	grams	0.035	ounces	oz
kg	kilograms	2.2	pounds	lb
t	tonnes (1000 kg)	1.1	short tons	
		VOLUME		
ml	milliliters	0.03	fluid ounces	fl oz
l	liters	0.125	cups	c
l	liters	2.1	pints	pt
l	liters	1.06	quarts	qt
l	liters	0.26	gallons	gal
m^3	cubic meters	35	cubic feet	ft^3
m^3	cubic meters	1.3	cubic yards	yd^3
		TEMPERATURE (EXACT)		
°C	Celsius temperature	9/5 (then add 32)	Fahrenheit temperature	°F

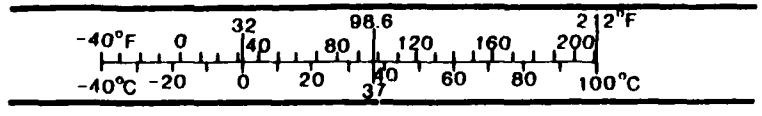

TABLE OF CONTENTS

LIST OF ILLUSTRATIONS

LIST OF ILLUSTRATIONS (continued)

LIST OF TABLES

1.0 INTRODUCTION

1.1 Problem Statement

Presently, the U.S. Coast Guard utilizes a soft, low carbon (1022) steel in mooring chain to anchor navigational buoys. The chain suffers a high wear rate due to the combined abrasion and corrosion encountered as the section of the chain resting on the bottom is dragged back and forth across the ocean bottom by currents and wave action. The high wear rate of the 1022 steel chain requires frequent checks by the Coast Guard buoy maintenance personnel with many moorings requiring frequent replacement of severely worn sections.

1.2 Objective

The objective of this research is twofold. As the mechanism that affects the buoy chain is a combination of a corrosion process and an abrasion process, the initial objective of this research is to isolate these two processes and identify their contributing roles in the material loss of the steel chain. The analysis of the two processes will provide a better understanding of the unique factors involved in the corrosive-wear process. Secondly, additional steel materials will be subjected to the corrosive-wear process and compared to the presently used material to determine what effects the steel's composition, hardness, and microstructure have on the corrosive-wear resistance. By determining the relative corrosive-wear rates, predictions of the improvement in chain life by the utilization of certain alloy steels can be achieved. Longer chain life may result in substantial savings by the Coast Guard.

1.3 Background

The safety of navigation upon the waters of the United States and its territories is the responsibility of the U.S. Coast Guard, which accomplishes this task through an intricate system of what are termed "aids to navigation". The primary component of the Coast Guard's system of aids to navigation is the buoyage system.

The importance of the buoy remaining on its charted position and attached to its mooring cannot be understated. Buoys mark the "highways" of the ocean in the same manner as painted lines and curbs mark roadways on land. They are relied and depended upon twenty-four hours a day by mariners who expect uninterrupted service of accurately placed buoys. If a buoy is missing from its station, there is the potential for a breakdown in the safe navigation of the marine industry. The possibility of a vessel grounding is increased together with the possibility of a collision with another vessel. Each year vessel groundings and collisions result in millions of dollars expended in the form of damage to vessels, pollution of the marine environment, and in some cases, loss of life. Occasionally, lawsuits have been brought against the U.S. Government and the Coast Guard in marine accidents alleging missing or misplaced buoys resulting in the cause of the mishap. Although invariably it is shown in most cases that human error is the ultimate cause in marine casualties, nevertheless, the importance of the buoyage system and ultimately the mooring system remains critical.

Today, the aids to navigation mission, including the system of buoyage, employs eighty vessels and forty bases. Over 23,000 buoys are currently in service as of January 1984. The mission requires approximately twenty percent of the Coast Guard's resources with a budget of $150 million and a manning of over 8,500 persons [3].

1.4 Chain Buoy Moorings

Although the system of buoyage has seen rapid technical progress, the use of steel chain as the material in the mooring of the buoys has essentially remained the same. The beginning of chain use is lost in history and as with many other basic mechanisms, the inventor and the date of origin are unknown. Steel chain was first used in the early moorings of navigational buoys and has continued in use to the present day [4].

The chain presently used by the Coast Guard for buoy moorings is a welded-link chain. Welded-link chain consists of interconnected endless loops of elliptical shape. The loops are made in automatic forming machines that cut the bar material to the correct blank length, bend the blank into the link

shape, thread another blank through the previously formed link, then repeat the process. After forming, the links are put together in shots (lengths of ninety feet) by one of several butt-welding processes.

The complete mooring system includes the chain attached to the buoy and a large concrete sinker. The buoy and its mooring system are shown in Figure 1.

A buoy moored in this fashion in the marine environment is subjected to wind, wave, and current forces which act directly on the buoy. The result of these forces is that the buoy, connected to the concrete sinker via the steel chain, is set into nearly constant movement. Even in extremely calm weather conditions, the buoy is still subject to tidal currents and waves caused by passing vessels. The constant movement of the buoy transmits motion to the attached length of chain. Also, below the surface, subsurface currents act on the chain and the concrete sinker. Both sections of the chain are therefore nearly constantly in motion. The section suspended in seawater follows the buoy while the section near the sinker is dragged along the sea bottom.

When buoys are deployed, the length of chain used for the mooring is determined by the particular type buoy being used, the water depth, the bottom type, and the marine environment where the buoy is being placed. The marine environment takes into account local winds, waves, and currents that can be expected for that location. The mooring is designed so that under the most severe designed environmental conditions, the entire length of chain is completely off the bottom with no upward angle at the sinker [5] as shown in Figure 2. As conditions diminish, subsequent amounts of chain will fall to the ocean bottom. Normally, the average amount of chain used at most locations is approximately two to three times the depth of water where the buoy is being deployed.

The chain used by the Coast Guard is carefully tested to ensure that the breaking strength of the chain safely exceeds the design loads anticipated in the actual buoy moorings. However, once the chain is placed on station with the buoy in the marine environment, the corrosive-wear process begins to

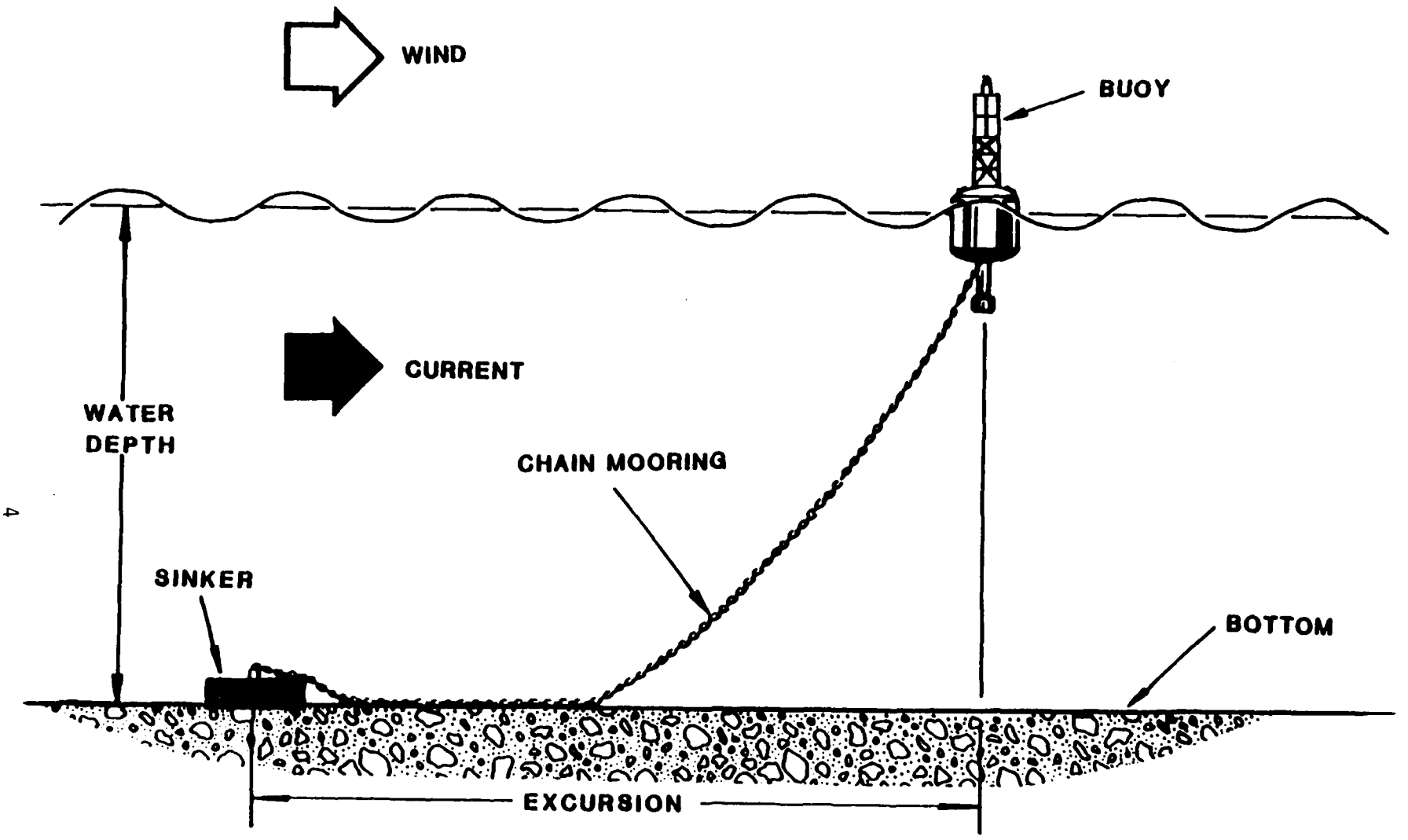

FIGURE 1. BUOY AND MOORING

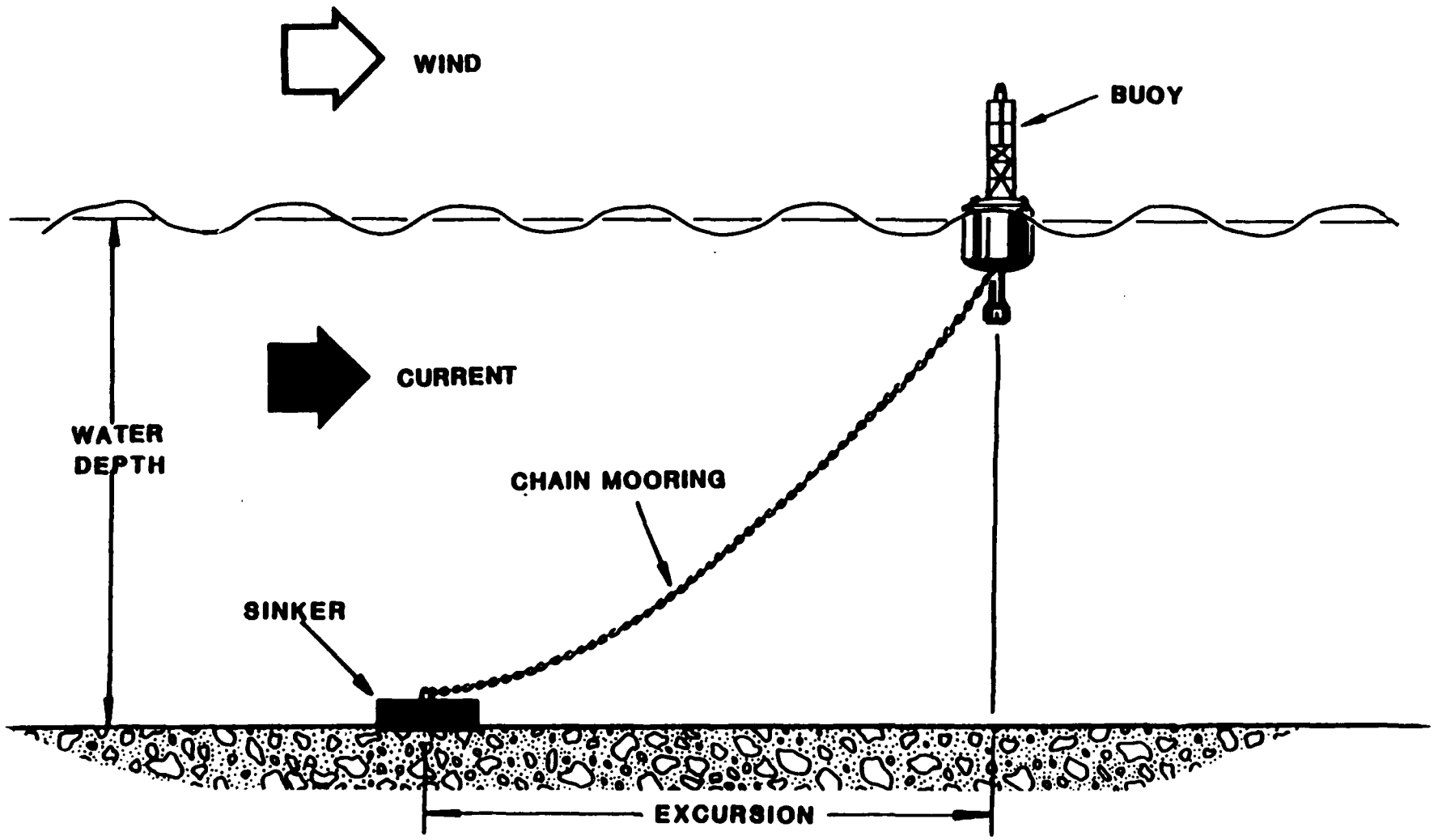

FIGURE 2. BUOY AND MOORING (MAX. CONDITIONS)

act on the chain. This process occurs when the chain is dragged across the sea bottom during buoy motion. If severe enough, large amounts of material in the bottom links of the mooring chain can be lost by corrosive-wear in relatively short periods of time. Material loss can result in tensile stresses on the link in excess of the link's breaking strength. Figures 3 through 9 graphically illustrate several buoy chain moorings which have undergone severe reductions in area. If this occurs, there is a high probability that ultimately a link will rupture due to the increased load felt on the link. Failure of the link may also occur as a result of fatigue due to the constant cyclic loading on the worn link. Because most moorings are lost when a buoy breaks its chain, there has been little research into the possible cause of the failure.

There is evidence that the early buoy and lighthouse tenders became aware of this problem as early as the late 1800's. Although most buoy moorings only required one inch to one and one-half inch diameter steel chain, it was standard practice to place chain of two and one-quarter to two and one-half inch diameter in the section of the mooring resting on the bottom, which is referred to as the chafe section [4]. This was obviously done in order to help compensate for the anticipated high loss of material and subsequent reduction in area resulting in an increased load on the chain links.

Failure of the mooring chain results in the buoy being released and set adrift. Not only does this reduce the effectivenes of the buoyage system of safe navigation, it results in the possible damage or total loss of the buoy.

1.5 Corrosive-Wear Principles

Corrosive-wear is a corrosion phenomenon involving two surfaces in contact with each other while subjected to a corrosive medium. It results in an accelerated rate of deterioration on a metal surface.

Wear involves two surfaces in contact with each other, usually with one surface not as hard as the other and therefore subject to material loss [6]. A driving mechanism is present to initiate motion between the two

FIGURE 3. ABRADED BUOY CHAIN

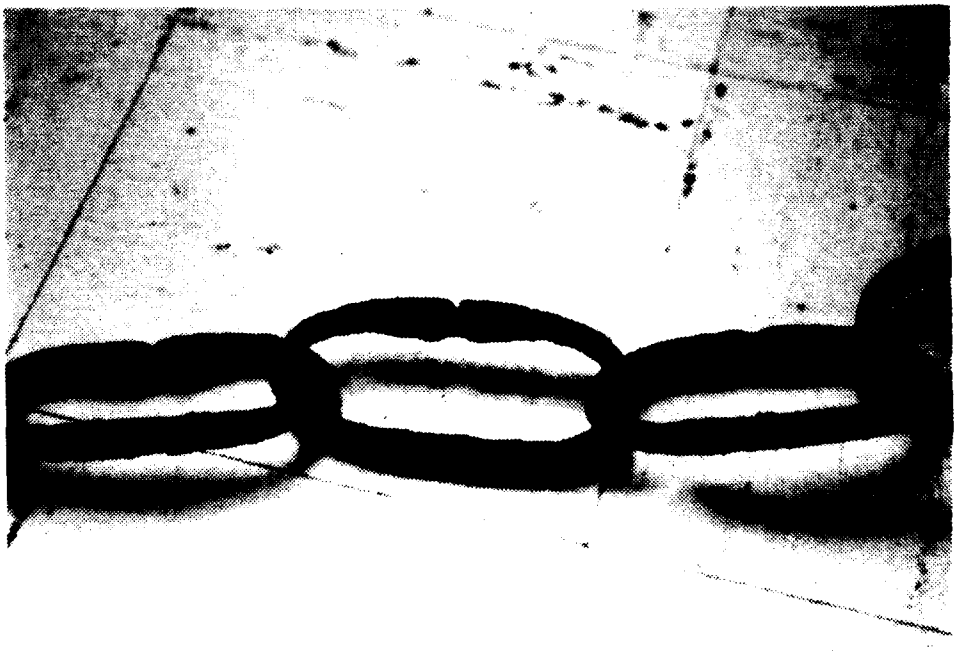

FIGURE 4. ABRADED BUOY CHAIN

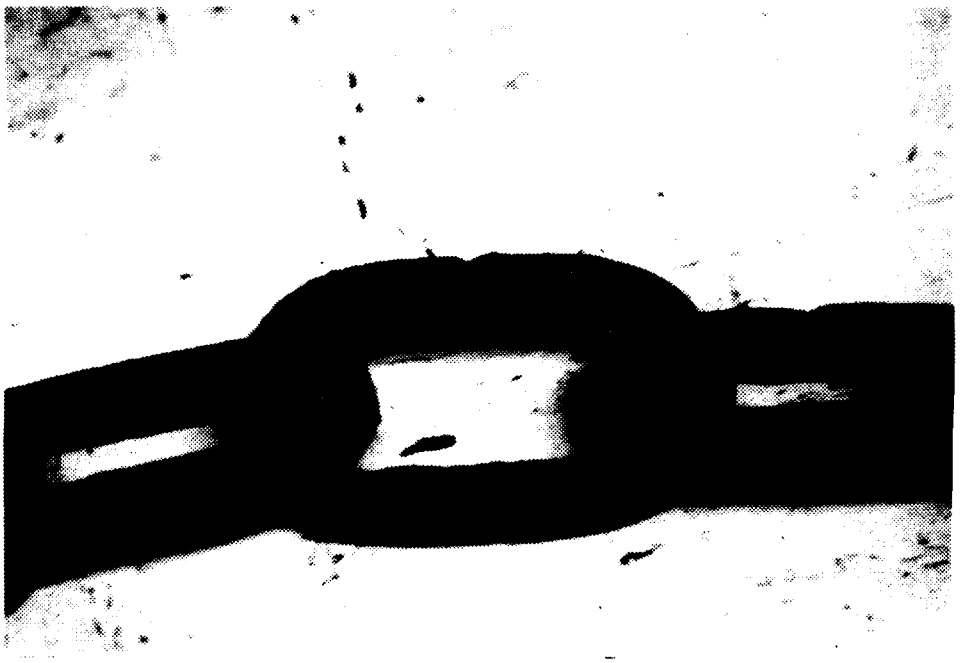

FIGURE 5. ABRADED BUOY CHAIN

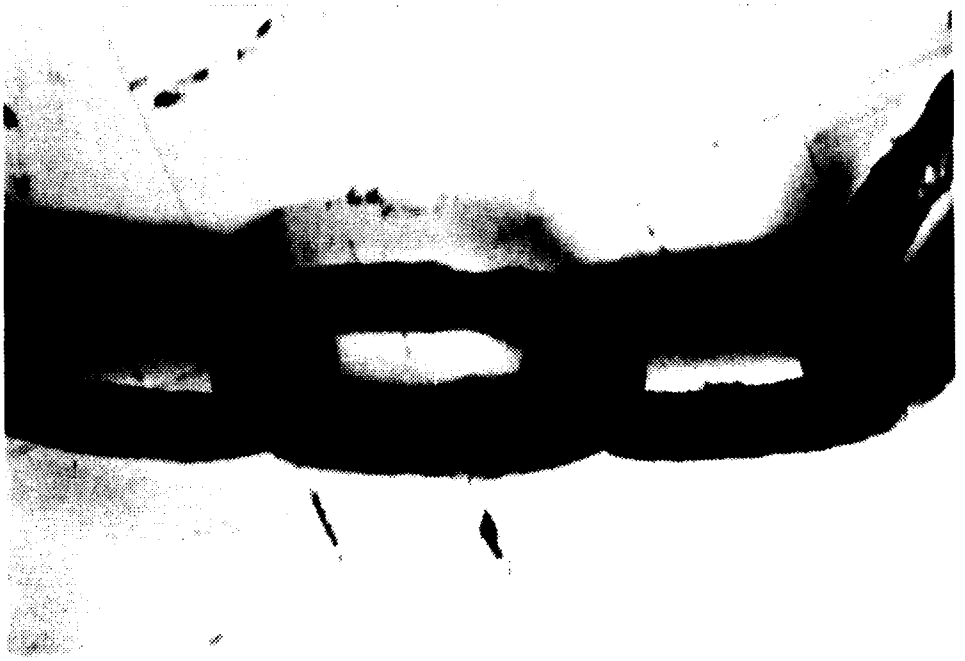

FIGURE 6. ABRADED BUOY CHAIN

FIGURE 7. ABRADED BUOY CHAIN

FIGURE 8. ABRADED BUOY CHAIN

FIGURE 9. ABRADED BUOY CHAIN

surfaces, setting up the abrasion process. The attack by the corrosive medium provides for a surface layer to form due to corrosion on the metal surface which can be easily abraded from the surface. As each new layer of corrosion products is formed, it too is eventually removed from the metal. The continual process results in a high loss of metal material. When the surface layer is removed, the newly exposed area of the metal is also subject to being directly abraded as it remains in contact with the abrading surface.

The degradation of buoy chain occurs in the same fashion. As the chain is moved about the ocean bottom, the soft porous layer on the links is removed by the abrasive surface of a sandy or rocky bottom and falls away from the steel links. The newly exposed metal area is then subject to a direct abrading process with the sand or rock particles. When the chain does become stationary, a new surface layer will form.

Most metals and alloys are susceptible to this type of corrosive-wear mechanism or other similar forms of erosion-corrosion. Many metals depend upon the formation of a surface layer for resistance to corrosion in the phenomenon called passivation [7]. As the thin passivating layer is removed by abrasion, these materials are normally rendered useless since the abrasive mechanism destroys the protective layer.

Soft metals are usually more susceptible to the corrosive-wear process than hard metals because they are more vulnerable to wear from the abrasive component of the process. This is commonly true of the low carbon content steels [7]. Inherently hard metals therefore usually provide better protection than soft metals in an abrasion dominated process.

1.6 Buoy Chain Corrosion Studies

Problems with the corrosive wear of buoy chain have also been investigated by the Canadian Coast Guard [8]. Commencing in 1954, a series of five tests over an 8-year period were conducted in the Bay of Fundy. The location was selected for its dynamic range of tides and strong currents. The severity of the environment was emphasized by the loss of the first two test buoys. The testing utilized various plain carbon and alloy steels on full length and composite moorings as shown in Table I.

Pertinent Data on Various Chains Tested

TABLE I

Properties of Steels Tested by the Canadian Coast Guard

Steel Identification	Specified Compositional Limits C %	Mn %	Si %	S %	P %	Cr %	Ni %	Mo %	Cu %	Yield Strength psi*	Yield Load lbs*	Chain Diameter Inches*	Fundy Test	Remarks
AISI 1026	0.22/0.28	0.60/0.90	-	0.05 max	0.04 max	-	-	-	-	39,300 (27.5)	-	1½ (0.0317)	A	AW
Wrought Iron	0.03	0.05	0.18	0.031	0.42	-	-	-	-	37,000 (25.9)	-	1½ (0.038)	A	AW
AISI 4615	0.13/0.18	0.45/0.65	0.20/0.35	0.04 max	0.04 max	-	1.65/2.00	0.20/0.30	-	90,500 (63.4)	65,000(1) (29,500)	1 (0.0254)	A	Q & T - 280 BHN
Wrought Iron	0.01	0.17	0.14	0.028	0.27	-	-	-	-	33,500 (23.4)	-	1½ (0.0317)	B	AW - 116 BHN
AISI 8620	0.18/0.23	0.70/0.90	0.20/0.35	0.04 max	0.04 max	0.40/0.60	0.40/0.70	0.15/0.25	-	122,300 (85.5)	-	1 (0.0254)	B	Q&T - 260 BHN
Manganese Steel	1.0/1.4	10.0/14.0	1.00 max	0.04 max	0.05 max	-	-	-	-	-	-	1 (0.0254)	B	Q - 235 BHN
AISI 4615	0.13/0.18	0.45/0.65	0.20/0.35	0.04 max	0.04 max	-	1.65/2.00	0.20/0.30	-	104,500 (73.1)	-	1 (0.0254	B	Q&T - 260 BHN
AISI 1008	0.10 max	0.25/0.40	-	0.05 max	0.04 max	-	-	-	-	35,700 (25.0)	-	1½ (0.038)	B	AW - 116 BHN
Stelcoloy	0.09	0.45	0.21	0.027	0.095	0.42	0.85	-	0.50	61,000 (42.7)	55,000(2) (25,000)	1 (0.0254)	C	AW - 159 BHN - Test Bar 202 BHN - Chain
Copper-Nickel	0.14	0.93	0.37	0.021	0.010	-	3.93	-	1.20	145,000 (101.0)	70,000(4) (31,800)	1 (0.0254)	C	Q&T - 388 BHN
AISI 1020	0.18/0.23	0.30/0.60	-	0.05 max	0.04 max	-	-	-	-	-	42,000 (19,070)	1½ (0.0317)	C	AW - 187 BHN
AISI 8620	0.18/0.23	0.70/0.90	0.20/0.35	0.04 max	0.04 max	0.40/0.60	0.40/0.70	0.15/0.25	-	-	-	1 (0.0254)	C	Carb.
Ni-Steel	0.09/0.11	0.65/0.75	0.10 max	0.03 max	0.06/0.08	0.18/0.21 Al	0.55/0.65	0.10/0.12	1.05/1.15	52,000 (36.4)	27,000(5) (12,250)	1 (0.0254)	C	AW
AISI 1027	0.22/0.29	1.20/1.50	-	0.05 max	0.04 max	-	-	-	-	-	64,000(3) (29,100)	1 (0.0254)	D	AW - 150 BHN
Stelcoloy	0.12	0.71	0.31	0.030	0.07	0.36	0.50	-	0.45	-	53,000(2) (24,100)	1 (0.0254)	E	AW
"	0.12	0.53	0.28	0.029	0.084	0.47	0.62	-	0.40	-	46,000(2) (20,900)	1 (0.0254)	-	In General Use
"	0.09	0.77	0.37	0.022	0.075	0.53	0.53	-	0.49	-	45,000(2) (20,400)	1 (0.0254)	-	" " "

(1) Test results obtained on pitted chain.

(2) Several different samples of Stelcoloy chain, made by different companies, were tested and are given here to show the range of properties encountered.

(3) This test was on new chain. Pitted chain showed a yield load of about 22,000 lbs. (9,980 Kg)

(4) The yield load shown refers to tests on new 5/8" (0.0159m) diameter chain to this approx. composition.

(5) Yield load obtained on tests on pitted chain.

* Figures in brackets are the yield strength in Kg/mm^2, the yield load in Kg and the chain diameter in meters.

Legend
AW - As-welded
Q&T - Quenched & Tempered
Carb. - Carburized

Although the testing was somewhat inconclusive, the materials that showed the most promise were Stelcolony, which is available commercially, and a higher content copper-nickel steel alloy. A comparison beteen these two alloys and heat-treated AISI 1020 steel is shown in Figure 10. In the first twenty-seven months the alloy steels lost approximately ten percent of their weight. The AISI 1020 samples lost from thirteen to seventeen percent and continued to corrode so that after forty-five months the losses were near twenty-five percent. The reductions in weight loss over time for the alloy steels (Cu-Ni and Stelcolony), as demonstrated in Figure 10, are attributed to the passivity of the steels, which forms a tightly adherent oxide layer on the surface. Barrel wear was not examined on these particular chains.

All the other alloy steels tested showed susceptibility to pitting. The AISI 4615 exhibited extensive pitting after only six and one-half months. In another test, chains of carburized AISI 8620 and AISI 1020 steel were declared unserviceable after thirteen months of exposure. Pitting was also evident on the Stelcolony samples. It was concluded that a nickel content of at least 0.58% was necessary to reduce pitting corrosion significantly.

By examination of the chains following testing, it was determined that the main causes of chain degradation were pitting corrosion, inter-link wear, and barrel wear. Barrel wear occurs due to the abrasion of the sides of the chain against a rough bottom surface. Inter-link wear is caused by the friction between connecting links. It was concluded that future mooring chain selection should be based primarily on general corrosion resistance and especially pitting corrosion. Failure of the mooring may result from pitting rather than overall weight loss. Secondly, the chain should have good wear resistance especially on bottom sections where the barrel wear occurs. By proper selection of alloy in elements, significant improvement in strength and wear resistance can be obtained.

Following the Bay of Fundy test program, the Canadian Coast Guard implemented 1-1/8 inch diameter alloy steel chain replacing the 1-1/4 and 1-1/2 inch diameter mild steel chains on many buoy moorings across Canada. Results have been highly favorable in most cases with certain exceptions. Intergranular corrosion of the alloy chain was observed in a few isolated cases. This was attributed to either improper bar rolling at the steel plant

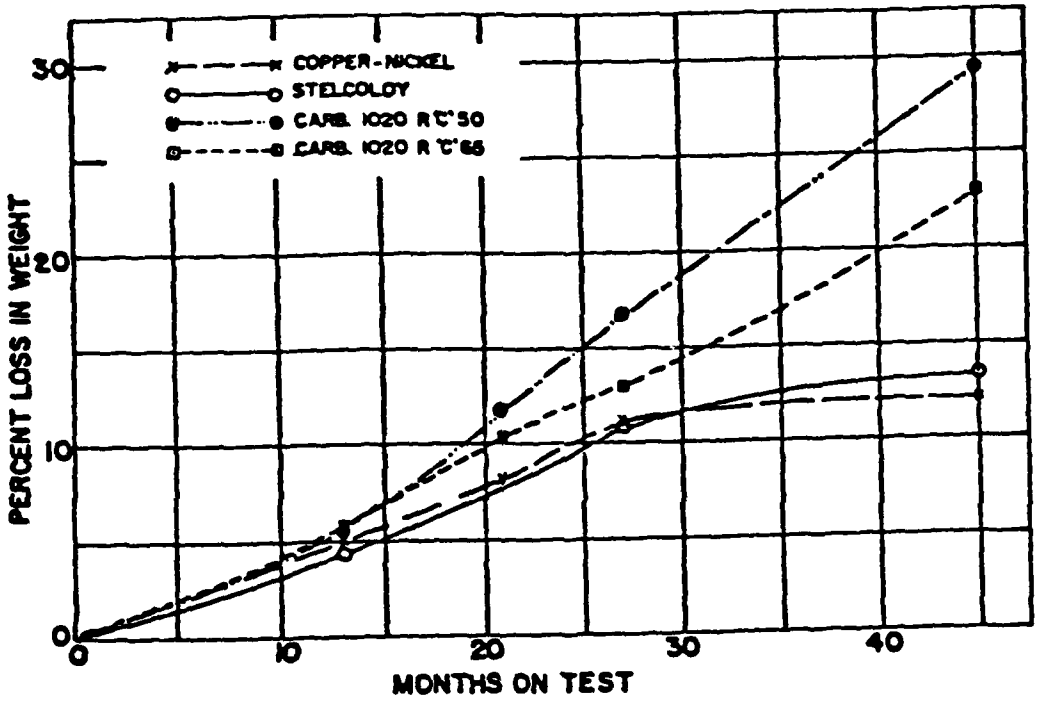

FIGURE 10. GRAPH SHOWING THE PERCENTAGE WEIGHT LOSS VS TIME FOR FOUR TEST CHAINS IN FUNDY TEST "C"

or the presence of certain chemicals in the water. Prevention could be accomplished through post-forming heat treatment.

Largely, it was observed that the alloy steel chain, with great strength and wear resistance or even equivalent performance to mild steel, allowed for buoy mooring down-sizing to obtain equal or better station life at a reduced cost.

2.0 APPROACH

2.1 Simulating the Chain Wear Mechanism

Before selecting the alternative steels to compare with the presently used 1022 steel, the task of designing the test apparatus was undertaken. The uniqueness of the corrosive-wear mechanism affecting buoy mooring chain makes it a difficult process to simulate.

Ideally, full-scale field tests on actual buoys would provide the most reliable data; however, these tests would require at least two full years under ideal conditions. An accelerated model of this process would provide valuable data in a relatively short period of time.

From Coast Guard buoy tender reports it was clear that the dominating factor in the process is the constant movement of the steel chain across the abrasive bottom. This movement not only removes the protective oxide layer formed on the chain links, it also directly abrades the steel links themselves. To simulate this type movement, a horizontal displacement motor was selected to provide the driving force for movement of the steel specimens during the tests. The motor provided a back and forth reciprocal motion similar to the motion actual chain moorings experience. A motor with a relatively low rpm ratio was chosen so as to provide a realistic approach to the actual frequency movement of the buoy chain. The Bodine motor chosen operated at 29 rpm, thus the steel specimen is cycled across the abrasive field approximately once every two seconds. This would correspond to a mooring chain attached to a buoy experiencing waves with 2-second periods. For most buoys, the wave periods associated with the maximum environmental conditions range from one second to ten seconds. Thus, with the use of the

Bodine motor at 29 rpm, the abrasion process, which is dependent on frequency, simulated a realistic situation that would occur to an actual buoy chain mooring under its near maximum design conditions.

Depending on the location where the buoy is stationed, the attached chain may rest on a sandy, muddy, rocky, or combination type bottom. Over the years, reports from Coast Guard field units have indicated that rocky and sandy type bottoms produce increased wear on chain moorings over soft or muddy bottoms. To simulate a sandy or rocky type bottom, an abrasive surface with approximately the same hardness and particle size should be used since wear rates are dependent on these factors. Since the testing utilized the same type of abrasive for each specimen, the abrasive characteristics were not critical.

Simulation of the chain wear mechanism was carried out in two different laboratory testing schemes. The first set of experiments were conducted in 1984 and will be referred to in the subsequent text as Experiment A. The second set of tests completed in 1985 will be referred to as Experiment B.

2.2. Materials

The steels selected for use in Experiment A for comparison with the presently used 1022 steel were 1045 and 4140 grade steels. These two grade steels were chosen to investigate the effect of increasing carbon content with the 1045 steel and the effect of alloying at about the same carbon content with the 4140 steel. A third approach was to examine the effect on a martensitic structure by heat-treating the 1022 steel. Table II provides all pertinent data on the selected steels.

Selection of the two comparison steels was geared towards providing similar type material composition yet increasing the structural strength and hardness. It is theorized that a similar but structurally harder material will provide a lesser wear rate due to an increase in wear resistance. By heat-treating the 1022 steel, a martensitic microstructure was obtained, thus also producing a structurally harder material than the original 1022 steel.

TABLE II

PROPERTIES OF MATERIALS TESTED

MATERIAL	COMPOSITION	YIELD STRENGTH	TENSILE STRENGTH	ROCKWELL HARDNESS	% ELONGATION
1022	.18-.23% C .70-1.0% Mn .04% P, max .05% S, max BALANCE Fe	52,000 psi	73,000 psi	77 Rb	35
1022HT	SAME AS ABOVE	140,000 Approx	188,000 Approx	41 Rc	12 Approx
1045	.43-.50% C .60-.90% Mn .04% P, max .05% S, max BALANCE Fe	59,000	90,000	100 Rb	25
4140	.38-.43% C .70-1.0% Mn .80-1.1% Cr .15-.25% Mo .20-.35% Si .035% P, max .040% S, max BALANCE Fe	60,500	95,000	89 Rb	26
4140HT	SAME AS ABOVE	56,000 Approx	85,000 Approx	84 Rb	30 Approx
4340	.38-.43% C .60-.80% Mn 1.65-2.0% Ni .70-.90% Cr .20-.30% Mo .20-.35% Si .035% P, max .040% S, max BALANCE Fe	68,5000	108,000	22 Rc	22
8740	.38-.43% C .75-1.0% Mn .40-.70% Ni .40-.60% Cr .20-.30% Mo .20-.35% Si .035% P, max .040% S, max BALANCE Fe	60,250	100,750	90 Rb	22

In Experiment B the steels were selected in order to determine the effects of various alloy additions on hardness and microstructure. The following alloy steels were chosen to compare with the presently used 1022 steel: ASTM 4140, heat-treated 4140, 4340, and 8740. All the alloy steels contain approximately the same amount of carbon. Their respective properties are also shown in Table II.

Presently, the Coast Guard purchases steel in quarterly contracts through a specification for mooring U.S. Coast Guard buoys, Specification No. 377. Qualified steels for use in the production of the buoy chain are referenced to a Federal military specification. The military specification used, MIL-S-16974, is for any grade carbon or alloy steel as long as the steel meets the proof load and breaking load requirements in the buoy mooring specifications. All the comparison steels chosen would be appropriate "qualified" steels for buoy mooring chain according to these two specifications.

The 1022 steel used in this research was obtained through several unused links of one and one-quarter inch diameter chain provided by the Coast Guard. Specimens were cut from the linear sections of the links. Specimens from the other steels were cut from bar stocks of the same diameter as the chain links and were obtained from local manufacturers.

The 1022 steel, used in both Experiments A and B, is a plain carbon steel with a microstructure consisting of unresolved pearlite within equiaxed ferrite grains as shown in Figure 11. The material is relatively soft due to its high ferrite to pearlite ratio.

The 1045 steel, used in Experiment A, is also a plain carbon steel with the only significant difference being the increased carbon content. Carbon is the principal hardening element in steels, and with each increment of carbon an increase in hardness and tensile strength of the steel in the as-rolled condition results. A trade-off to the increased hardness and strength is a reduction in ductility and weldability. The choice of the 1045 grade steel also provides an alternative material which is similar in production technique and in cost. An increase in the amount of coarse

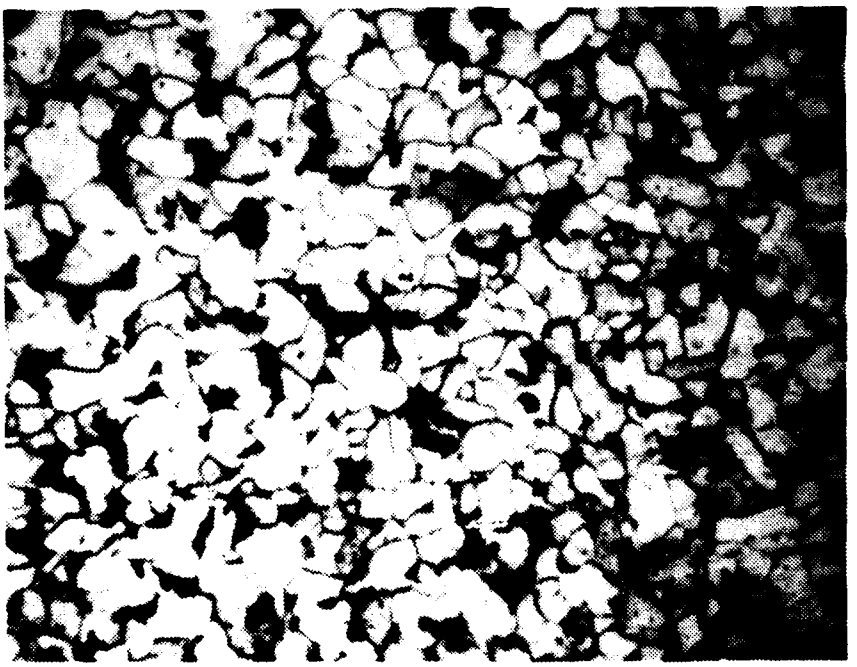

FIGURE 11. MICROSTRUCTURE PHOTO OF 1022 STEEL (X288)

pearlite in the microstructure as a result of the carbon content increase can be seen in Figures 12 and 13, where it is visible as the dark areas in the photographs.

The 4140 grade steel is very similar to the 1045 grade steel in carbon content (.40 to .45 percent) but in addition it contains several trace elements which tend to increase its strength and hardness as well as its resistance to corrosion such as chromium, molybdenum, and silicon. Microstructural examination of the steel, as displayed in Figures 14 and 15, revealed a predominately pearlitic structure mixed with ferrite. The 4140 steel used in Experiment A and shown in Figure 14, contained much finer pearlite and ferrite than the coarser structure of the 4140 used in Experiment B, which is shown in Figure 15. The carbide plates of the pearlite are more visible due to increased carbon content over the 1022 steel.

Heat treatments of the 1022 steel in Experiment A and of the 4140 in Experiment B were conducted in order to observe the effects of altering the microstructures without changing the compositions. Through heat treatment of the 1022 steel, a martensitic structure was obtained as shown in Figure 16. This increased the hardness of the steel as well as the tensile strength. Heat treatment of the 4140 steel consisted of austenitizing at 1600^{o}F for a 1-hour period followed by a slow cooling over a 24-hour period. The heat-treated steel is softer than the original steel. The reason for this can be observed in Figure 17, where a coarse ferrite is the dominant feature. Compared to the small, isolated, and elongated ferrite grains in the cold-rolled 4140, the annealing of the heat-treated 4140 allowed for reforming and growth of the ferrite structure. However, the hardness was still above that of the 1022 steel due to increased carbon and alloy content.

Higher alloy additions, especially nickel, were contained in the 4340 steel used in Experiment B. This steel was one of the hardest steels tested due to the solution-hardening effects of the nickel. Shown in Figure 18, the structure consisted of small, finely dispersed ferrite and pearlite grains.

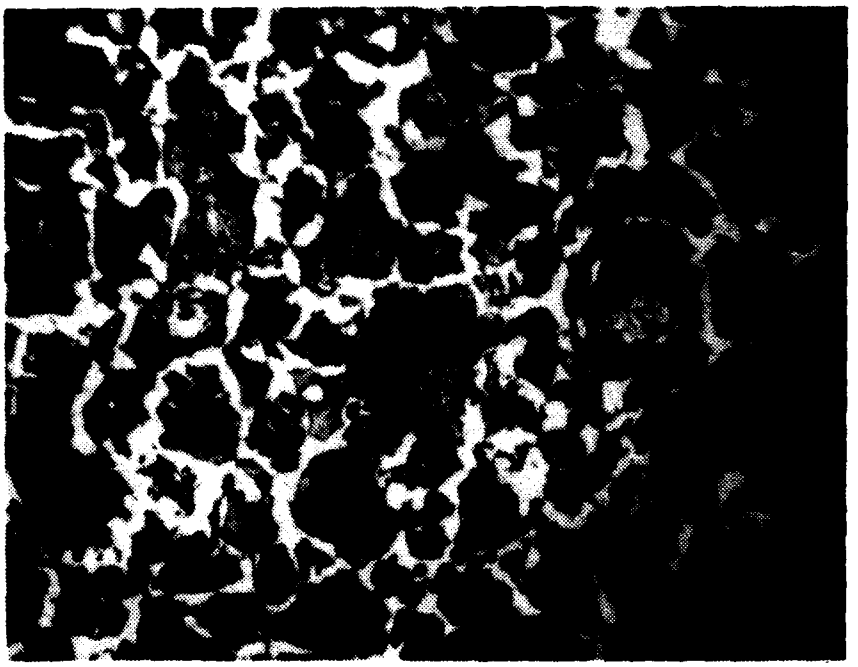

FIGURE 12. MICROSTRUCTURE PHOTO OF 1045 STEEL (X288)

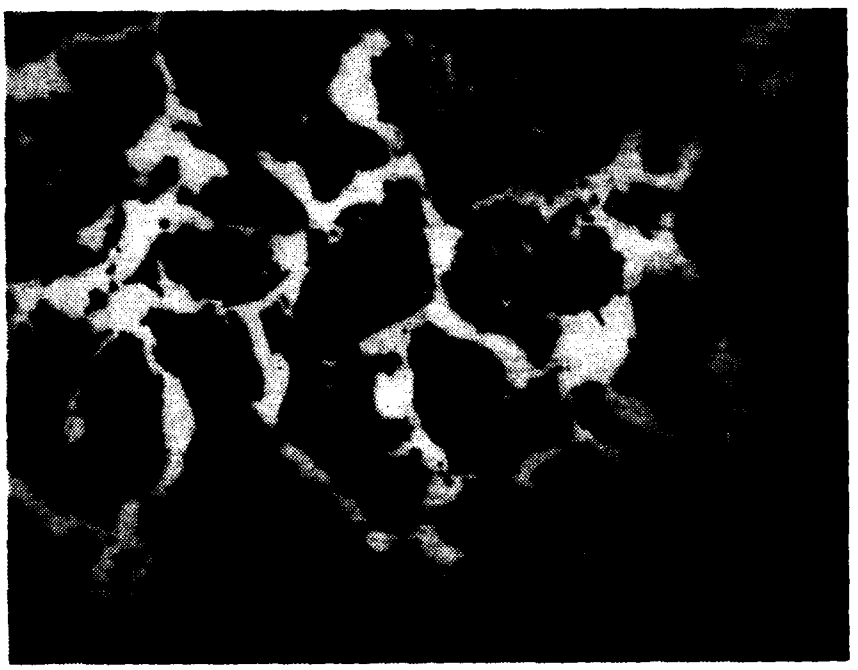

FIGURE 13. MICROSTRUCTURE PHOTO OF 1045 (H. MAG.) STEEL (X576)

FIGURE 14. MICROSTRUCTURE PHOTO OF 4140 STEEL (X288): EXPERIMENT A

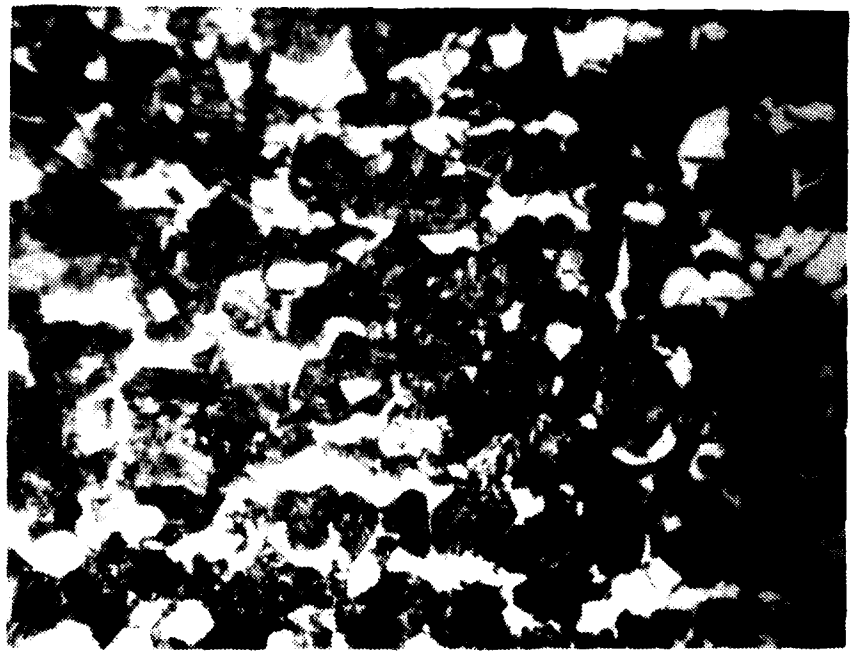

FIGURE 15. MICROSTRUCTURE PHOTO OF 4140 STEEL (X288): EXPERIMENT B

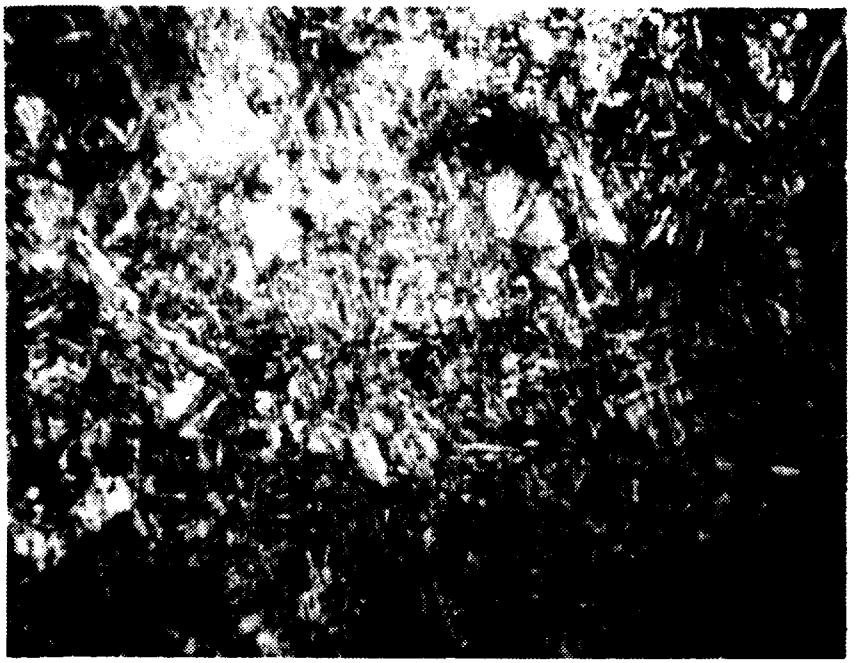

FIGURE 16. MICROSTRUCTURE PHOTO OF 1022 HT STEEL (X288)

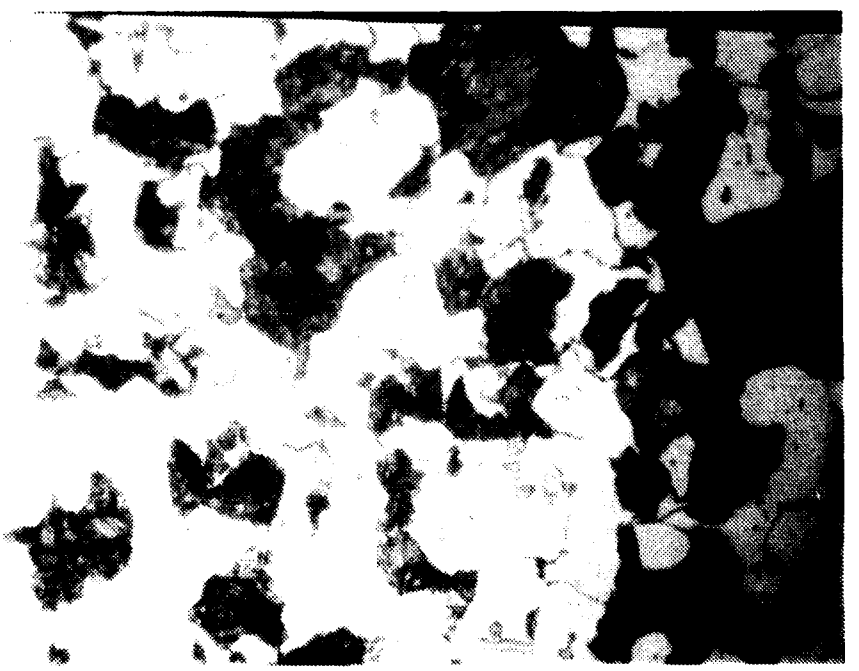

FIGURE 17. MICROSTRUCTURE PHOTO OF 4140 HT STEEL (X288)

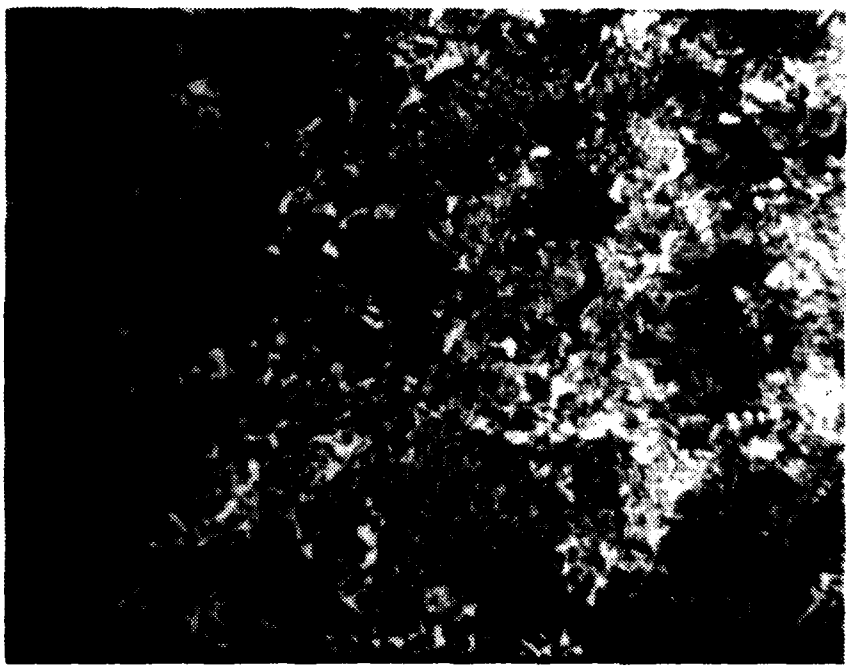

FIGURE 18. MICROSTRUCTURE PHOTO OF 4340 STEEL (X288)

Another material tested in Experiment B was an 8740 grade steel. Of approximately the same composition as the 4340, except for a reduced nickel content, the material was slightly softer. The structure of the 8740 steel is shown in Figure 19. The microstructure resembled that of the 4140 steel, with approximately the same ferrite grain size, volume fraction, and mechanical properties.

3.0 EXPERIMENT PROCEDURES

3.1 Undisturbed Corrosion Tests

Undisturbed corrosion tests were conducted in Experiment A to provide a basis for analysis of the corrosion aspect involved in the corrosive-wear mechanism. The tests involved allowing a selected steel specimen to corrode undisturbed while immersed in volumes of distilled water or seawater.

Steel specimens of one and one-quarter inch diameter and approximately seven-eighths inches long were prepared by surfacing one face side of each specimen to a smooth finish. This was performed by the use of a Buehler Roll Grinder. Four different SIC grit size paper were used: 240, 320, 400, and 600 mesh. A smooth finish on one face was achieved by grinding the specimen on each size grit paper starting with the 240 size and continuing to finish with the 600 size.

Once a smooth finish was achieved, the remaining unprepared surface area of the specimen was painted with a protective insulating coating. The protective coating used was a mixture of a rubber-based tool grip compound thinned by a turpentine-based thinner. The mixture was prepared by pouring several ounces of the tool grip compound into a petri dish and then adding the thinner to arrive at the desired consistency.

Prior to the start of the test and after the specimen's coating had sufficiently dried, the specimen was weighed by use of an analytical balance. A total of six weight measurements were taken and then averaged to determine the pre-test weight. The balance was initially zeroed and then re-zeroed after every two successive measurements.

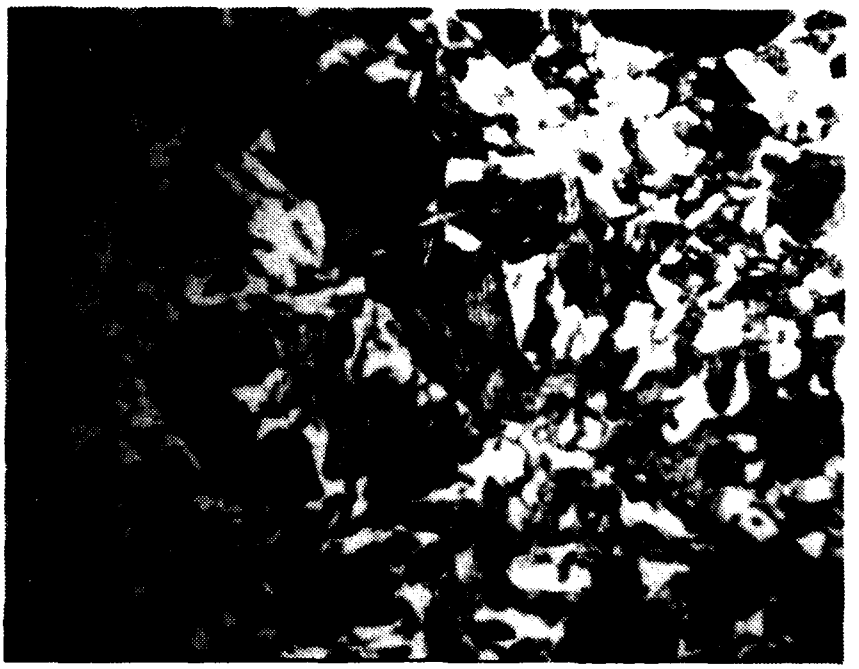

FIGURE 19. MICROSTRUCTURE PHOTO OF 8740 STEEL (X288)

A small specimen holder was designed and constructed of non-conducting plastic material to hold the specimen during the test. The holder consisted of a hollowed-out shell that the steel specimen fit up into leaving only the unprotected prepared surface exposed. A small plastic set screw on the side of the shell held the specimen in place. The shell was attached to a one-quarter inch diameter plastic rod from which it was suspended into the test bath.

The undisturbed corrosion tests were conducted using baths of distilled water and baths of seawater and with all four materials being tested: 1022, heat-treated 1022, 1045, and 4140 steels. The seawater used for the tests was obtained from the Narragansett Bay and had a pH of 8.3. Each bath of distilled water and seawater was prepared by drawing approximately 500 ml from the respective reservoirs into a glass beaker.

On one side of each specimen approximately one-quarter inch from the prepared surface, a 3/32-inch hole was drilled and tapped. This served as the point where a small wire was attached via a brass 3/32-inch screw to provide an electrical connection. Once the connection was made and the screw secured, the connection was painted with a thin layer of the prepared protective coating mixture.

Prior to the start of the test, a standard calomel electrode was placed into the bath. The electrode lead was connected into the input side of a data bank. The electrical connection leading from the steel specimen was used to read the output voltage from the data bank. A direct voltage potential reading was recorded as well as an offset reading referenced to the calomel electrode. Data sheets were prepared for each test to record all voltage potentials, weights, and other pertinent data.

To initiate the test, the specimen holder with attached steel specimen was suspended in the bath. Voltage potential readings were recorded at periodic intervals during the test. Each test was allowed to proceed until a well-stabilized voltage reading was achieved, usually within 120 to 180 hours.

At the termination of the test, the specimen holder containing the specimen was removed from the bath. The steel specimen was removed from the holder and the attached electrical wire and screw removed from the specimen. The specimen was cleaned with warm tapwater and all oxide particles were brushed away. The specimen was then sprayed with methanol to drive off the water moisture and allowed to dry.

After the specimen was completely dry it was weighed on the analytical balance in the same manner as it had prior to the test. Six measurements were taken and averaged to arrive at a final post-test weight. The total material weight loss and the ending voltage potentials were recorded on each specimen's data sheet.

3.2 Corrosive-Wear Tests: Experiment A

A plastic rectangular tank eighteen inches by twelve inches by twelve inches deep served as the reservoir for the distilled water and seawater used in the tests. A continuous duty Bodine electric motor was attached to the tank to deliver the driving force required for movement of the steel specimens. The motor was fitted with a plastic cam to provide the horizontal back-and-forth motion desired for the steel specimens. The 1/20 horsepower motor operated at 29 rpm and with a stroke of 4-3/4 inches. An acrylic 3/4-inch diameter rod served as a shaft and attached to the motor drive cam via a plastic arm and rod holder. The 2-1/2 foot shaft led from the motor across the top of the tank reservoir and was supported by two sets of dual 1-inch diameter plastic ball bearings. The sets of ball bearings were mounted on each side of the tank and provided for smooth unobstructed movement of the shaft. A small weight was attached to the end of the shaft which extended over the outside edge of the tank. The weight served to balance the shaft due to the weight of the cam and rod holder at the other end of the shaft.

A plastic carriage rode on the shaft and provided a platform from which the steel specimens could be suspended. The carriage consisted of a 3-1/2 inch by 1-3/4 inch rectangular base through which the shaft passed and a triangular 7-1/2 inch long arm extending down into the tank reservoir. The

same specimen holder used for the undisturbed corrosion tests was used for the corrosive-wear tests.

To attach the holder and specimen to the carriage, an additional support piece was designed and constructed of plastic. This piece mounted onto the lower end of the triangular arm of the carriage and provided three supports through which the 1/4-inch diameter rod of the specimen holder passed. The holes of the support were bored so that the 1/4-inch rod of the specimen holder could slide freely up and down through the supports. A sliding guide piece was attached between the two top supports. This piece, which mounted to the 1/4-inch rod of the specimen holder through a drilled hole and set screw, allowed the specimen holder to move only up and down as a steel specimen was moved across the abrasive. The guide piece allowed for a steady controlled back-and-forth motion of the steel specimen across the abrasive.

Mounted on the top of the 1/4-inch diameter rod of the specimen holder was a plastic hollowed-out shell similar to the shell which was used to hold the steel specimens. This shell served as a platform for weights to be placed in order to transfer a load to the steel specimen as it was abraded. Although different weights could have been placed on the platform shell, a standard weight of 100 grams was used for all of the tests. All equipment of the carriage apparatus and specimen holder were constructed of plastic or non-metallic materials so as not to interfere with the potential voltage readings being observed. Plastic screws were used to secure the various components wherever possible. Several metallic screws were required on some pieces. However, once secured in place, they were thoroughly coated with the protective rubber-based mixture used to coat the steel specimens.

Inside the tank, an abrasive disc was used as the abrasive mechanism to which the steel specimens were subjected. The type disc used was a 10-inch diameter aluminum oxide abrasive cut-off wheel. After each test, the disc was repositioned to subject a fresh area to the abrasion process. The disc was replaced with a new disc once all available areas of the disc were used.

A platform was constructed of wood and placed inside the tank on which the abrasive disc was mounted. The platform raised the level of the

disc up to the approximate position of the bottom of the specimen holder. Once the platform was positioned inside the tank, it was leveled and secured. The abrasive disc was held in place on the platform by two standard construction bricks. Figure 20 shows the motor and tank set-up and Figure 21 shows an enlarged view of the carriage and specimen holder.

At the start of each corrosive-wear test, the tank was filled to a level of approximately 3/4 full. Depending on the type test being conducted, the tank was filled with either distilled water or seawater from two large reservoirs housed within the laboratory. The level of the water in the tank allowed for a depth over the abrasive disc of approximately 3-1/2 inches. A standard calomel electrode was mounted to one side of the tank and suspended into the bath.

The steel specimens used for the corrosive-wear tests were prepared in the same manner as the specimens used for the undisturbed corrosion tests. Each specimen was prepared on the roll grinder, coated with a thin layer of the protective mixture and weighed prior to the start of a test as before. To initiate the test, the steel specimen being tested was placed into the specimen holder which was raised above the water level of the tank. The steel specimen was secured in place with a plastic set screw. An electrical connection to the specimen was now made by attaching a small wire with a screw into the side of the specimen as had been done in the undisturbed corrosion tests. A 3/32-inch brass screw held the wire into the hole which had been drilled and tapped into the side of the specimen. Once the connection was secured, it was painted with a thin layer of the prepared protective coating mixture.

As in the undisturbed tests, the calomel electrode wire lead was connected into the input side of the data bank. The electrical connection leading from the steel specimen was then connected into the second input side of the data bank. A multi-meter was used to read the output voltage from the data bank. When the electrical connection coating had sufficiently dried, the specimen holder was lowered into the bath and the 100 gram load was placed on the top of the specimen holder platform. To start the test the motor was then switched on.

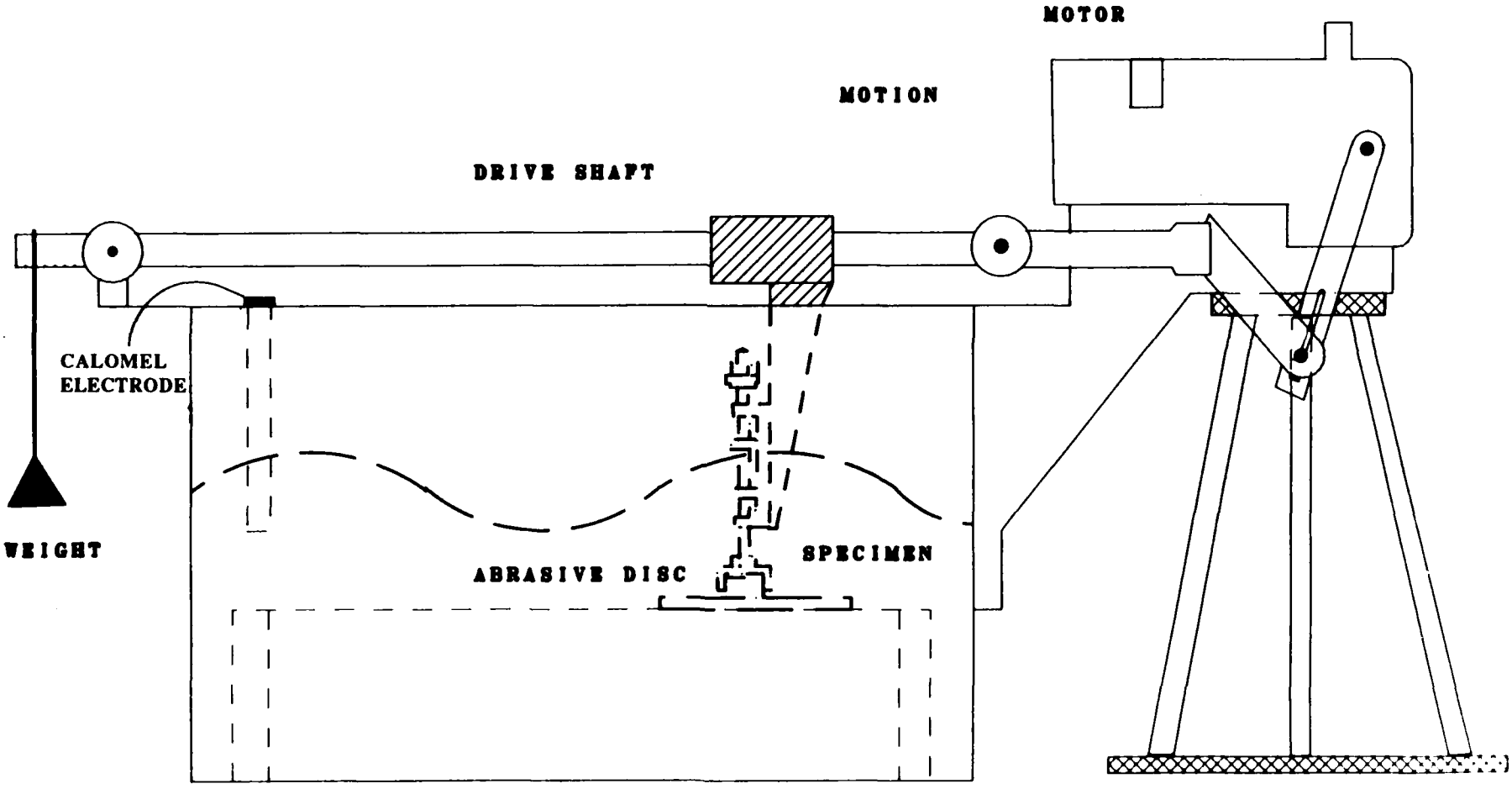

FIGURE 20. TANK AND MOTOR SET-UP APPARATUS: EXPER'MENT A

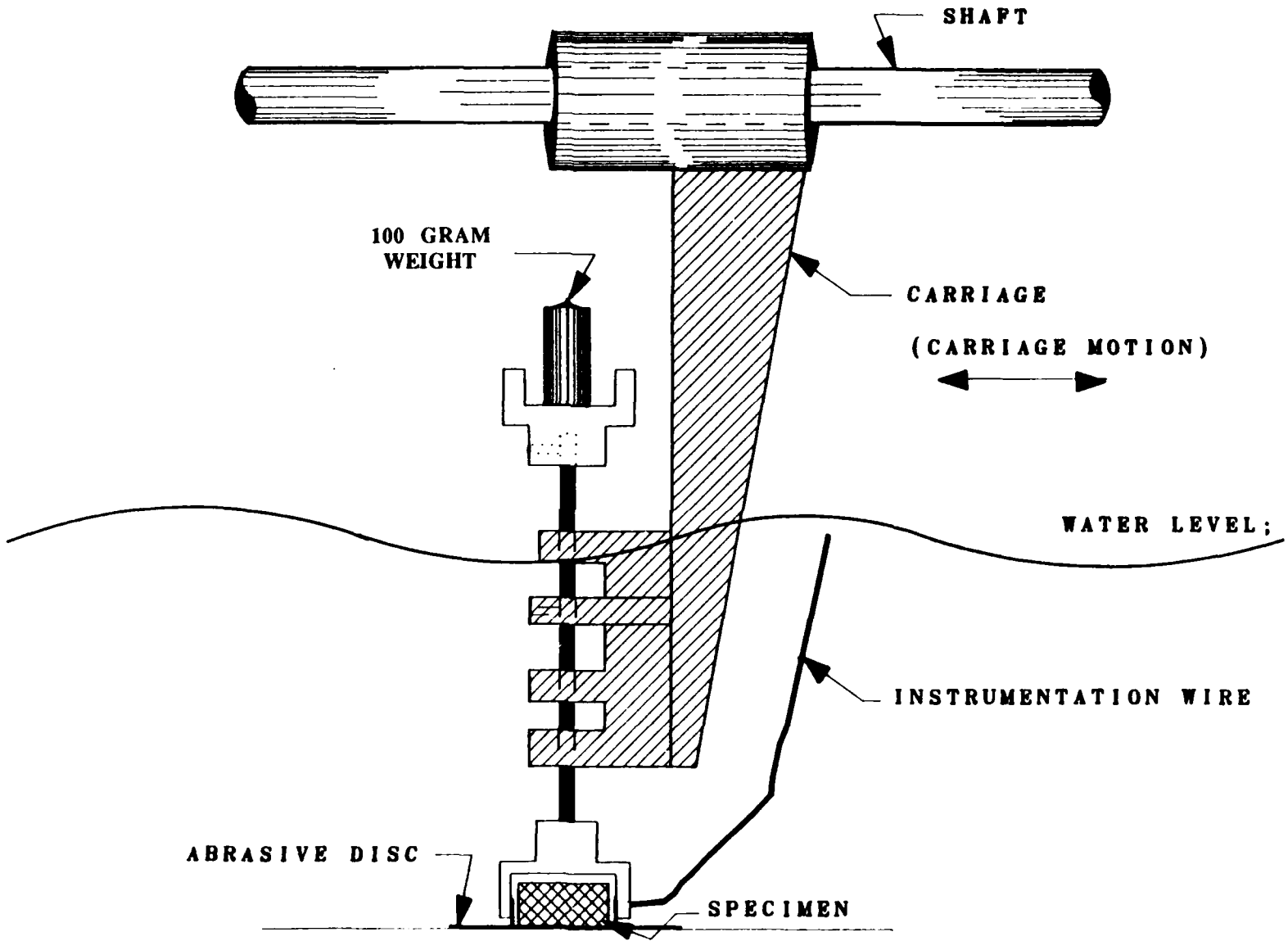

FIGURE 21. CARRIAGE AND SPECIMEN HOLDER APPARATUS: EXPERIMENT A

Each test was allowed to run for a predetermined period of time. During the test, voltage potential readings were recorded at one-half and one hour intervals. A direct voltage potential reading was recorded as well as an offset reading referenced to the calomel electrode. Similar data sheets to the ones used for the undisturbed corrosion tests were used to record the voltage potentials, the weight measurements and any other pertinent data.

The test concluded when the predetermined period of time for the test expired. A last set of voltage readings were recorded and the motor was switched off. The carriage was lifted out of the water and the specimen was removed from the holder. The electrical wire and the screw were removed so that the specimen could be cleaned. The specimen was cleaned by immersion under running warm tap water and all oxide particles were brushed away. The specimen was then sprayed with methanol to drive off the water moisture and allowed to dry. At the end of each test the tank was drained and cleaned prior to the start of another test.

Once the specimen was completely dry, it was weighed to arrive at a post-test weight. Weight measurements were taken by the same procedure that was used for the undisturbed tests. The total material weight loss for the time duration of the test was recorded on the specimen's data sheet.

Initially, corrosive-wear tests were performed using 1022 steel specimens submerged in distilled water and then in seawater. The distilled water tests were conducted so as to isolate the corrosive nature of the seawater and to observe its role in the corrosive-wear mechanism. The results of the distilled water abrasion tests would be compared with that of the seawater tests to determine its contributing role. The 1022 steel specimens were tested for durations of 3, 6, 15 and 24-hour periods in distilled water and for durations of 3, 6, 9, 12, and 24-hour periods in seawater.

Additional corrosive-wear tests were conducted with the two comparison steels and with the heat-treated 1022 steel in seawater. Steel specimens of 1045, heat-treated 1022, and 4140 were tested for durations of 3, 6, 9, 12, and 24-hour periods in the seawater environment. These tests were conducted to compare the wear loss rates and potentials of the three different steel specimens with that obtained in the 1022 tests.

3.3 Corrosive-Wear Tests: Experiment B

The apparatus and procedures used to test the various steels in Experiment B differed from that of Experiment A in several ways. In Experiment A, due to the nature of the apparatus, there were variations in the abraded areas of the specimen's surface. This resulted in the use of a wear coefficient in order to account for differences in abraded surface area. The apparatus in Experiment B was specifically designed to eliminate this problem by producing specimens with uniformly worn surfaces. Voltage potential measurements were not taken in Experiment B since they were determined not to be a valid indication of the corrosive-wear properties of a steel. The elaborate surface preparations used in Experiment A were discontinued since it was found not to be a significant factor affecting the wear rates.

The apparatus used in Experiment B, shown in Figures 22 and 23, consisted of an aluminum base plate, electric motor, drive shaft, bellow seals, linear bearings, shaft bushing guides, and a plastic tank which contained seawater, whetstone, whetstone platform, and specimen carriage. Sketches of the individual components are given in Appendix A.

The design features of the apparatus allowed only for reciprocating motion of the specimen on the whetstone. Linear bearings supported the weight of the drive shaft and also restricted the shaft movements to linear and rotational motions. Horizontal keyways cut into both sides of the drive shaft at each end contained teflon keys which passed through the teflon shaft bushing guides. These restricted rotation of the shaft. The teflon specimen carriage was attached to the shaft by four screws which tightened the carriage around the shaft. A pin passing through the carriage and shaft insured that no motion of the carriage occurred along or about the shaft. The specimen carriage also contained an aluminum key which matched keyways cut into the steel specimens. Movement of the specimen was limited to a vertical motion. The steel spring in the specimen carriage controlled the vertical motion and kept the specimen in contact with the whetstone.

The corrosive-wear testing of the materials commenced with the weighing of the specimens. The Gram-atic balance was zeroed initially and

FIGURE 22. CORROSIVE-WEAR TESTING APPARATUS: EXPERIMENT B

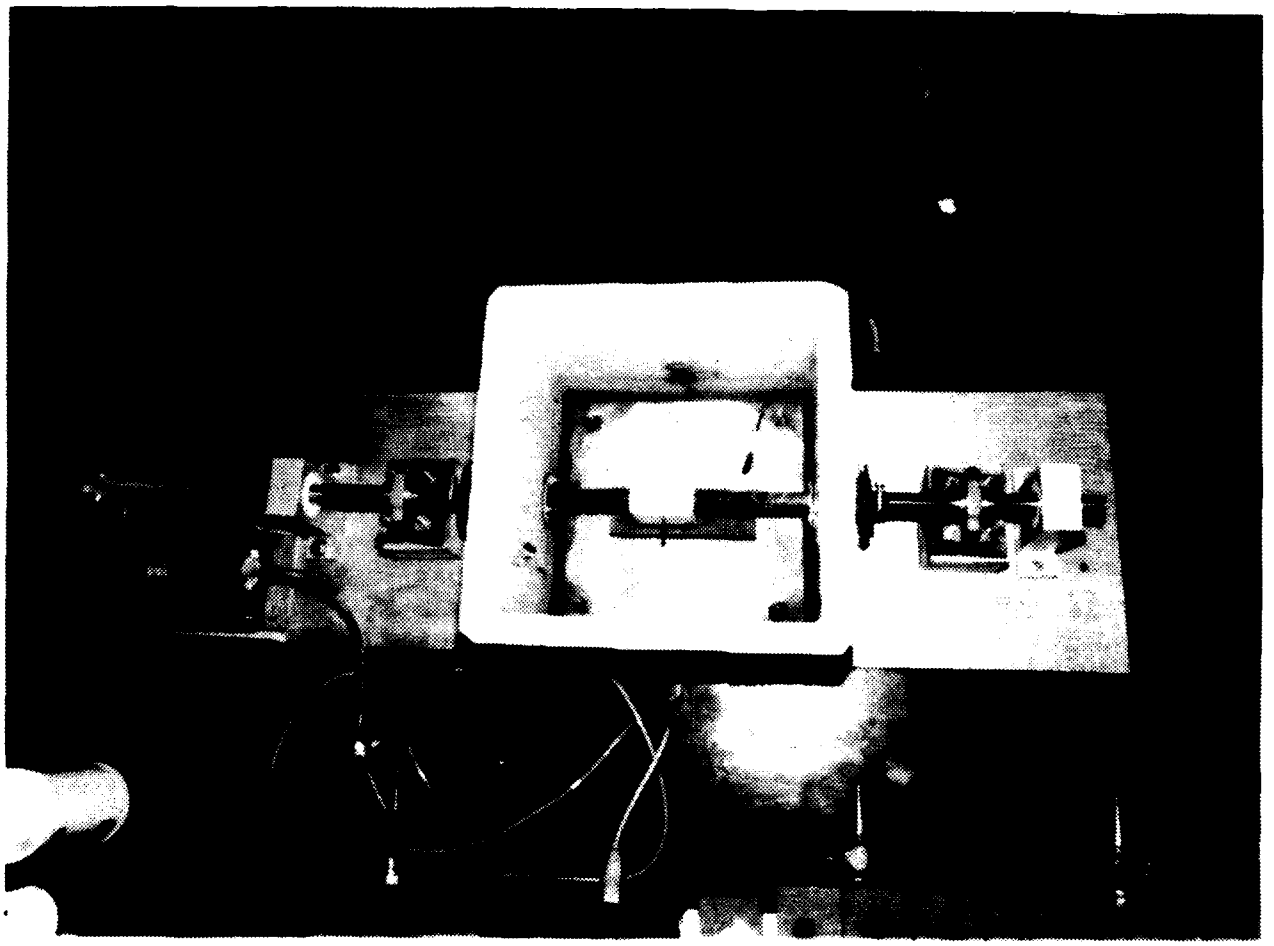

FIGURE 23. CARRIAGE AND SPECIMEN HOLDER: EXPERIMENT B

re-zeroed after two successive measurements. After a total of six measurements were obtained, the masses were averaged yielding the value for the specimen's initial mass.

The spring was placed into the specimen carriage followed by the steel specimen. A fresh whetstone was then placed on top of the whetstone platform. The carriage was placed in position and the set pin inserted. The plastic tank was filled with seawater to a level just below the drive shaft. The seawater was obtained from the Narragansett Bay and had a pH of approximately 8.3.

Testing of the steels was conducted for periods of 3, 6, 9, 12, and 24 hours. A new specimen and whetstone were used for each run. After each 24 hours of successive testing, the seawater was drained from the tank, the tank was flushed out, and then refilled.

Following each run, the specimens were removed from the carriage. The specimens were washed with tap water, then sprayed with methanol. Following a drying period of approximately thirty minutes, the specimens were re-weighed using the same procedure a previously described. After the final masses were recorded, the amount of material removed from the specimens was obtained by subtracting the initial from final masses. The material loss from each specimen was then plotted as a function of time for each steel.

3.4 Microstructure Analysis

To observe the microstructure of an abraded surface of a particlular steel specimen, electron microscopy was utilized. This allowed for a detailed analysis of how the corrosive-wear mechansim affected each grade steel specimen. The type scanning electron microscope (SEM) used was a Cambridge Stereoscan model S4.

The SEM was used to observe the microstructure of all four materials in Experiment A subjected to the corrosive-wear mechanism, including the 1022, heat-treated 1022, 1045, and 4140 steels. Polaroid Type 55 land film was used to photograph specific surfaces observed.

4.0 RESULTS AND DISCUSSION

4.1 Undisturbed Corrosion Tests

The results of the undisturbed corrosion tests are graphically illustrated by the potential plots shown in Figures 24 through 30. The plots show the potential of each material tested immersed in distilled water or seawater as a function of time. Data points for the plots were obtained from each material's individual data sheet. An exponential function was used to obtain a best fit curve through the data points.

As is evident by the potential plots, the materials tested in distilled water (1022, 1045, and 4140) had increased potentials when tested in seawater. The 1022 steel had an increased potential of 40 mV whereas both the 1045 and 4140 increased in potential by approximately 90 mV. This is an expected result since the seawater is a more corrosive environment then the distilled water due to the high chloride ion content.

The 4140 steel obtained the lowest potential (620 mV) in distilled water. The 1045 steel at 658 mV was only slightly higher than that of the 1022 steel at 650 mV.

In seawater, the heat-treated 1022 steel and the 1045 steel reached the highest potential at 745 mV. The 4140 steel was considerably less at 707 mV and the 1022 was even lower at 690 mV.

The heat-treated 1022 steel would be expected to reach a high potential due to the reformation of the grain boundaries in producing the martensitic microstructure during heat-treatment. The 1045 steel would also be expected to reach a higher potential due to the increased carbon content over the 1022 steel. The 4140 steel, although similar in carbon content to the 1045 steel, reached a potential much lower than the 1045. This can be attributed to the additions of chromium and molybdenum in the 4140 steel which are instrumental in producing a more corrosion-resistant material.

Table III displays the results obtained for the material weight losses during the undisturbed corrosion tests.

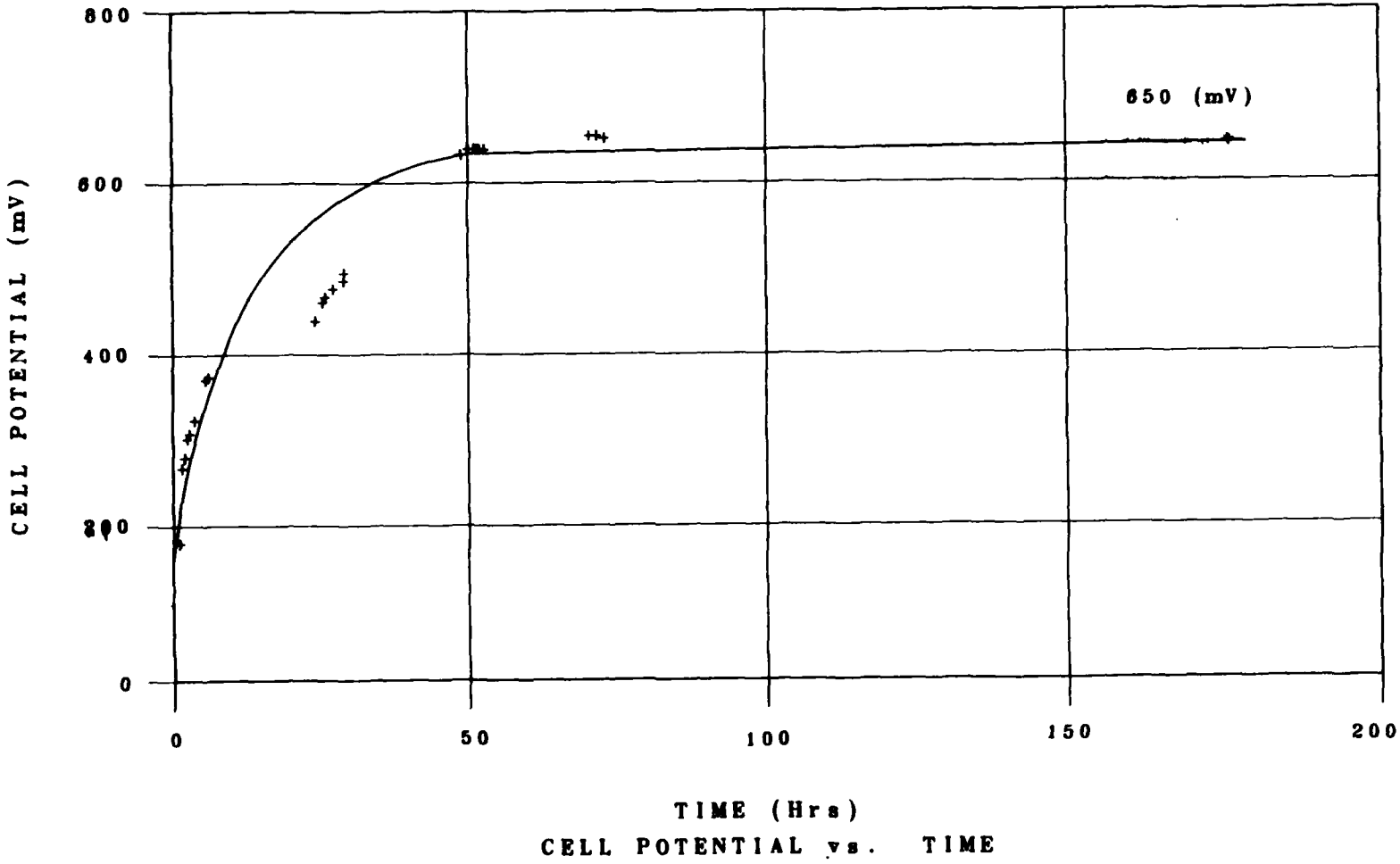

FIGURE 24. CG 1022 UNDISTURBED CORROSION IN DISTILLED WATER

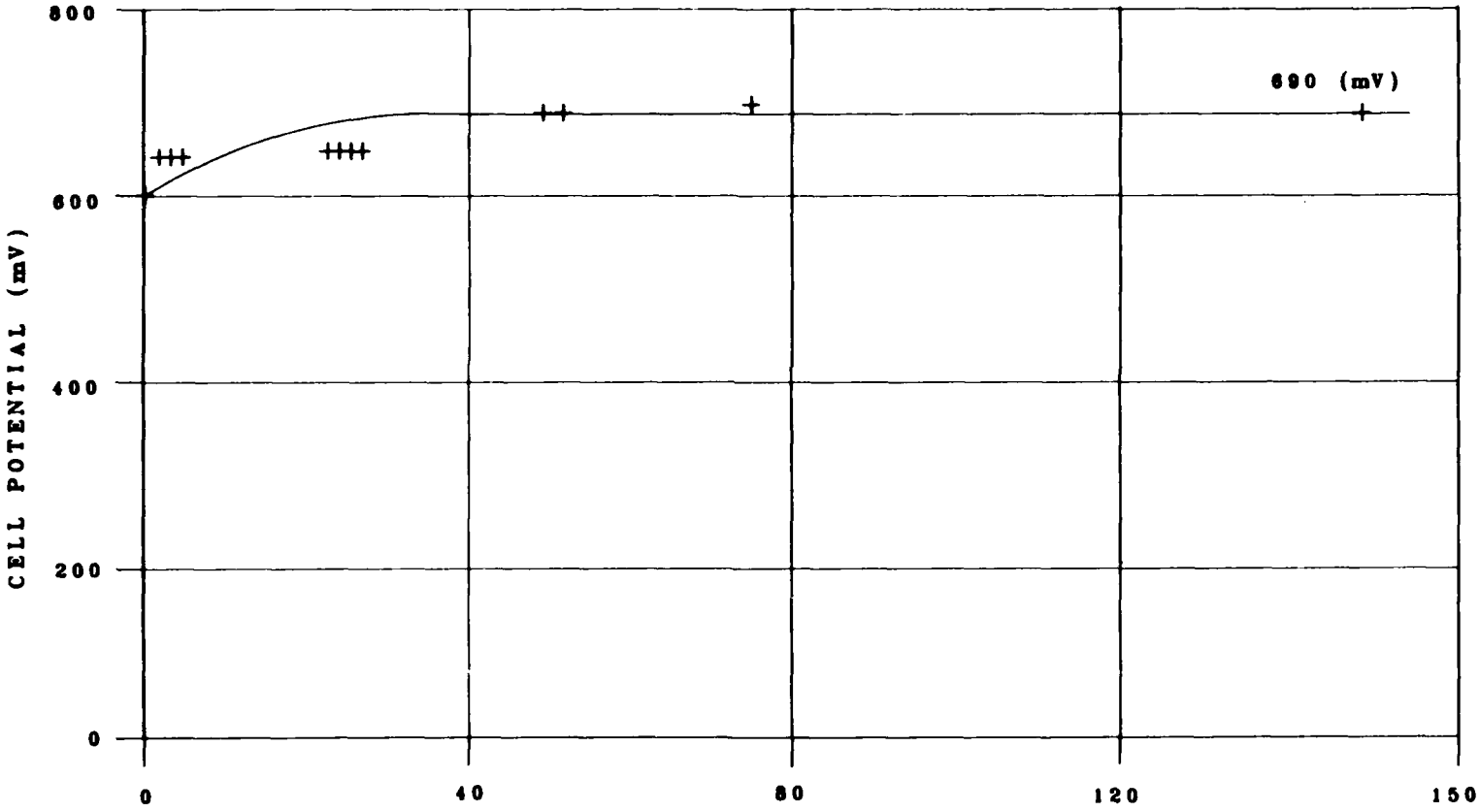

FIGURE 25. CG 1022 UNDISTURBED CORROSION IN SEAWATER

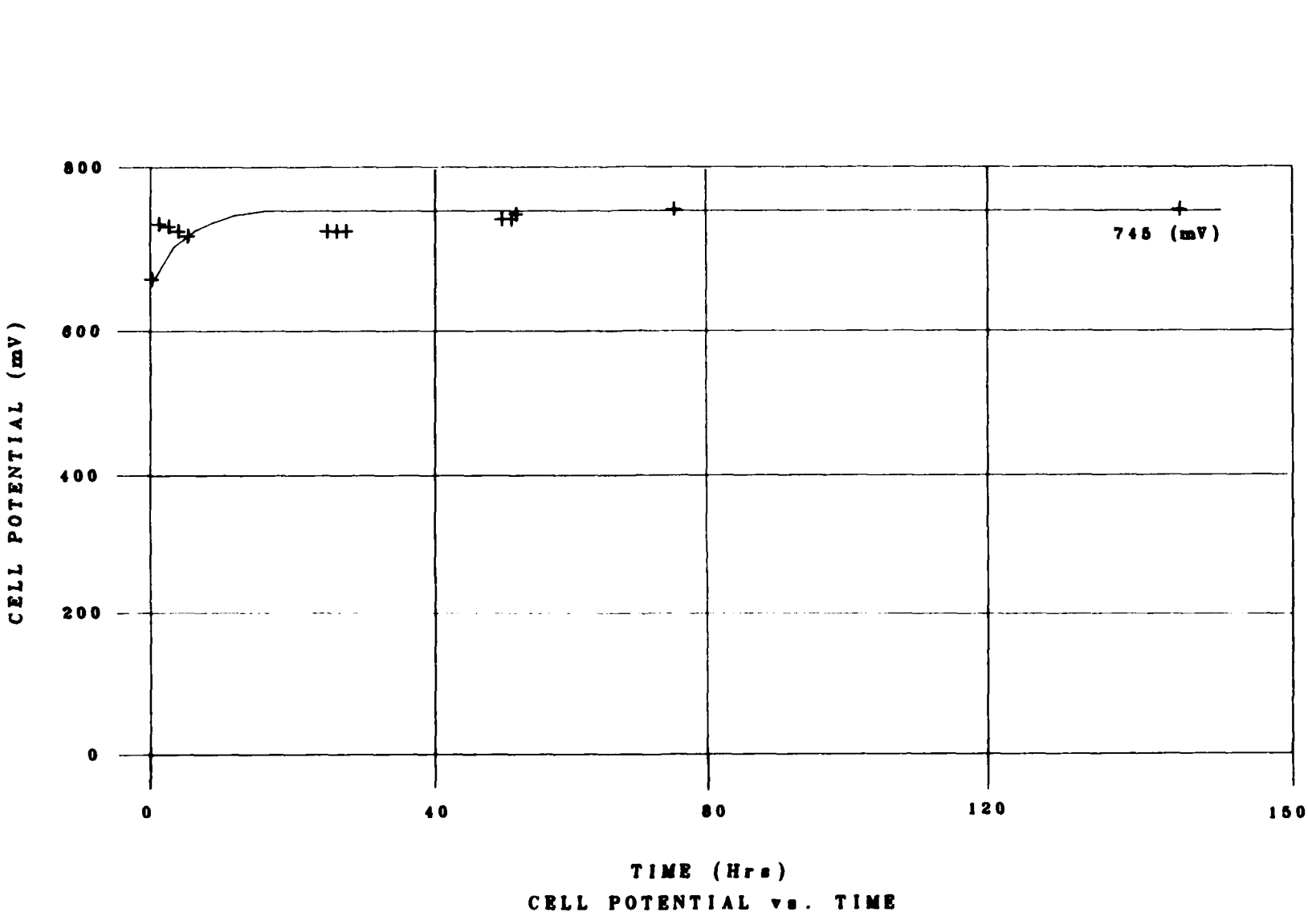

FIGURE 26. CG 1022 (HEAT-TREATED) UNDISTURBED CORROSION IN SEAWATER

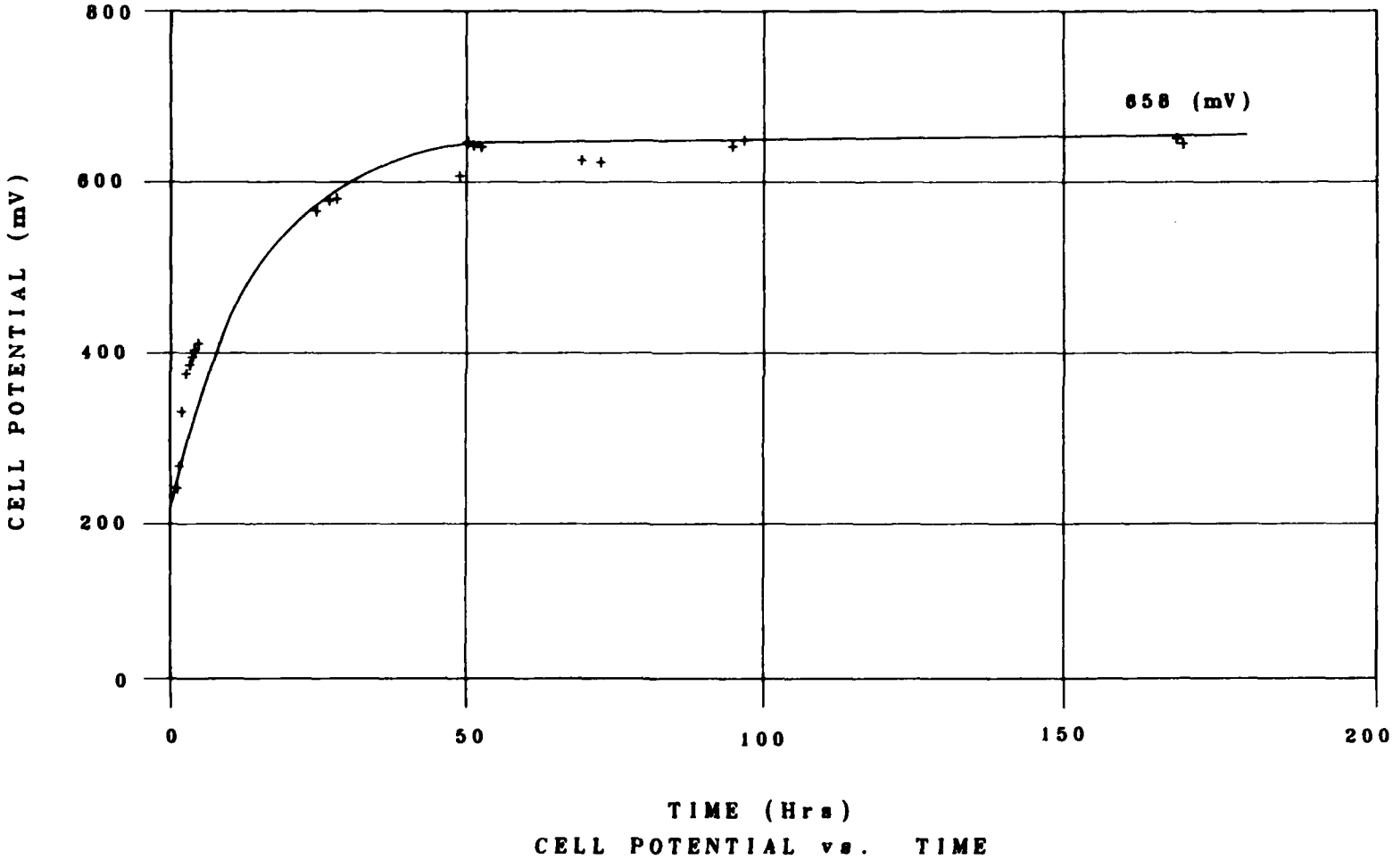

FIGURE 27. CG RYERSON 1045 UNDISTURBED CORROSION IN DISTILLED WATER

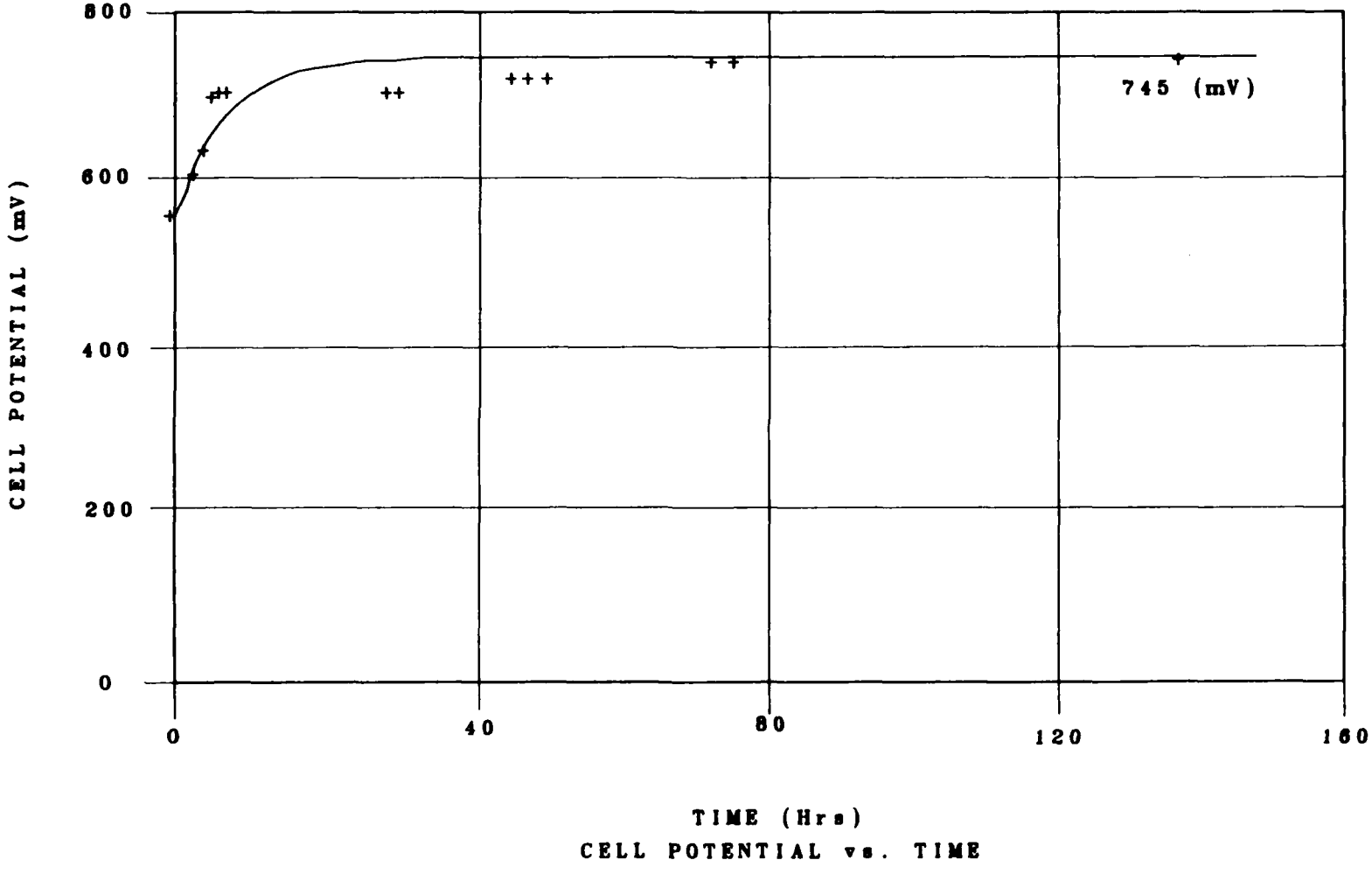

FIGURE 28. RYERSON 1045 UNDISTURBED CORROSION IN SEAWATER

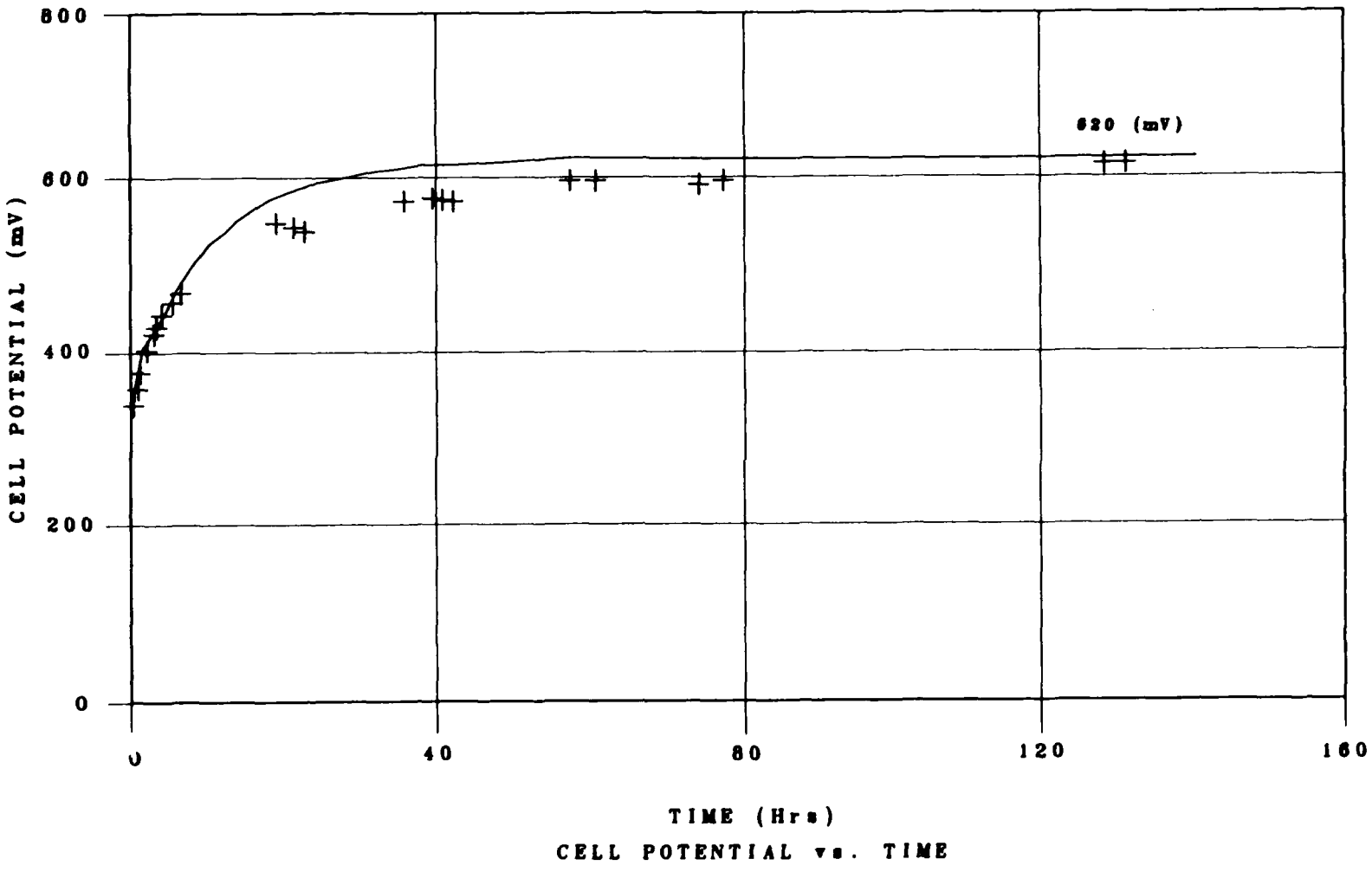

FIGURE 29. RYERSON 4140 UNDISTURBED CORROSION IN DISTILLED WATER

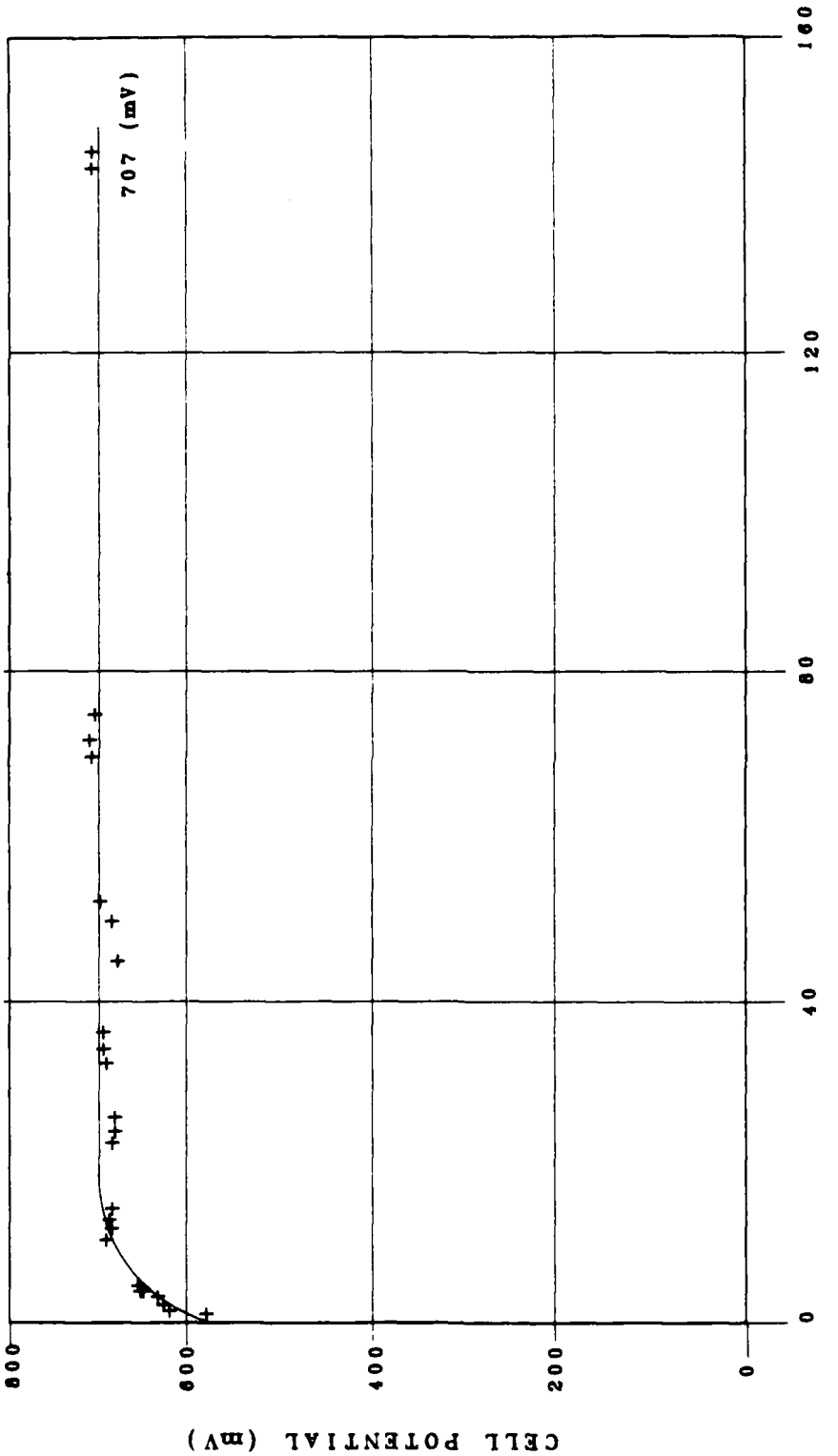

FIGURE 30. RYERSON 4140 UNDISTURBED CORROSION IN SEAWATER

TABLE III

UNDISTURBED CORROSION TEST MATERIAL LOSSES

MATERIAL	ENVIRONMENT TYPE	MATERIAL LOSS	CELL POTENTIAL
1022	Distilled Water	11.3 g/hr*	650 mV
1022	Seawater	14.6	690
1045	Distilled Water	13.9	658
1045	Seawater	15.3	745
4140	Distilled Water	14.7	620
4140	Seawater	14.2	707
1022HT	Seawater	16.4	745

*($\times 10^{-5}$)

HT: Heat-treated at 1650 deg. F for 30 min. and water quenched.

For the 1022 steel, the amount of material lost in the seawater was substantially higher than that lost in the distilled water, which would be expected. Approximately twenty-nine percent more material was lost on an hourly basis in the seawater environment. Figure 31 illustrates the distilled water and seawater environment comparison projected over a twenty-four hour period on a loss/area basis.

As with the 1022 steel, the 1045 steel also experienced a higher loss per hour rate in the seawater environment. The increase at ten percent was not nearly as high as the 1022 steel.

The 4140 steel had essentially similar material loss rates for both environments. Although the distilled water rate is slightly higher than the seawater rate, a difference of only (.5) is not relatively significant as compared to the differences obtained in the 1045 and 1022 steels.

The 1045 and 4140 steels both experienced higher material loss rates than the 1022 steel in both the distilled water and the seawater environments. A heat-treated 1022 specimen was tested in the seawater environment in order to compare it to the original 1022 steel. The material loss rate for this heat-treated steel was higher then that of the original 1022 steel in seawater as well as the 1045 and 4140 steels in seawater.

By examining the undisturbed-corrosion results, a relationship between cell potential and material loss was observed. Higher cell potentials, which indicate higher oxidation rates, would result in a higher material loss as observed. There are several factors which determine oxidation rate such as material composition and microstructure which must be investigated furthur to determine the extent of their influence.

4.2 Corrosive-Wear Tests: Experiment A

The corrosive-wear tests produced results in two specific areas. First, the testing of the 1022 steel in distilled water and seawater provided insight into what extent the medium affects the corrosive-wear process. Secondly, the corrosive-wear testing on the 1045, 4140, and heat-treated 1022

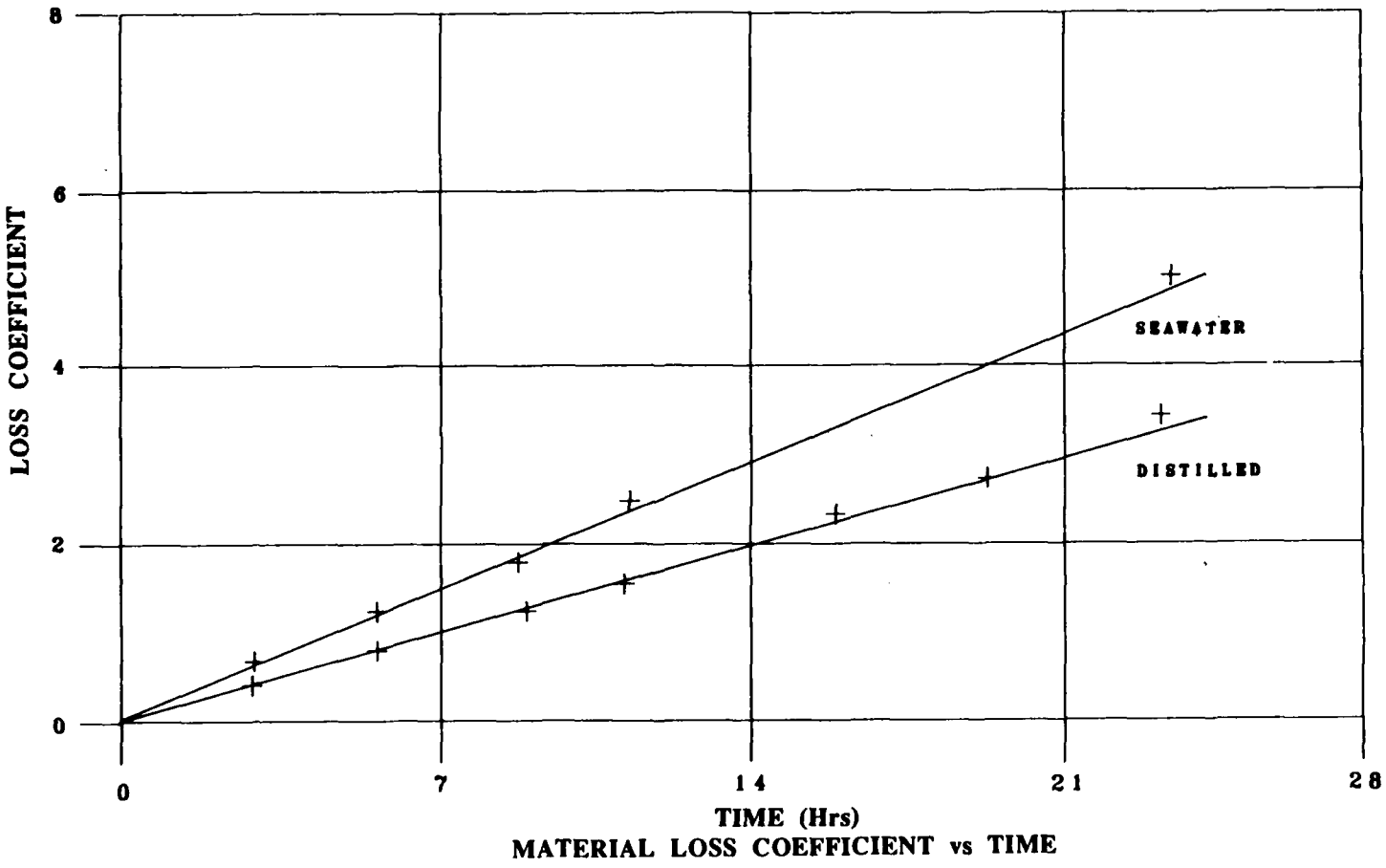

FIGURE 31. UNDISTURBED CORROSION OF CG 1022 SEAWATER VS DISTILLED WATER

steels provided a basis for comparing them with the presently used 1022 steel in order to determine which materials display the best performance when subjected to conditions of corrosive-wear.

In Figure 32, the corrosive-wear cell potential plot of the 1022 steel in distilled water over a twenty-four hour period is given. In Figures 33 through 36, the corrosive-wear cell potential plots of the 1022, 1045, 4140, and heat-treated 1022 steels in seawater are given over a twenty-four hour period. As with the other cell potential plots described previously, the HP9816 graphics computer and HP9872A plotter were used to generate the graphs with an exponential function utilized to provide a best fit curve through the data points.

As evident in the plots of the corrosive-wear tests, a stabilized potential was reached at a much faster rate than in the undisturbed corrosion tests. This results in a relatively flat curve compared to the curves of the undisturbed corrosion tests.

The corrosive-wear test of the 1022 steel in distilled water reached a much lower potential than the potential it had reached in the undisturbed corrosion test in distilled water. A potential drop on nearly 100 mV (650 mV for undisturbed compared to 551 mV for corrosive-wear) was obtained. The seawater corrosive-wear test resulted in a likewise decrease in potential than the undisturbed corrosion test in seawater; however, only a 20 mV difference (690 mV for undisturbed compared to 670 mV for corrosive-wear) was obtained between these two tests.

The three comparative steels also obtained lower potentials in the corrosive-wear tests than in the undisturbed tests. The 4140 steel obtained a drop of 87 mV whereas the 1045 steel and the heat-treated 1022 steel each decreased by 125 mV. Thus, the potentials obtained by all four materials in the seawater corrosive-wear tests were less than what was obtained with the same four materials in the undisturbed corrosion tests in seawater. This lowering of the potential is apparently due to the wear process. It has been shown that decreasing potential during combined wear and corrosion was indicative of an increasing weight loss of a material [9]. As the specimen is

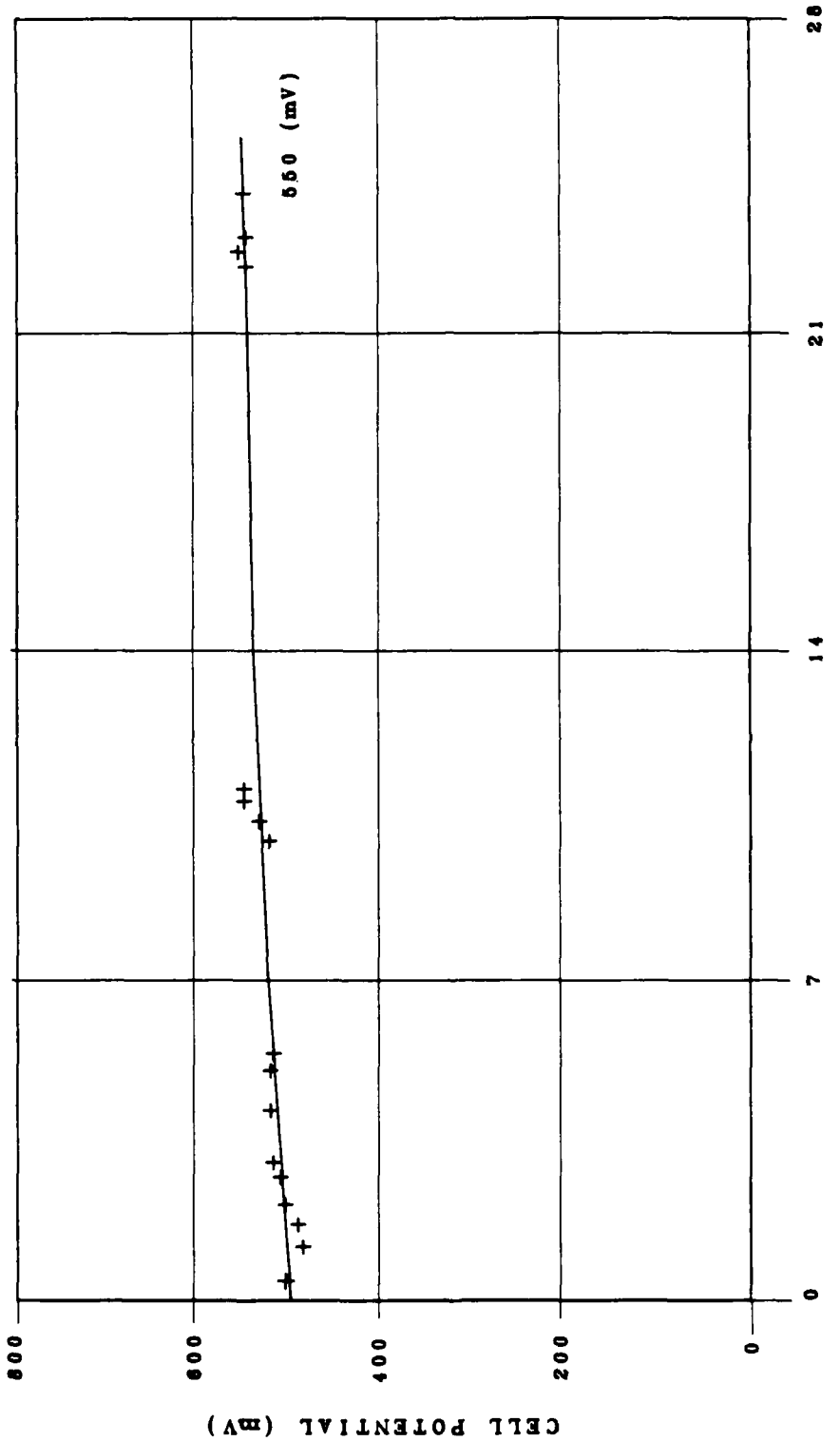

CELL POTENTIAL vs. TIME

FIGURE 32. CG 1022 CORROSIVE-WEAR IN DISTILLED WATER

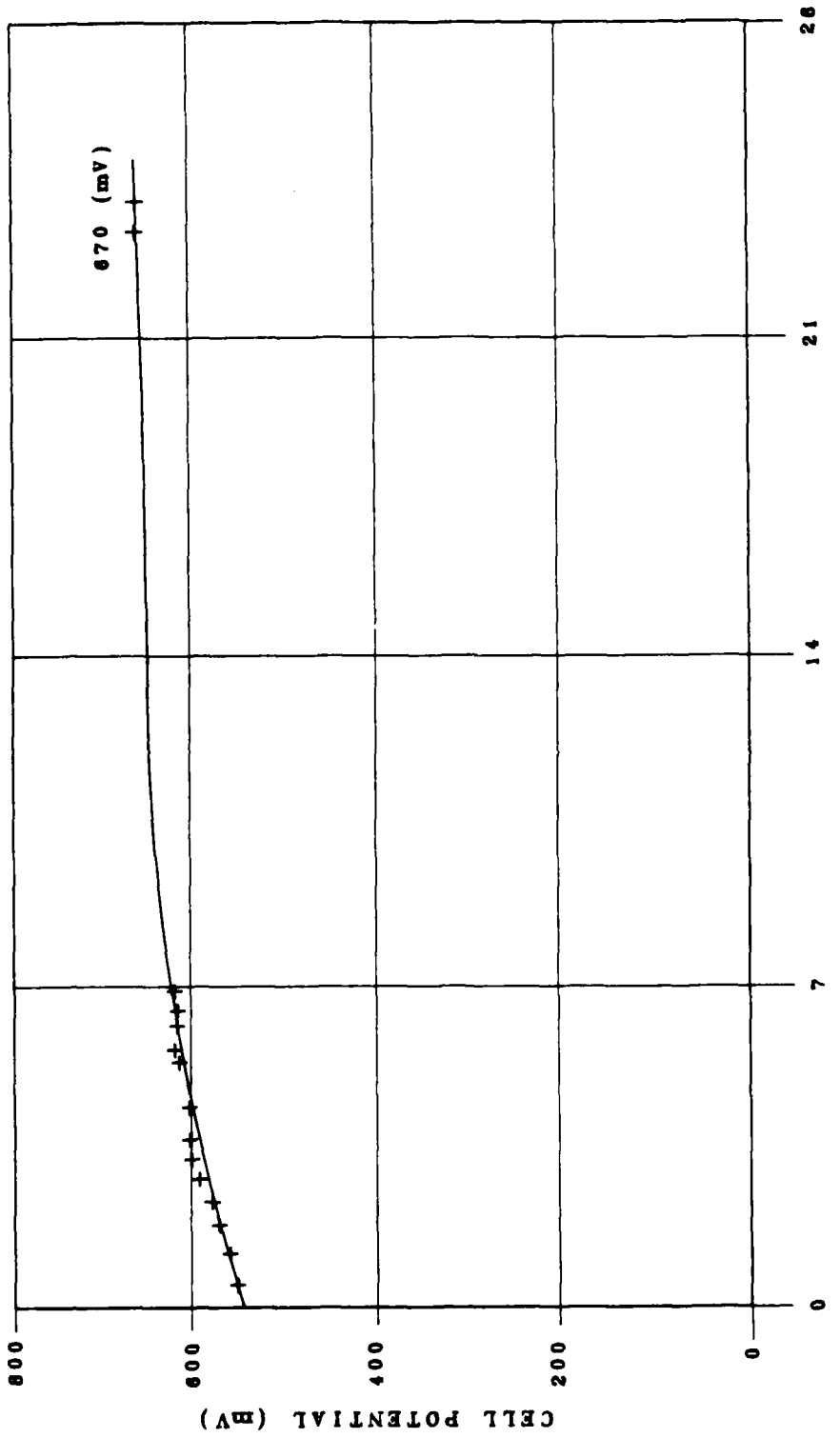

CELL POTENTIAL vs. TIME

FIGURE 33. CG 1022 CORROSIVE-WEAR IN SEAWATER

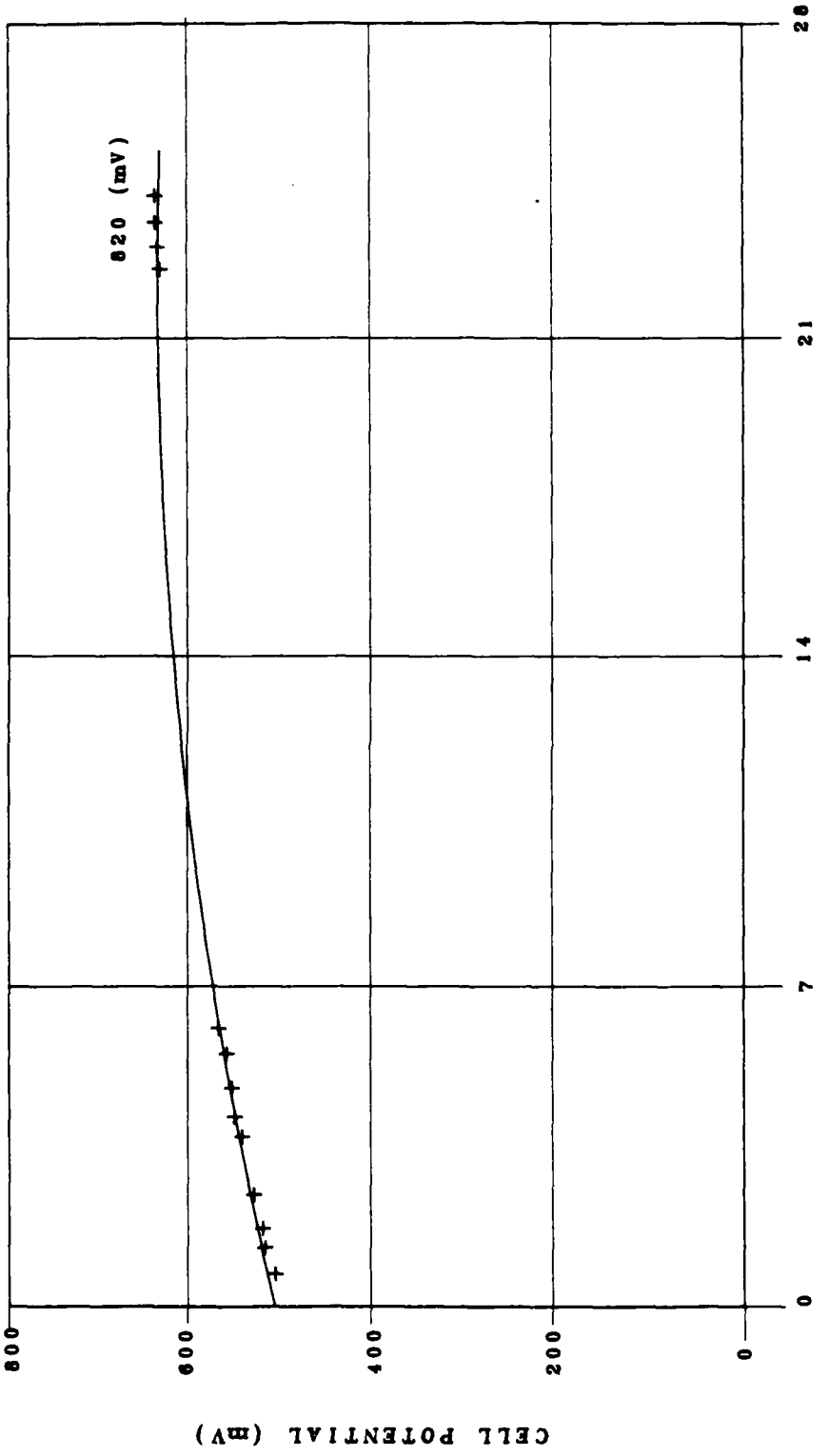

CELL POTENTIAL vs. TIME

FIGURE 34. RYERSON 1045 CORROSIVE-WEAR IN SEAWATER

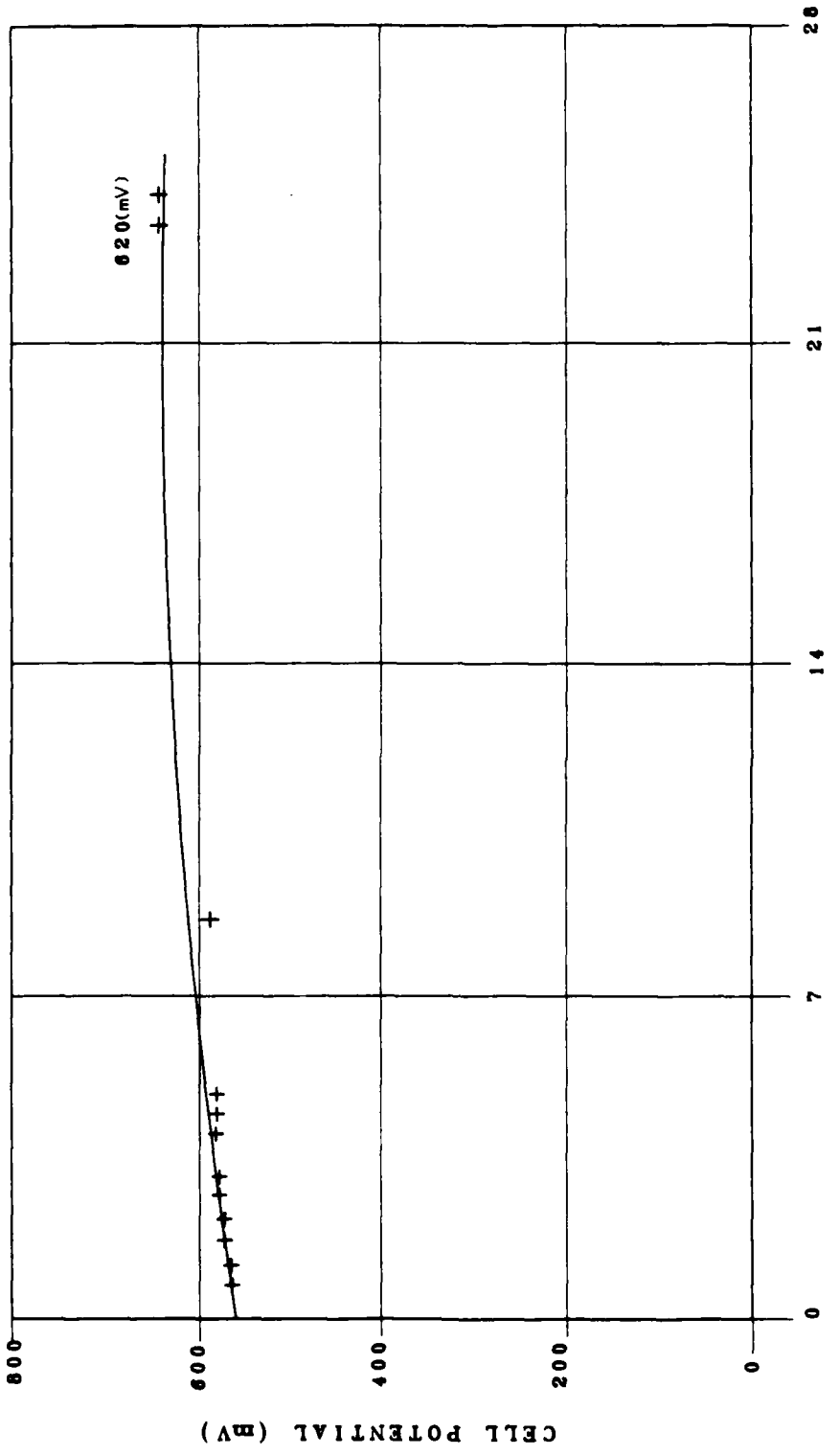

FIGURE 35. RYERSON 4140 CORROSIVE-WEAR IN SEAWATER

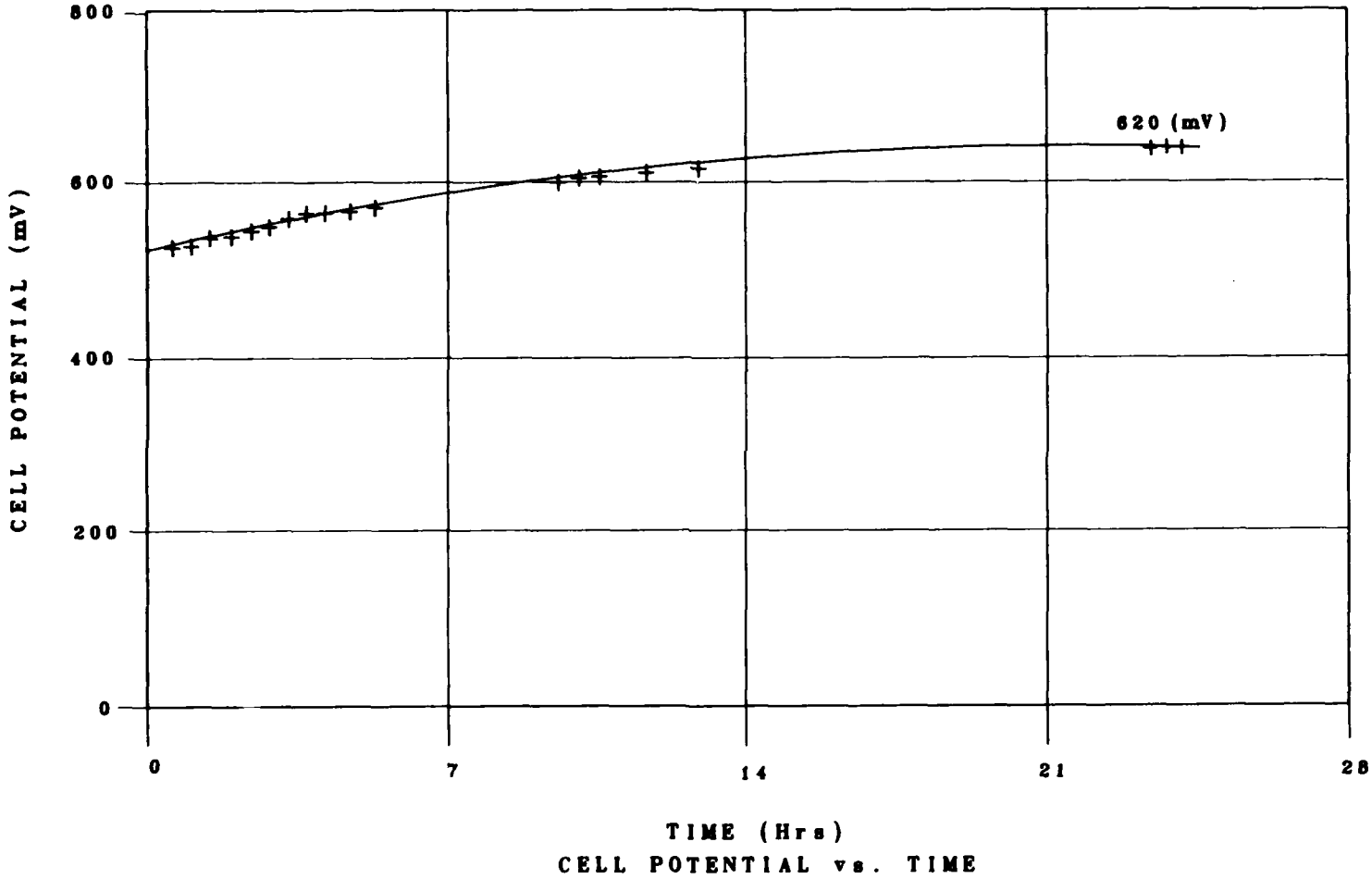

FIGURE 36. CG 1022 (HEAT-TREATED) CORROSIVE-WEAR IN SEAWATER

moved across the abrasive any stabilized film on the surface of the specimen is removed and fresh metal is exposed. Thus, the process of forming a new film layer begins once again.

In comparing the three alternative materials (the 1045, 4140, and heat-treated 1022 steels) to the original 1022 steel, they all obtain similar type plots although they all reached lower potentials than the 1022 steel. Also, the potential plots of the 1045, 4140, and heat-treated 1022 steels are all similar to each other in that they all stabilize at a potential of approximately 620 mV.

Tables IV and V provide the material loss data of each specimen during its specified test duration time. Because each specimen contacted the abrasive surface in a slightly different manner, the amount of pressure applied to the abraded surface of the specimen varied during each specimen test. The applied pressure (P) on the abraded surface can be calculated using the equation:

$$P\ (\text{dynes/cm}^2) = \textit{Applied Load / Abraded Surface Area}$$

Since the applied load was constant (98,100 dynes) for all the specimens, the applied pressure was only dependent on the abraded surface area. This necessitated the measurement of the amount of area abraded on each specimen at the conclusion of its test. In order to make direct comparisons between steels, a loss coefficient (L) was developed based on the expression:

$$L\ (\text{g/cm}^2) = \text{Mass Loss (g) / Abraded Surface Area}$$

In Figures 37 through 41, the material loss coefficients are plotted as a function of time for each steel tested. The graphs were generated in the same manner as previous graphs; however, a power function polynomial was used to obtain the best fit curve through the data points.

Of particular importance is the shape of the curves for each material. There appears to be an incubation period which is characterized by a rapid increase in the material loss coefficent. This phenomena is usually

TABLE IV

MATERIAL LOSS COEFFICIENTS IN DISTILLED WATER

MATERIAL	TIME (HRS)	MASS LOSS	AREA ABRADED	LOSS COEFFICIENT	
1022	3	.02527 g	1.40 cm2	1.800 g/cm2	$x10^{-2}$
1022	6	.04342	1.89	2.303	
1022	15	.07650	2.08	3.682	
1022	24	.03249	0.84	3.882	

TABLE V

MATERIAL LOSS COEFFICIENTS IN SEAWATER

MATERIAL	TIME (HRS)	MASS LOSS	AREA ABRADED	LOSS COEFFICIENT
1022	3	.02435 g	1.65 cm2	1.476 g/cm2 $x10^{-2}$
1022	6	.03044	1.36	2.239
1022	9	.03783	1.12	3.384
1022	12	.04067	1.38	2.945
1022	24	.06455	1.12	5.771
1022HT	3	.01813	2.03	0.892
1022HT	6	.03075	2.18	1.411
1022HT	9	.03613	1.49	2.426
1022HT	12	.03850	1.69	2.278
1022HT	24	.09840	5.58	1.763
1045	3	.01863	2.19	0.853
1045	6	.01778	0.95	1.875
1045	9	.01976	0.76	2.614
1045	12	.02964	0.76	3.921
1045	24	.07043	1.01	6.942
4140	3	.02975	2.43	1.226
4140	6	.02094	3.07	0.683
4140	9	.04040	2.83	1.428
4140	12	.04998	4.61	1.085
4140	24	.07323	5.86	1.250

HT: Heat-treated at 1650 deg. F for 30 min. and water quenched.

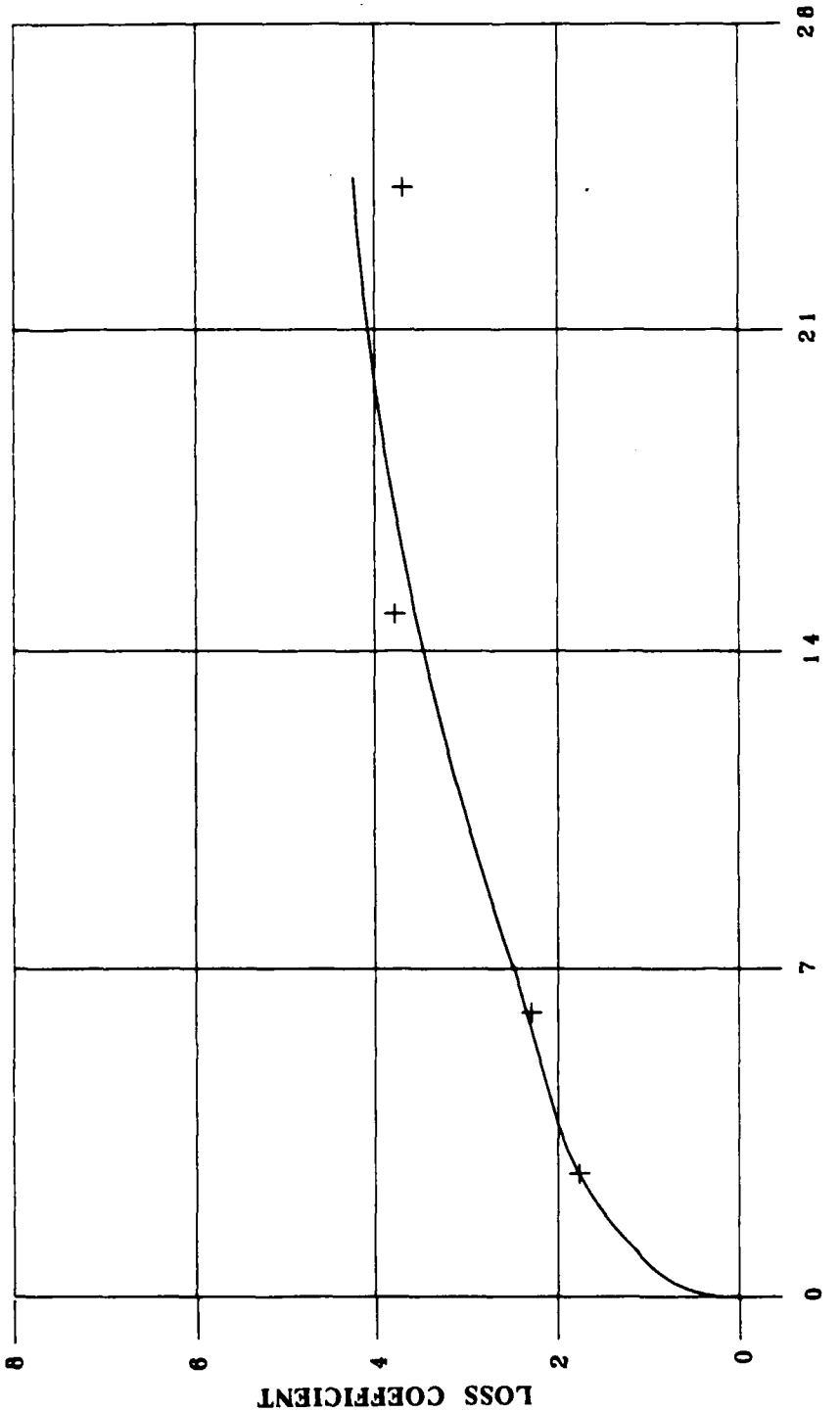

FIGURE 37. CG 1022 (HEAT-TREATED) CORROSIVE-WEAR IN DISTILLED WATER

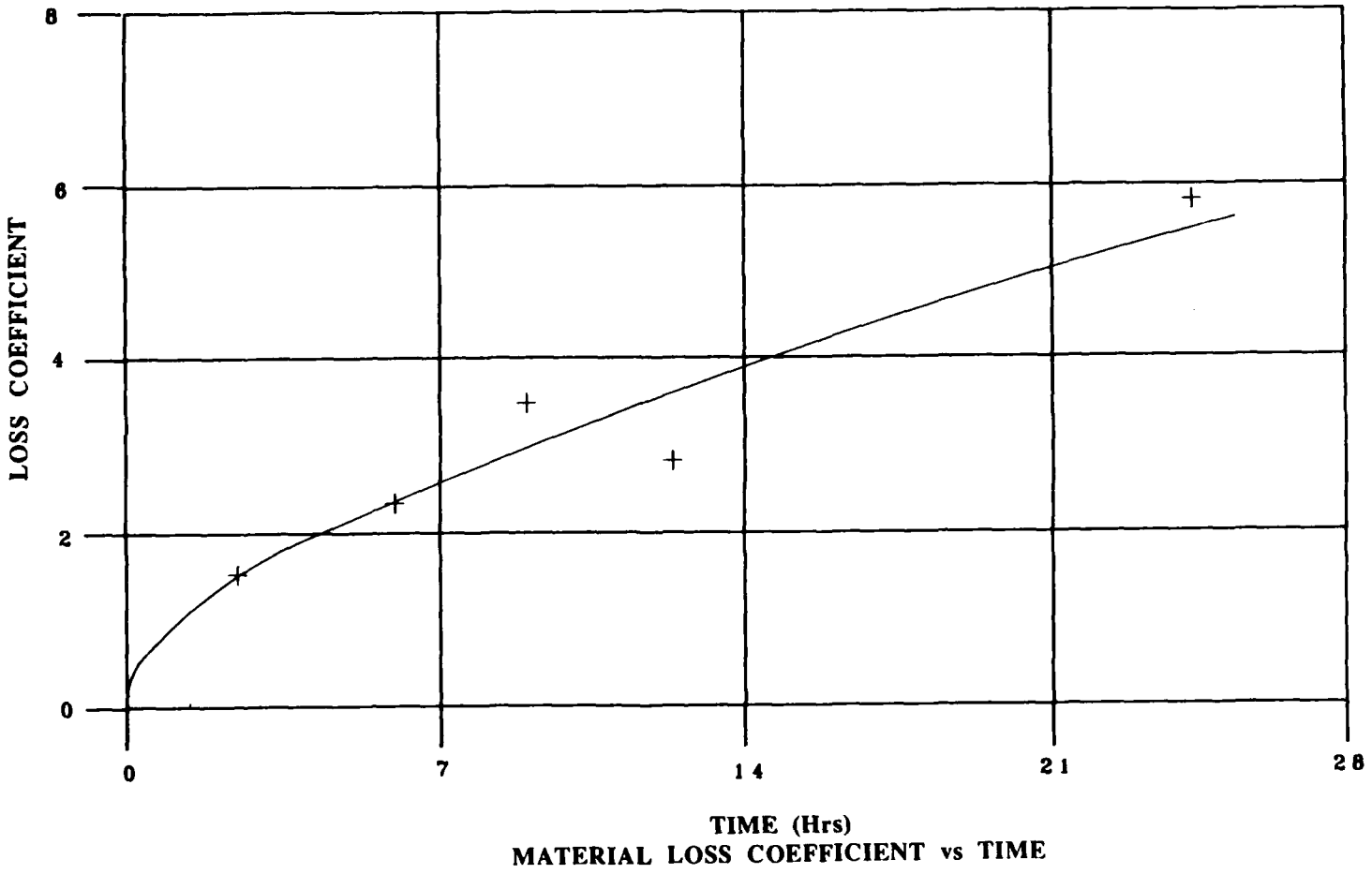

FIGURE 38. CG 1022 CORROSIVE-WEAR IN SEAWATER

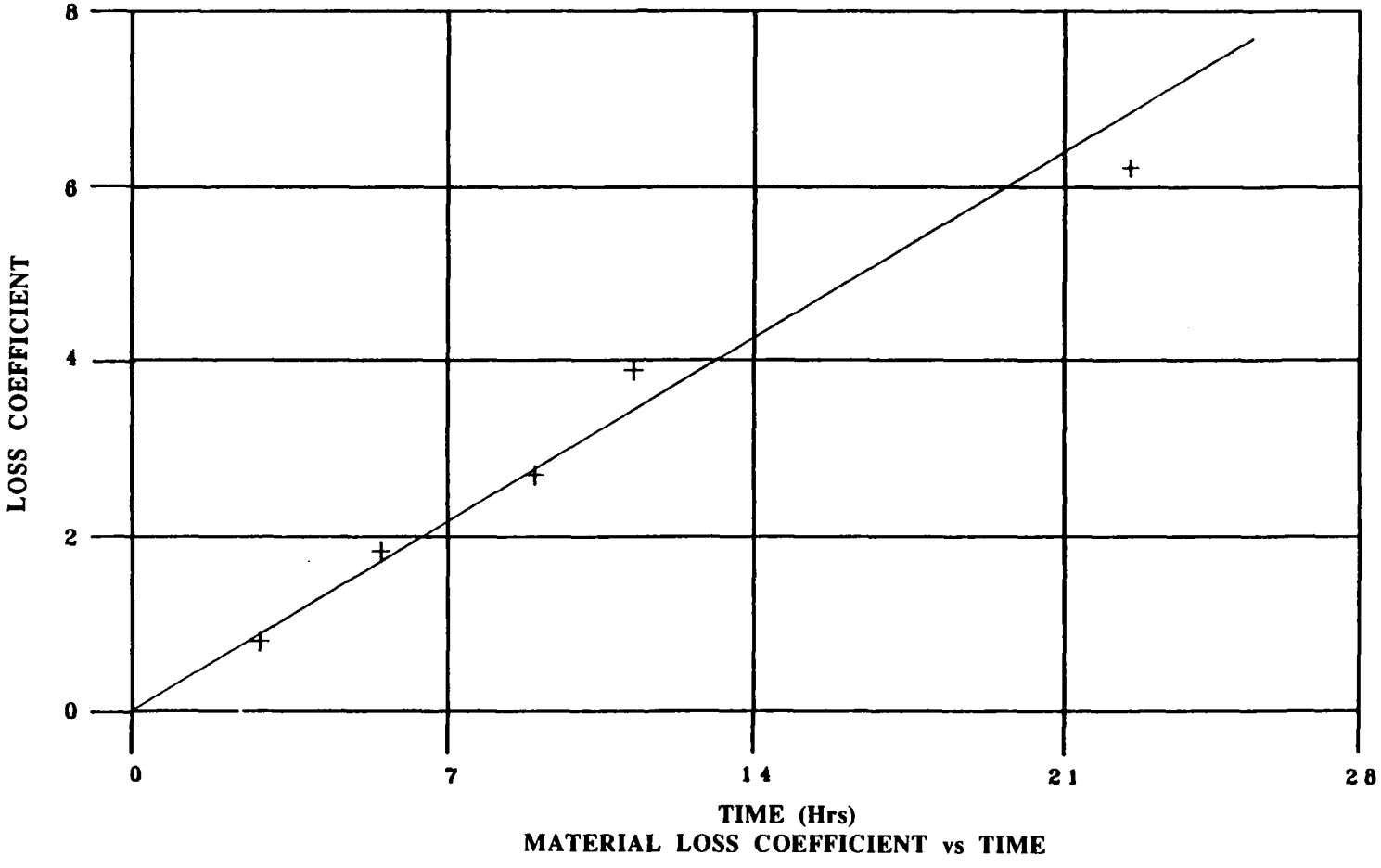

FIGURE 39. RYERSON 1045 CORROSIVE-WEAR IN SEAWATER

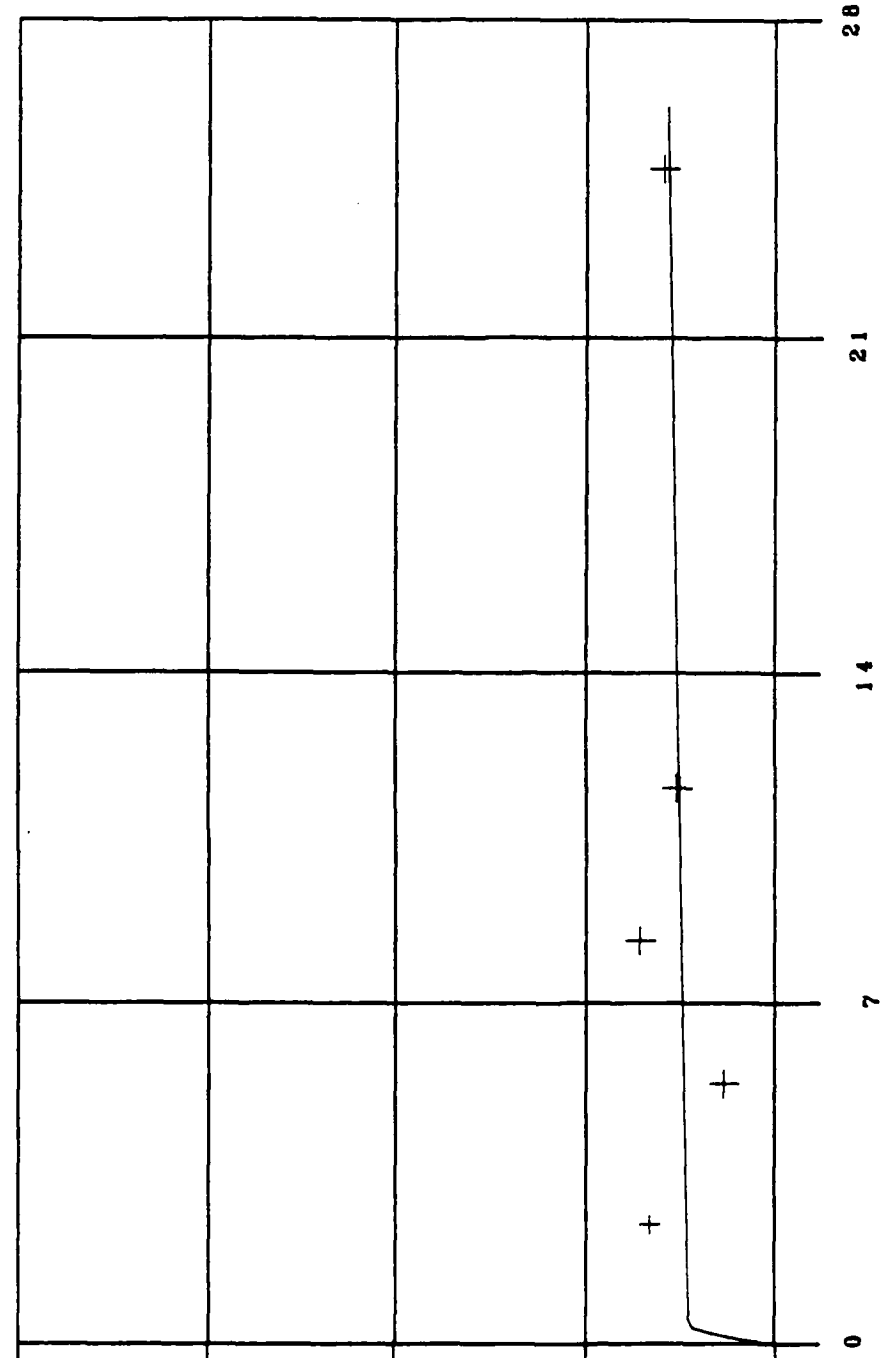

FIGURE 40. RYERSON 4140 CORROSIVE-WEAR IN SEAWATER

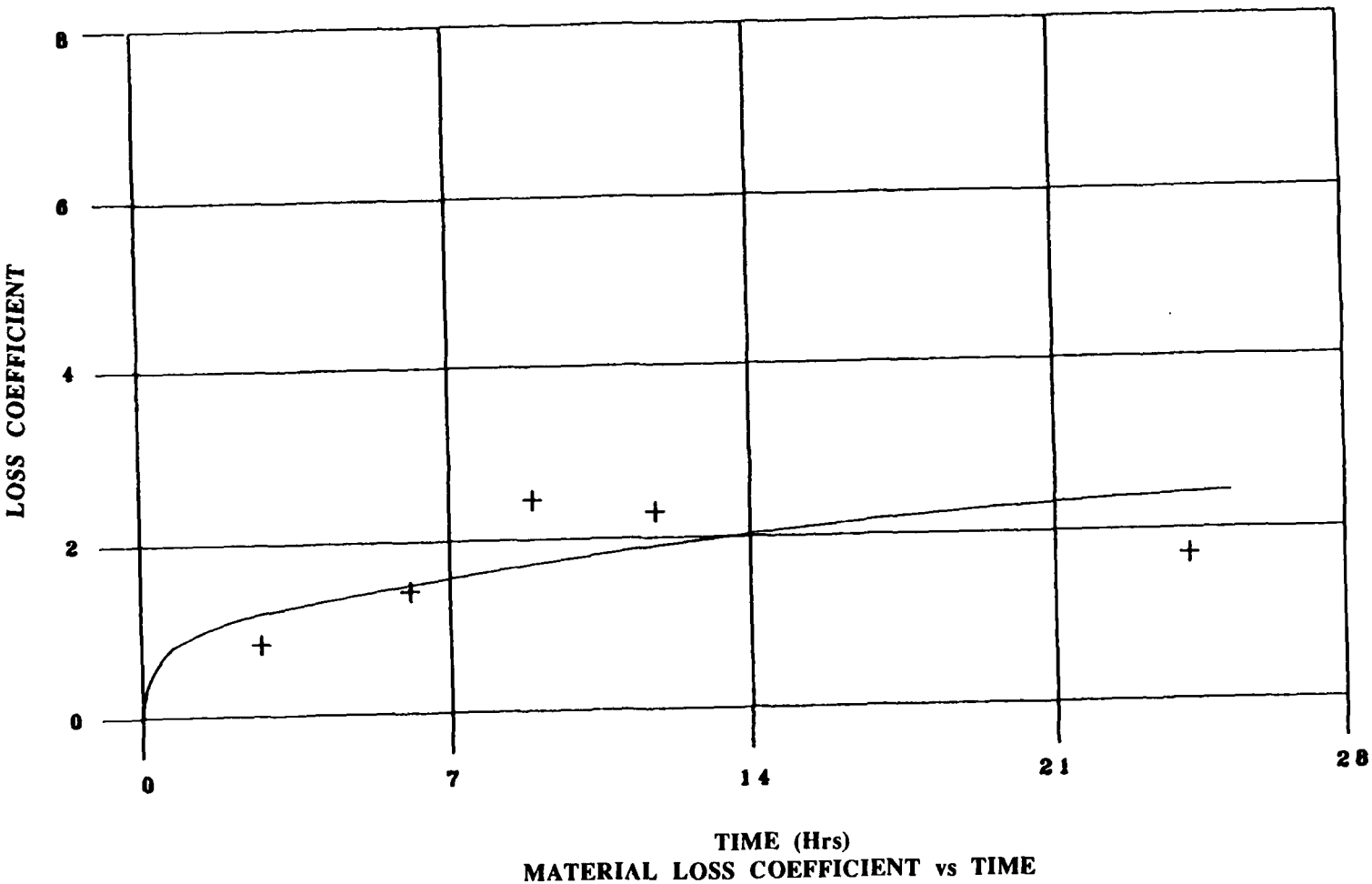

FIGURE 41. CG 1022 (HEAT-TREATED) CORROSIVE-WEAR IN SEAWATER

characteristic of a wear process due to the abrasive cutting grooves into the material being abraded. Following the incubation stage is a steady state region. During this phase the surface of the specimen undergoes consistent wear due to the reduction of asperities on the abrasive thus eliminating groove cutting on the abraded surface. Wear can occur through delamination of the subsurface [10]. It is this region that characterizes the wear which occurs most often on a metal surface.

The plots of material loss coefficients versus time of the four materials provide the most significant results. Each plot provides an indication of that material's rate of loss of material when subjected to the corrosive-wear process. Although actual slope values are given for each curve, they are only indications as to the general steepness of the curves in the steady-state wear region. Materials with higher slopes would indicate higher corrosive-wear rates occuring on the surface. Therefore, materials with smaller slopes would suggest a material of better performance and thus better suited for use in the corrosive-wear process, such as experienced by buoy chains.

The material loss coefficient plots of the 1022 steel in distilled water and in seawater (Figures 37 and 38) are quite similar in form. The distilled water test was of lower profile than the seawater test and begins a slight decline indicating a leveling off in the rate of loss of material in the process. This was not observed in the seawater test. The lower profile and the leveling off observed in the distilled water test resulted in a curve with a slope of less than that seen in the seawater test curve.

The greater rate of loss of material in the seawater environment confirms what is expected by theory and what has been experienced in actual practice. Due to the corrosive nature of the seawater, it would be expected to result in higher loss of material, thus, higher material loss coefficients. Reports from Coast Guard buoy maintenance crews have reported similar effects. It appears that chain on buoys moored in rivers or in brackish water do not suffer the severe loss of material that chain moorings of ocean seawater buoys do.

Comparing the slopes obtained from the material loss coefficient curves shows that the 4140 performed the best when exposed to corrosive-wear. This exceeded the performance of the presently used 1022 steel, as did the heat-treated 1022. Both these steels displayed the incubation and steady-state wear periods. The 1045 steel did not show an incubation period; however, steady-state wear occured continuously at a higher rate than the 1022 steel.

It is interesting to note the order of magnitude of the material losses obtained in the corrosive-wear tests with that obtained in the undisturbed corrosion tests. Table VI contains a summary of the material losses obtained in the undisturbed corrosion tests and the corrosive-wear tests expressed as losses per area on an hourly basis. The material losses in the undisturbed corrosion tests are one to two orders of magnitude less than the corrosive-wear tests. This would indicate that at the frequency used for this research, the material loss is essentially due to the wear rather than the corrosion process.

4.3 *Corrosive-Wear Tests: Experiment B*

The corrosive-wear testing, in this experiment, yielded material loss measurements of the steel specimens for a given amount of exposure time. The results for each of the steels tested are presented in Table VII. This data provides a method of comparing other steels with the material presently use for Coast Guard buoy chain, 1022 steel. Corrosion potential measurements, performed in Experiment A, were not taken in this experiment since it was previously determined that abrasive-wear was the major loss mechanism of corrosive-wear.

Visual observations of the abraded surfaces of the specimens and whetstones revealed that wear occurred across the entire face of the specimens. Thus, the abraded area was constant for all specimens and eliminated the need for determining the abraded areas of the specimens. The wear patterns observed were identical regardless of material tested or exposure time. The wear pattern that occured in the center of the specimen in the direction of motion was different from the wear that occurred along the

TABLE VI

SUMMARY OF WEIGHT LOSSES IN SEAWATER: EXPERIMENT A

MATERIAL	ENVIRONMENT TYPE	MATERIAL LOSS ($x10^{-5}$)
1022	UNDISTURBED CORROSION	1.84 g/cm2-hr
1045	UNDISTURBED CORROSION	1.93
4140	UNDISTURBED CORROSION	1.79
1022HT	UNDISTURBED CORROSION	2.07
1022	CORROSIVE-WEAR	240.46
1045	CORROSIVE-WEAR	289.25
4140	CORROSIVE-WEAR	52.08
1022HT	CORROSIVE-WEAR	73.46

TABLE VII

EXPERIMENT B MATERIAL LOSSES (mg)

Material	Test Duration (hrs)				
	3	6	9	12	24
1022	19.7	29.0	49.7	---	57.1
4140	25.7	12.9	28.0	39.2	36.8
4140HT	25.4	20.0	40.9	42.0	67.5
4340	10.1	29.2	34.3	25.3	32.9
8740	15.3	17.6	28.1	30.2	33.7

HT: Heat-treated at 1650 deg. F for 30 min. and water quenched.

edges. This was attributed to the presence of abrasive and specimen wear particles which were forced out from the center of the specimen as it moved along the whetstone like the bow of a ship forcing water aside.

The graphs of material loss as a function of exposure time for each steel are given in Figures 42 through 46. As with Experiment A, there were two distinct regions on the graphs. An initial incubation period of approximately 12 hours occurs with each steel. This region is characterized by high wear rates due to the abrasion process. Fresh abrasive removes relatively large amounts of material in this stage. This region could be termed a "conditioning" region where the metal surface is changing so as to accomodate the abrasive surface for minimum abrasion. Following the incubation period is a region of steady-state wear. It is this region which is of major importance for buoy chain application since the majority of the lifetime of a buoy chain is spent in the steady-state wear region. The steady-state wear region therefore provides an indication as to which materials will provide longer life. The steady-state wear rates are determined by the slope of the material loss versus time curve in that region. The wear rates of each steel are given in Table VIII. Smaller slopes have lower wear rates and would indicate them to be more suitable for corrosive-wear prevention.

The material presently used for mooring chain, 1022 steel, showed a slope of (0.46). The material which exhibited the lowest steady-state wear was the 4340 steel. Having a slope of (0.10) its wear rate was approximately four and one-half times less than the 1022 steel. The 4140 steel showed half the wear rate of the 1022 steel with a slope of (0.19); however, when heat-treated, the wear rate was three times higher than the 1022 steel. The 8740 steel was similar to that of the 4140 steel with a slope of (0.21).

The results indicate that the 4340 steel would be the most desirable material for buoy chain, followed by the 4140 cold-rolled, then the 8740 steel. The 1022 steel is relatively poor in comparison with the alloy steels, except when the 4140 steel was heat-treated.

The results from Experiment B were consistent with those from Experiment A. The materials which showed the lowest wear rates were the 4340,

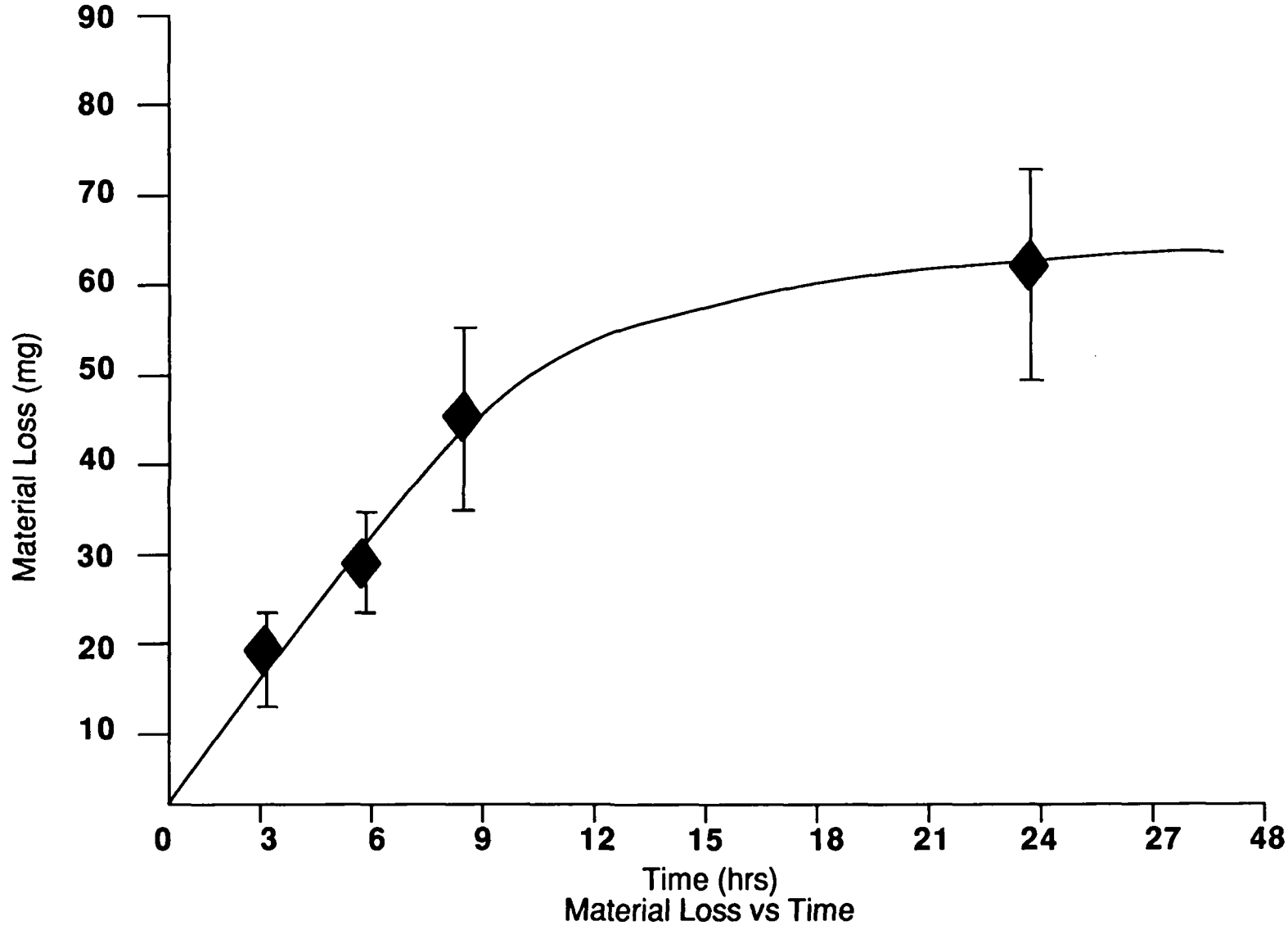

FIGURE 42. CORROSIVE-WEAR OF CG 1022 IN SEAWATER

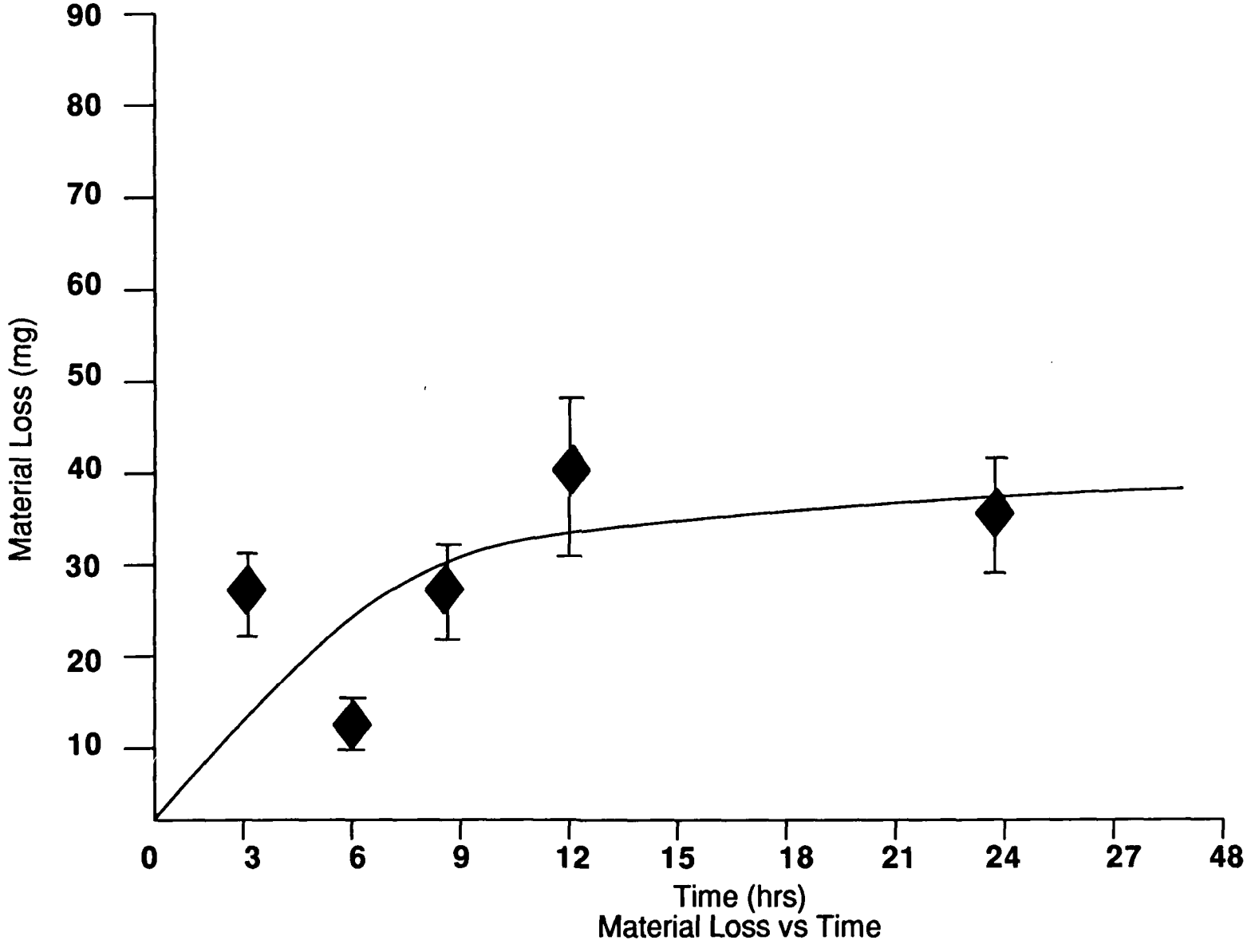

FIGURE 43. CORROSIVE-WEAR OF ASTM 4140 IN SEAWATER

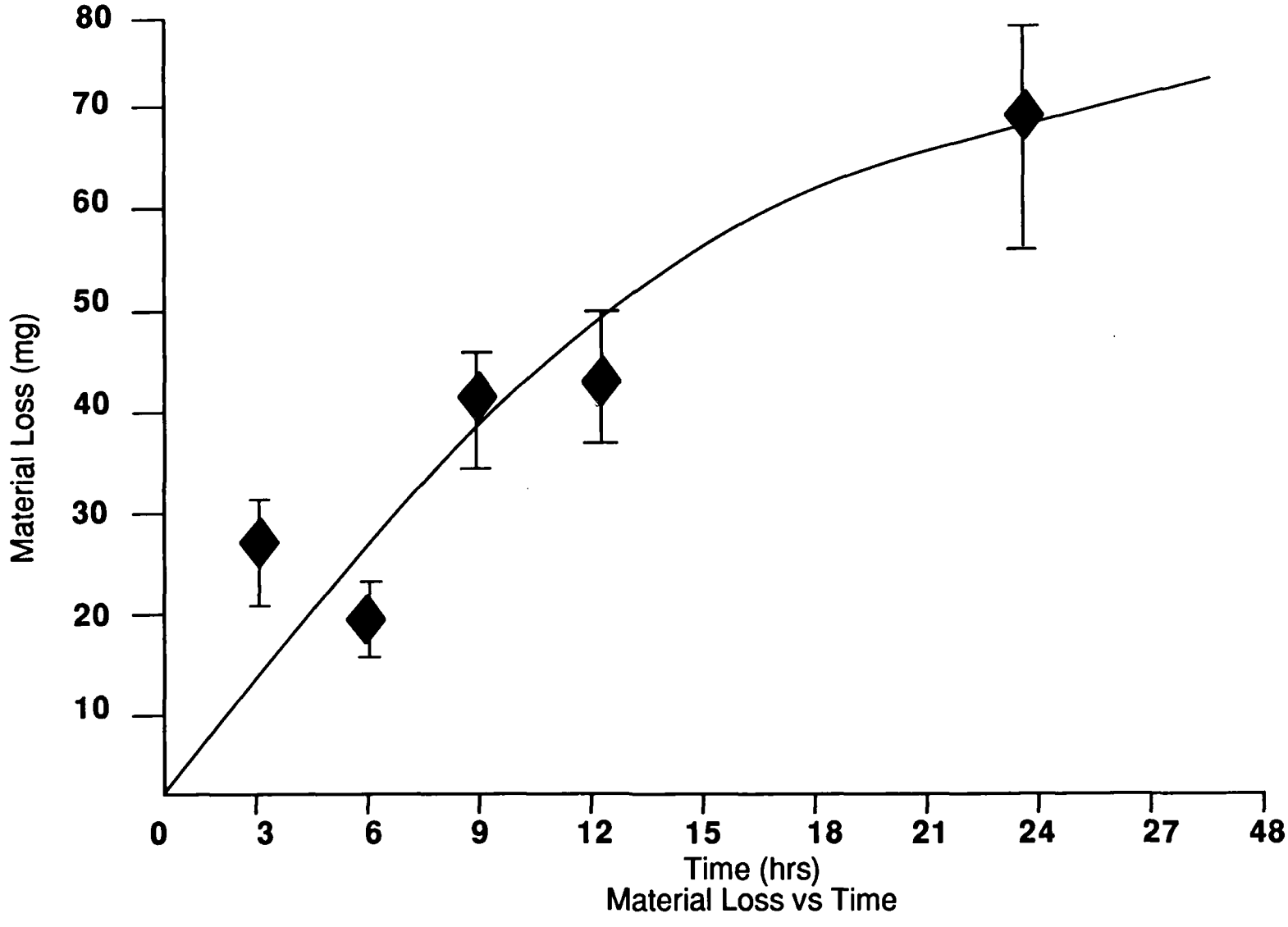

FIGURE 44. CORROSIVE-WEAR OF HEAT-TREATED ASTM 4140 IN SEAWATER

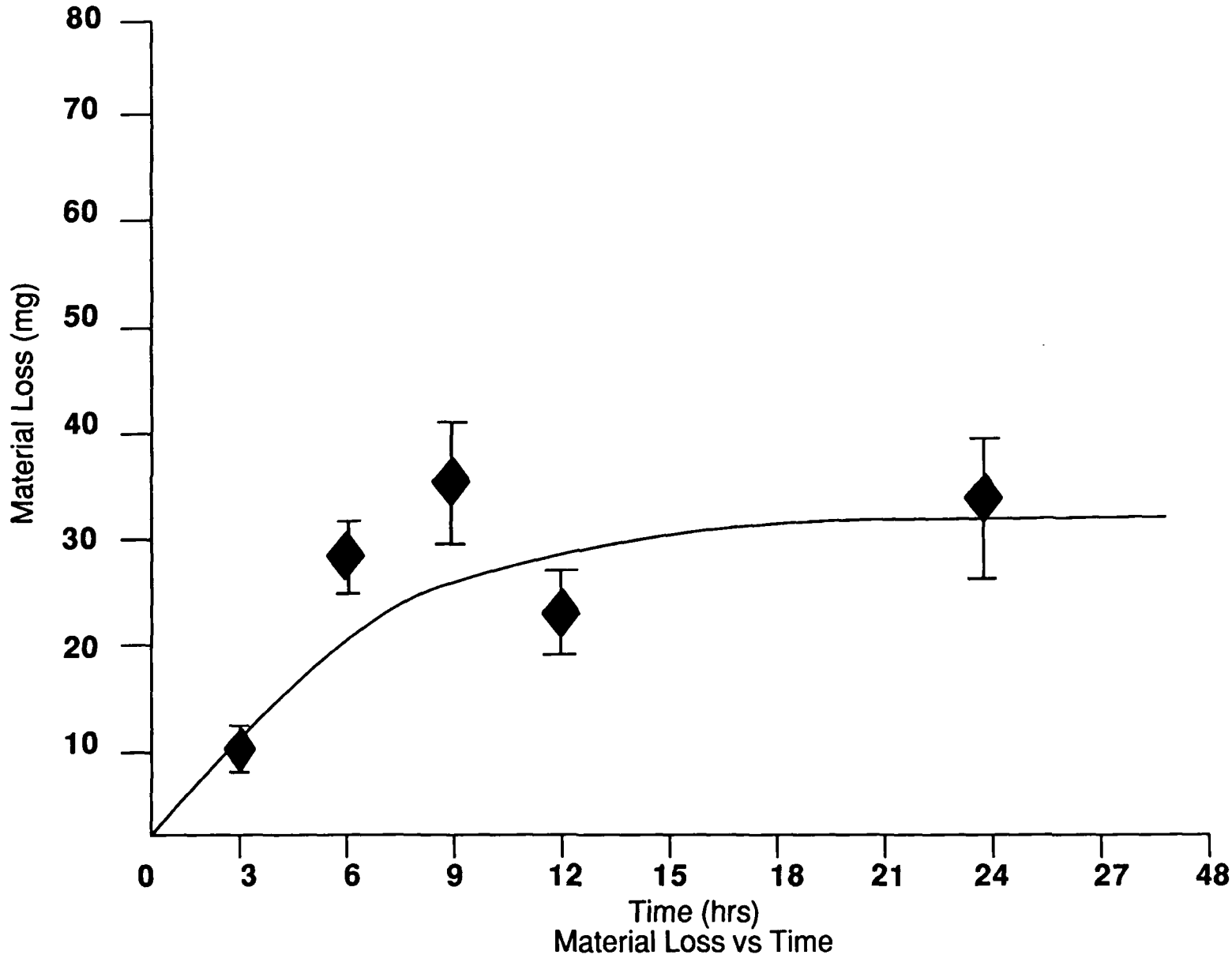

FIGURE 45. CORROSIVE-WEAR OF ASTM 4340 IN SEAWATER

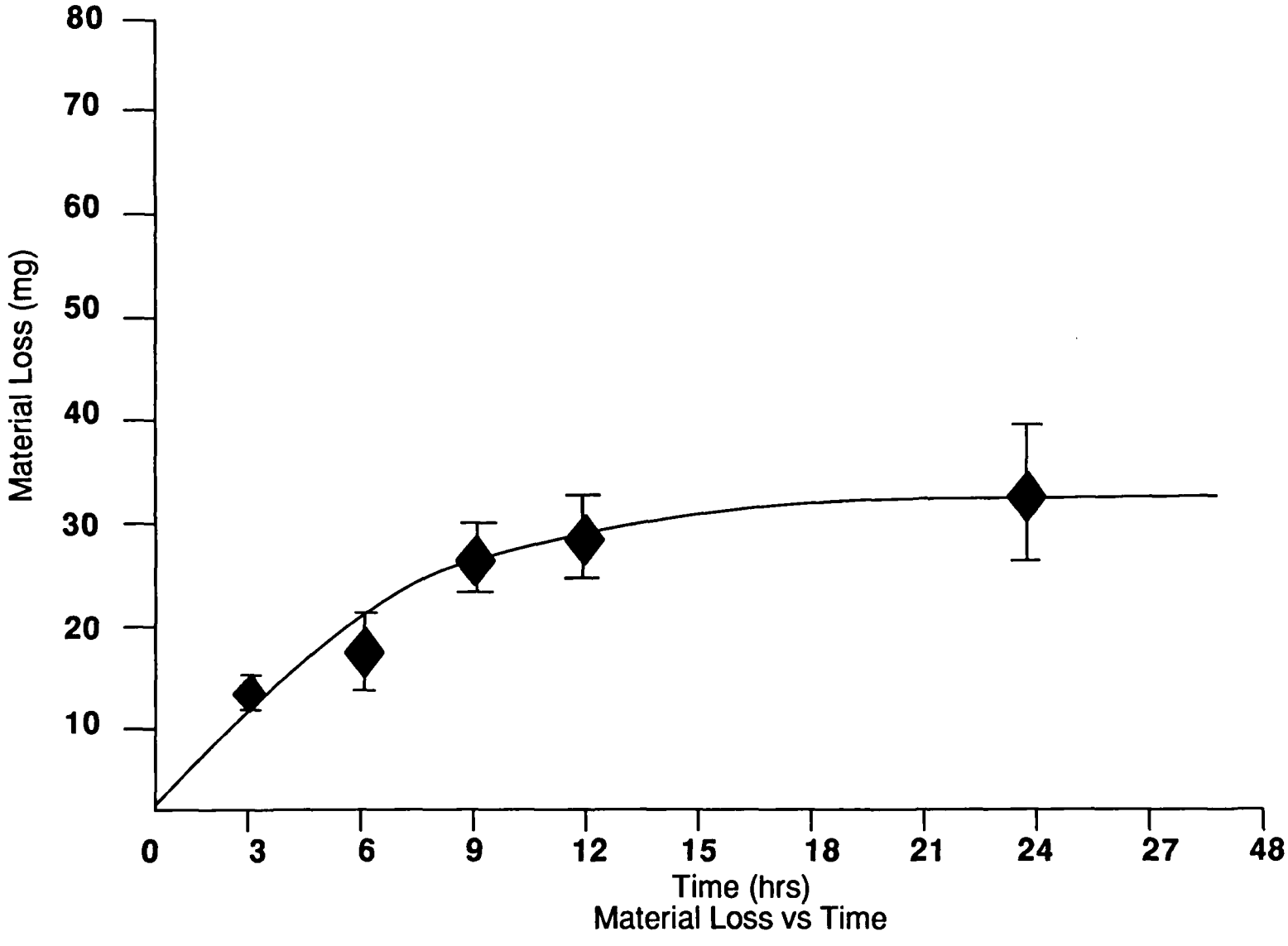

FIGURE 46. CORROSIVE-WEAR OF ASTM 8740 IN SEAWATER

TABLE VIII

SLOPE OF MATERIAL LOSS VS TIME CURVES

MATERIAL	WEAR RATE (mg/hr)
1022	0.46
4140	0.19
4140HT	1.42
4340	0.10
8740	0.21

4140, and 8740 steels. All three alloy steels contain small amounts of solution-hardened ferrite, which was shown previously to provide a greater wear resistance than plain carbon steels in which little solution-hardening exists. The exceptionally low wear rate of the 4340 steel is attributed to the presence of only a very small amount of ferrite in the microstructure, further increasing the hardness of the steel due to the large amount of pearlite present.

Of interest is the change in wear rate upon heating of the 4140 steel. Prior to heat-treating, the wear rate was one-half that of the 1022 steel. After heat-treatment, the wear rate was three times higher even though it contained twice the carbon content and was still harder than the 1022 steel. The reason for the difference can be observed in the microstructures of the steels. Originally, the 4140 microstructure was predominately pearlite with ferrite elongated in the rolling direction which is normal to the sliding motion during testing. The surface undergoing abrasion therefore has a high area fraction of pearlite with little ferrite. After heat-treatment, an equiaxed ferrite was formed along with pearlite due to slow furnace cooling. In this case, the area of ferrite on the surface was much greater than in rolled material. Additionally, the pearlite would be mechanically weaker due to increased coarsening. The soft ferrite phase would be easily removed by the abrasive, while the coarser pearlite in the 4140 in comparison to the 1022 steel would enable the abrasive to remove the ferrite plates in the pearlite. In a finer pearlite the closeness of the carbide plates would prevent removal of a significant amount of ferrite. In addition, a coarse pearlite allows greater dislocation movement and therefore larger pile-up stresses at the ferrite-pearlite interface which can fracture carbide plates and increase delamination.

All these factors would increase the wear rate of the heat-treated 4140. Similar features were found for the 1045 steel in Experiment A. The 1045 consisted of grain boundary ferrite with a coarse pearlite and it had an increased wear rate with respect to the 1022 steel of similar structure to that used in Experiment B and tested under the same conditions. The data found during this investigation furthur emphasizes that not only composition but microstructure of the material must be considered when comparing the abrasive wear of materials.

In considering the cold-rolled 4140, 4340, and 8740 steels, the order of wear resistance followed the volume fraction of ferrite in the material. The 4340 contained only a very small amount of a fine grained ferrite phase in a pearlite matrix and exhibited the best wear resistance. The cold-rolled 4140 and 8740 contained significantly larger amounts of ferrite than the 4340 cold-rolled steel but with the 8740 having a slightly larger volume fraction than the 4140 steel. The order of wear resistance was again following the ferrite content with the 8740 slightly less wear resistant than the 4140 in the cold rolled condition. The pearlite in all these structures were of approximately the same fineness which was similar to that of the heat-treated 4140. Using the same arguments as above, the ferrite phase would be easily removed by abrasive action while the pearlite would be more difficult than the ferrite due to the harder carbide phase resisting abrasion. Therefore, the wear resistance would be expected to increase with decreasing ferrite content with the same pearlite spacing.

The data in the research indicates that moderate changes in ferrite to pearlite ratio result in large changes in wear rate. For example, a change in ferrite content from approximately five percent in 4340 cold-rolled steel to thirty percent in the 4140 and thirty-five percent in the 8740 resulted in increasing the wear rates of just under two and just over two times. The controlling factor of wear rate in corrosive-wear of buoy chains for ferrite-pearlite structures appears to be the ferrite to pearlite ratio. The control of this ratio by suitable alloy selection, heat-treatment, and processing techniques would therefore seem to hold promise in improving buoy chain wear resistance.

An additional factor not investigated in this research but of major consideration is the corrosion behavior of alloy steels when used for buoy chain. Steels with more then 0.8% nickel were shown to be the most desirable in terms of corrosion resistance [11]. During initial material selection this point was considered and resulted in choosing the 4340 steel which has 1.8% nickel. The investigation into corrosive-wear in this experiment concluded that 4340 should be the best choice for wear resistance as well.

Although Experiments A and B compared both the 1022 and 4140 steels under similar corrosive-wear conditions, the results were slightly different.

In Experiment A, the wear rate of the 1022 steel was found to be approximately 19 times higher than the 4140 steel. In Experiment B, the wear rate of the 1022 was found to be only twice that of the 4140. The reason for this difference can be explained by comparing the microstructures of the 4140 steels used in both experiments. In Experiment B, the 4140 was cold-drawn producing grains of ferrite and pearlite arranged in a linear fashion paralell to the rolling direction but normal to the wear direction. The structure of the 4140 used in Experiment A shows an evenly dispersed equiaxed ferrite within the pearlite. However, in that experiment the loads during abrasive-wear were not distributed over such a large area as in Experiment B. The increased wear rate of the 1022 steel with increasing load would be expected due to the majority of the structure being ferrite. It is unlikely that increasing the load would produce such a rapid increase in wear rate in the highly pearlitic structure of the 4140 steel, which is also mechanically stronger. The change in wear rate with load is therfore suggested as the reason for the discrepancy in the data between the two tests.

In Experiment B, the majority of the uncertainty in the data was attributed to the loading of the specimens. Variations in the friction between the aluminum key and specimen, compositons of the whetstones, and loading by the spring produced an uncertainty of approximately 35%. This measure of uncertainty was obtained by multiple experiments. In addition, an accuracy of one-half a milligram was achieved during mass loss measurements. The error bars are shown for each of the materials in Figures 42 through 46.

The possibility exists that the reduction in wear rates of the steels over time may be due to the degradation of the abrasive. If this were true, the slope of the curve in the incubation period would be a more accurate reflection of the steady-state wear of the steels. Chain moorings are commonly in continual contact with some abrasive such as rock, gravel, and sand; therefore, it is believed that the experiments do reflect what actually occurs to the chains.

4.4 Microstructure Analysis

Figures 47 through 54 are representative photos of the abraded-corroded surfaces observed utilizing the SEM.

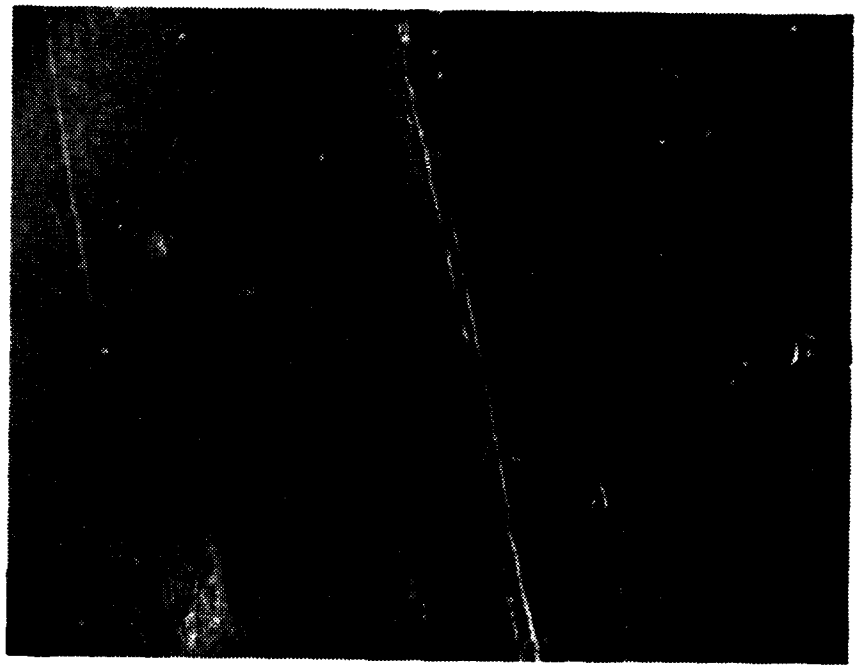

FIGURE 47. SEM PHOTO OF 1022 ABRADED SURFACE (X530)

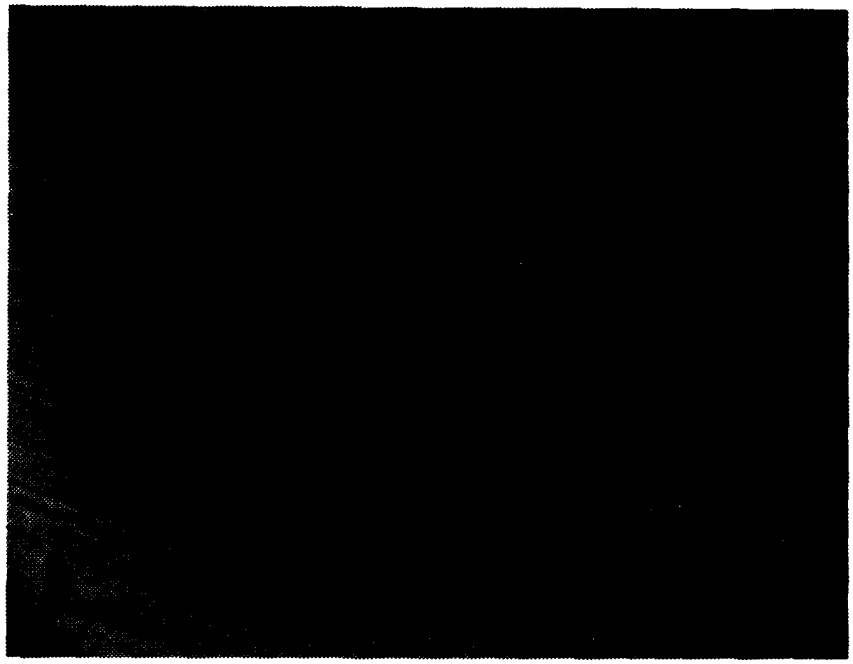

FIGURE 48. SEM PHOTO OF 1022 HT ABRADED SURFACE (X530)

FIGURE 49. SEM PHOTO OF 4140 ABRADED SURFACE (X530)

FIGURE 50. SEM PHOTO OF 1022 CORRODED SURFACE (X530)

FIGURE 51. SEM PHOTO OF 1045 CORRODED SURFACE (X540)

FIGURE 52. SEM PHOTO OF 4140 CORRODED SURFACE (X525)

FIGURE 53. SEM PHOTO OF 1022 HT CORRODED SURFACE (X530)

FIGURE 54. SEM PHOTO OF 1045 INTERFACE SURFACE (X530)

In Figure 47, the abraded surface of the 1022 steel can be seen as deep gouges and cuts. This is indicative of the softness of the low carbon content 1022 steel. In comparison, the abraded surface of the heat-treated 1022 steel and the 4140 steel, which are much harder materials, show very fine cuts and scratches. These are shown in Figures 48 and 49. The difference in abraded surfaces would explain the lower material loss rates obtained by these two steels.

The corroded surfaces of the 1022 and 1045 steels (Figures 50 and 51) show the massive porous layers characteristic of plain carbon steels which offer little protection against general corrosion. In Figures 52 and 53 the corroded surfaces of 4140 steel and the heat-treated 1022 steel are observed. These surfaces are quite different in that they lack the heavy thick layers, especially the 4140 steel which exhibits the largest resistance to corrosion provided by the addition of chromium and molybdenum. A thin uniform surface layer was evident on the 4140 steel which provided improved performance against the corrosive environment by being able to form rapidly if damaged. Additionally, once present, the layer would decrease corrosion effects rapidly. Such a film may also decrease the friction between the metal and abrasive unlike the heavy layers on the 1022 and 1045 steels. The heat-treated 1022 shows numerous cracks in the oxide layer which is commonly seen in steels of martensitic microstructure and clearly offers little protection against the corrosive environment. Figure 54 shows the interface of an area of abrasion and corrosion observed in the surface of the 1022 steel. Interface areas of the other steels showed similar combined areas of wear and corrosion.

5.0 CONCLUSIONS

The purpose of the laboratory corrosive-wear testing was to provide a relatively quick method of comparing steels for buoy chain-mooring applications. The comparison is based on the type of wear that would be experienced by the bottom sections of chain. Results of the research provide an insight into a complex and unique mechanism that has not been seen in prior in depth analysis as well as a better understanding of the effects of a combined wear and corrosion process.

The wear process accounts for the majority of the chain degradation. This can be observed in areas having a sand, rock, or gravel bottom where the chafe section of the chains exhibit a much higher degree of wear than the suspended section of chain. This was also observed in the laboratory testing where the material loss rates obtained in the undisturbed corrosion tests as compared to the rates obtained in the corrosive-wear tests portrayed how devasting the mechanism can be to a particular material.

While the wear component has been shown to be the dominating factor of the mechanism, it appears that it is dependent upon the frequency of the abrasion process. Although the actual relationship between the abrasion frequency and wear rate has not been determined, it is obvious that an increase in the number of cycles over a given time will increase the wear rate since the material will have been exposed to additional abrasive surface. Therefore, on the laboratory studies, the designed frequency and amplitude of the motion of the specimen against the abrasive surface was similar to that of a chain mooring under maximum environmental conditions.

There are several obvious environmental factors which influence the wear rates of chain such as wind, wave, and current forces. As discussed by Kohler [2], there are many other factors which can also affect the wear rate. The laboratory experiments were designed to eliminate most of these influences while allowing for material properties to be observed.

In Experiment A, the results of the corrosive-wear tests with the presently used 1022 steel and the three alternative materials, heat-treated 1022, 1045, and 4140 steel, provide a remarkable portrayal of how each material is affected by the corrosive-wear process. The results of the 1045 steel are quite surprising given that it is a structurally harder material than the 1022 steel yet, it had an increased material loss rate. The increase in hardness is not nearly as substantial as the heat-treated 1022 steel which resulted in a reduced material loss rate as compared to the original 1022 steel. The better performance of the heat-treated 1022 appears to be the result of the increased strength and hardness in the martensitic microstructure which is better suited to an abrasion process. The 4140 steel produced the best wear resistance with a material loss rate of five times less than that of the presently used 1022 steel. The 4140 was able to achieve a

loss rate at a strength and hardness less than that of the heat-treated 1022 steel through the addition of several alloying elements. It would appear that the addition of manganese, chromium and molybdenum to the 4140 steel produced a greater effect on the ability to resist the corrosive-wear process than the overall increase in strength and hardness.

In Experiment B, the results showed that the 4340 steel is best suited for the bottom section of a chain mooring. The wear rate of this steel was less than one-fourth that of the presently used, 1022 steel and almost half that of the 4140 steel, which was shown to be the best of steels examined in Experiment A. This confirms what has been determined previously, that the corrosive-wear behavior of steels is determined by their microstructure particularly the ferrite to pearlite ratio in the microstructure. Lower ferrite to pearlite ratios indicate better wear resistance. Increased hardness in the steel itself will not guarantee improved wear resistance. Alloy steels which are solutioned-hardened demonstrate increased wear resistance.

In summary, it is hypothesized that substantial savings can be achieved through use of the 4340 steel in chain moorings where frequent mooring replacement has been necessary in the past. The steel should also be much less susceptible to pitting attack than the other steels, due to its high nickel content. Although the greatest benefits of the steel would be realized in the chafe section, the increased strength of the alloy would allow for a reduction in the diameter of the chain if used in the entire mooring as compared to conventional requirements. This would decrease the weight of the mooring in addition to the cost, while providing a longer usable life.

5.1 A Final Look

A section of chain from an adrift buoy that had broken its chain mooring has provided a quick analysis and final conclusion from this research.

The section of chain (approximately 60 ft. in length) was removed from a drifting First Class Can Buoy that was recovered by the U.S. Coast Guard Cutter Redwood, a 157 ft. buoy tender. No official data was available on the buoy or chain but estimates by the servicing personnel were that it had been

deployed for approximately two to three years. The upper portion of the chain (originally one inch diameter) was in good condition; however, the lower portion where the chain had broken had undergone severe material loss due to corrosive-wear. To estimate the length of time the buoy chain has been subjected to the corrosive-wear mechanism, which resulted in the material loss, the rates obtained by this research were used. The calculations are as follows:

Diameter of original chain link = 2.54 cm
Diameter of worn chain link = 1.08 cm (average value)

Taking the chain link as an ellipse which can be rationalized as essentially a cylinder of steel that has been reshaped, the volume of the link can be calculated

Ellipse length	= 30.6 cm
Volume of original link	= 155.05 cm^3
Volume of worn link	= 28.03 cm^3
Volume loss from corrosive-wear	= 127.02 cm^3
Density of steel	= 7.8 g/cm^3
Total mass lost from corrosive-wear	= 990.76 g

To estimate the length of time the chain link was exposed to the corrosive-wear mechanism, the area of the link affected can be estimated. As a conservative approach, the minimum abraded area from the chain link is 9.5 cm long by 1.5 cm wide on the ocean floor and 2.0 cm^2 from link on link abrasion. Thus:

Total minimum area	= 16.25 cm^2
Area loss rate for corrosive-wear of chain	= 990.76 g / 16.25 cm^2 = 60.97 g/cm^2
Lab loss rate for 1022 steel chain in corrosive-wear	= 240.4 x 10-5 g/cm^2 hr
Time for actual chain loss rate	= 25,362 hr
	= 2.89 yrs

To compare this value with how long it would take for a 4140 steel chain to achieve this same amount of material loss, the rate determined by the laboratory experiments in this research can be used. As before:

Area loss rate	= 60.97 g/cm^2
Lab loss rate for 4140 steel chain in corrosive wear	= 52.08 x 10-5 g/cm hr
Predicted life of 4140 chain for corrosive-wear	= 117,070 hr = 13.36 yrs

The value of 2.89 years for the 1022 steel is very realistic based upon previous estimates by servicing personnel. The value of 13.36 years for the 4140 steel chain in an increase of over four and one-half times that of the 1022 steel chain.

REFERENCES

1. May, D.R., Abrasive-Corrosion of Buoy Chain, URI Thesis, 1984.

2. Kohler, C.A., Corrosive-Wear of Alloy Steels for Buoy Chain, URI Thesis, 1985.

3. Aids to Navigation, U.S. Coast Guard Mission Series, CG 378-6, Department of Transportation, March, 1978.

4. Johnson, Arnold-Burges, The Modern Lighthouse Service, Washington: U.S. Government Printing Office 1889. IX, p. 137.

5. Buoy Mooring Selection Guide for Chain Moorings, Ocean Engineering Report, COMDTINST M16511-1, dtd December 22, 1978, U.S. Government Printing Office.

6. Scott, D.M., "Treatise in Material Science and Technology", Wear, Vol. 13, Academic Press, New York, 1973.

7. Fontanna, M.G. and Greene, N.D., Corrosion Engineering, McGraw-Hill, New York, 1967.

8. Laing, A.K., Buhr, R.K., and Gertsman, S.L., Navigational Buoy Mooring Chains, Technical Report by the Canadian Department of Mines and Technical Surveys, 1965.

9. Brown, S.A., and Simpson, J.P., "Crevice and Fretting Corrosion of Stainless Steel Plates and Screws", Journal of Biomedical Materials Research, Vol. 15, 1981, pp. 867-878.

10. Suh, N.P., Jahanmir, S., and Abrahamson, E.P., "The Delamination Theory of Wear", Progress Report to the Advanced Research Project Agency, DOD, Materials Processing Laboratory, Department of Mechanical Engineering, Massachusetts Institute of Technology, Cambridge, Mass., Sept. 1974.

11. Wayne, J.F., Rice, S.L., Minakawa, K., and Nowotny, H., "The Role of Microstructure in the Wear of Selected Steels", Wear, Vol. 85, 1983, pp. 93-106.

APPENDIX A

APPARATUS COMPONENTS: EXPERIMENT B

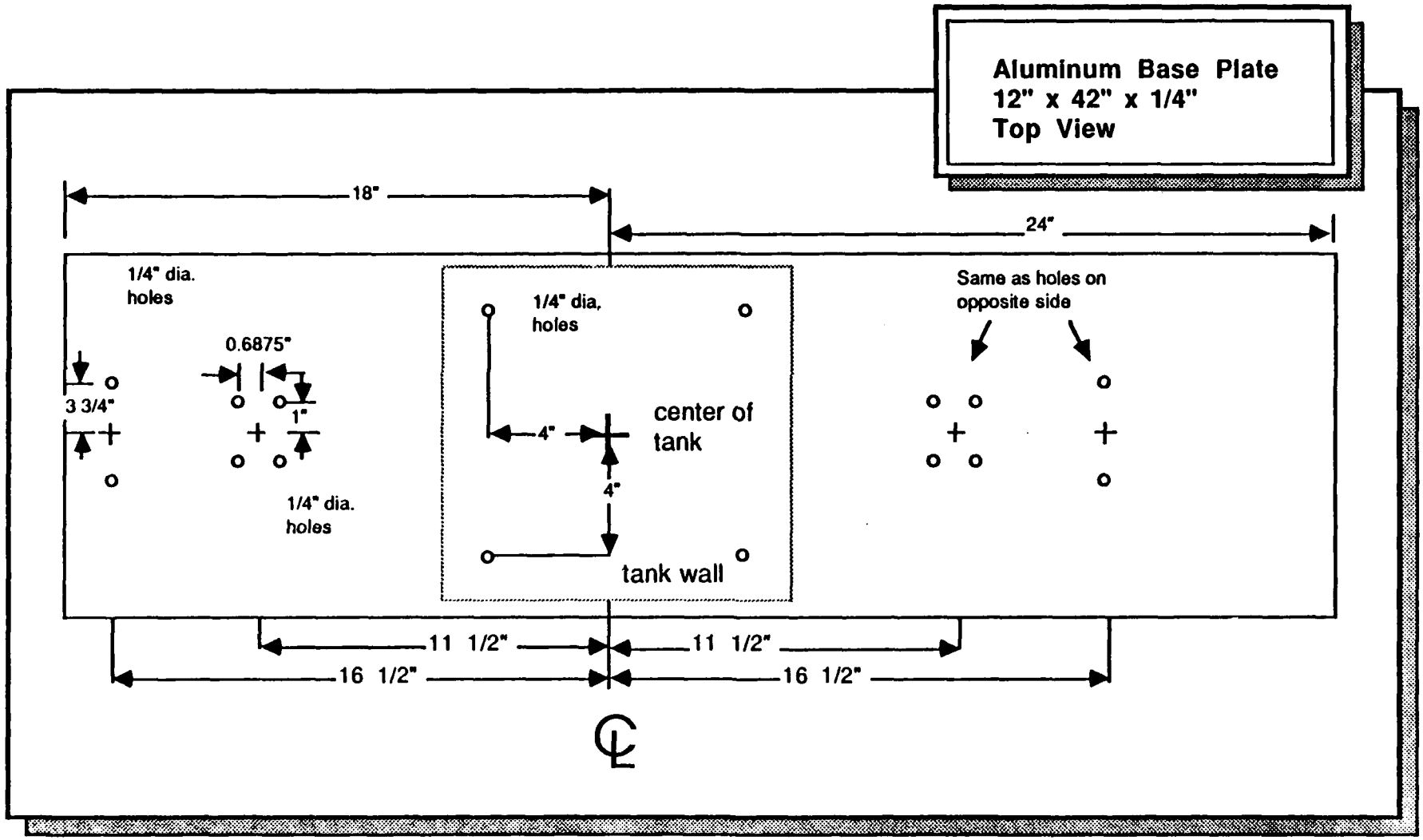
Aluminum Base Plate
12" x 42" x 1/4"
Top View
18"
24"
1/4" dia.
holes
0.6875"
3 3/4"
1"
1/4" dia.
holes
1/4" dia.
holes
4"
center of
tank
4"
tank wall
Same as holes on
opposite side
11 1/2"
11 1/2"
16 1/2"
16 1/2"

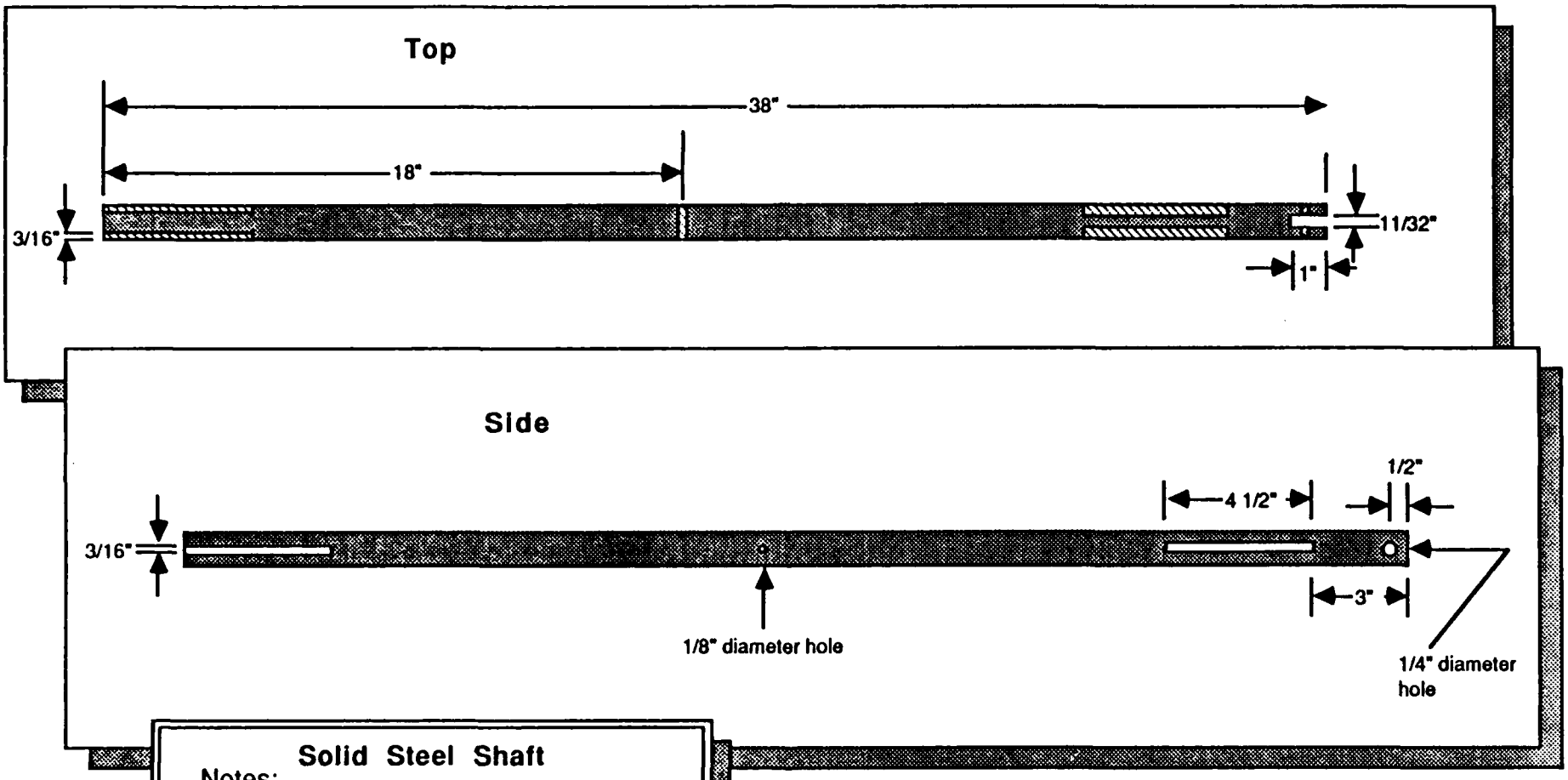

Solid Steel Shaft

Notes:

1) 3/4" nominal diameter shaft
2) Both keyways are 3/16" wide, 3/16" deep and 4 1/2" in length
3) 1/4" diameter hole drilled through slotted end

AD-A172 434 CORROSIVE-WEAR OF BUOY CHAIN(U) COAST GUARD RESEARCH AND DEVELOPMENT CENTER GROTON CT C A KOHLER ET AL. JUL 86 CGR/DC-05/86 USCG-D-21-86 2/2

UNCLASSIFIED F/G 11/6 NL

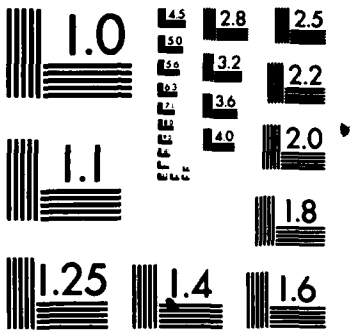

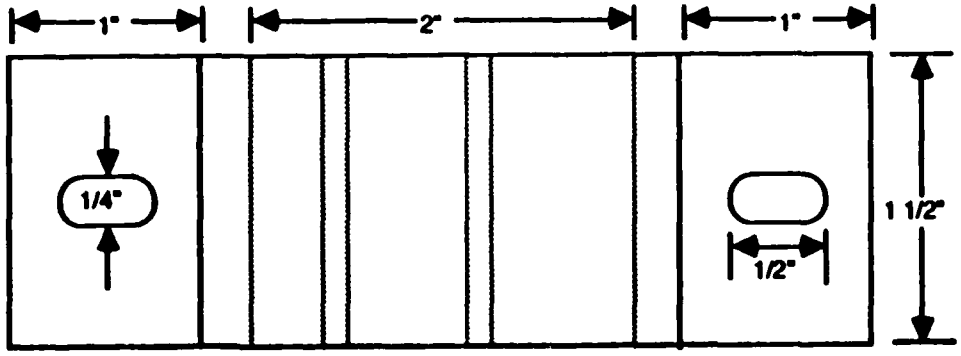

Top

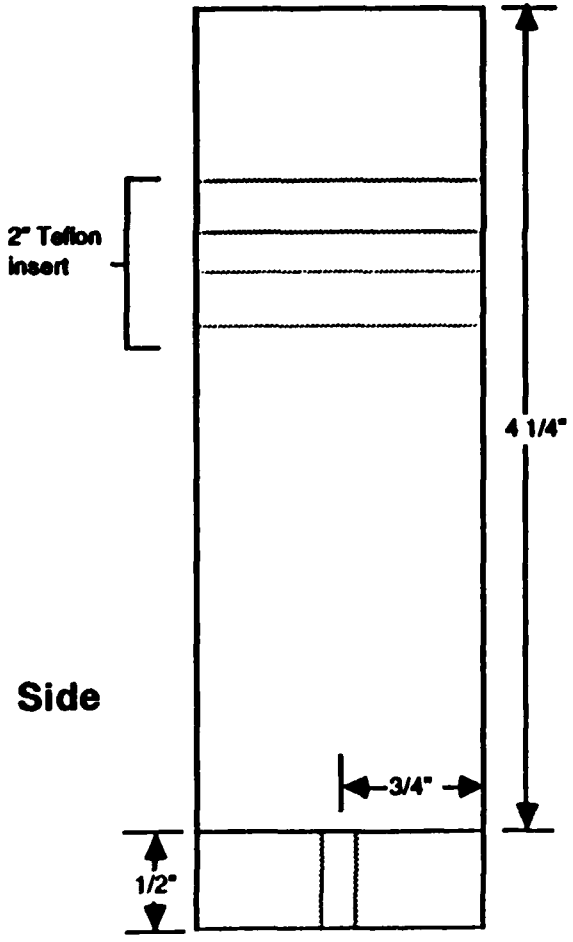

Side

Front

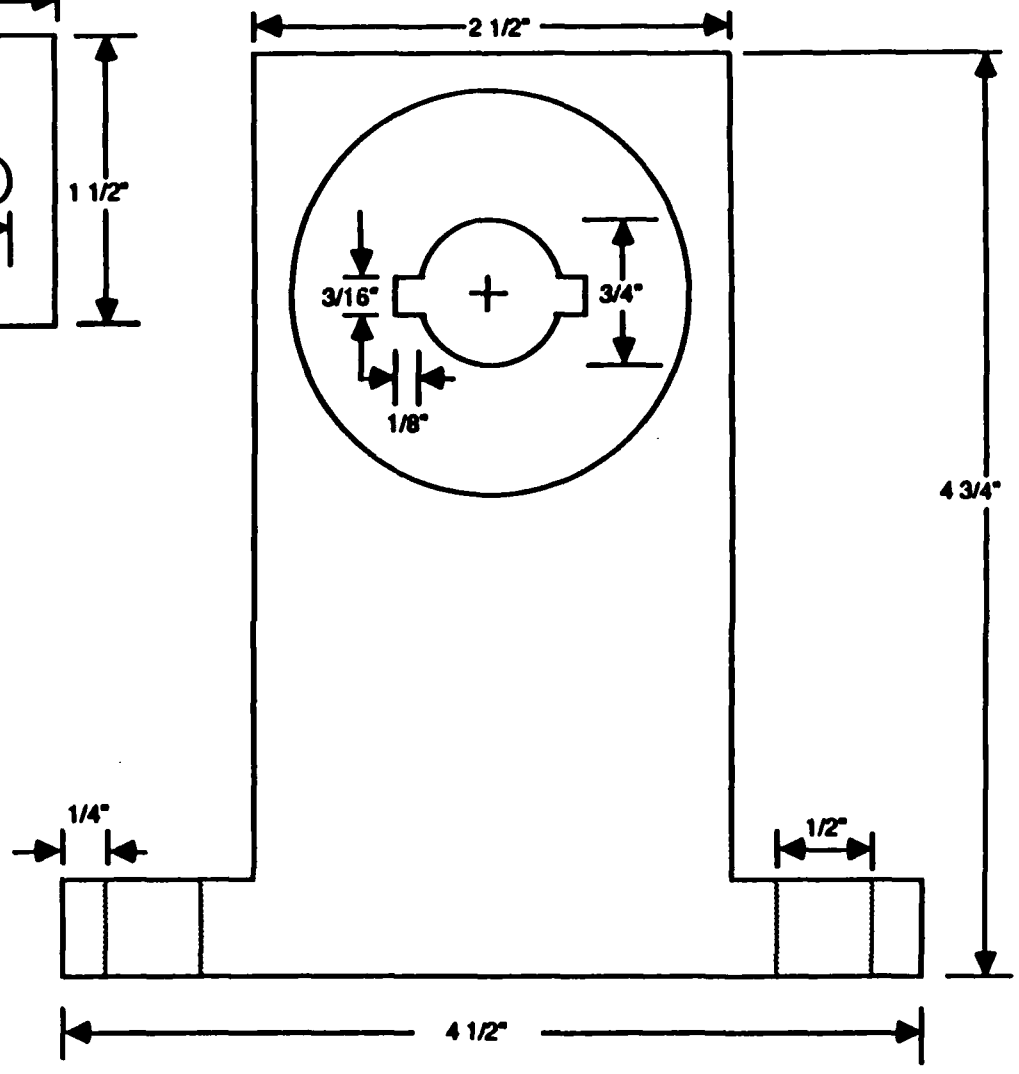

Shaft Bushing Guide

Notes:

1) Machined from aluminum block
2) Teflon 2" bushing insert

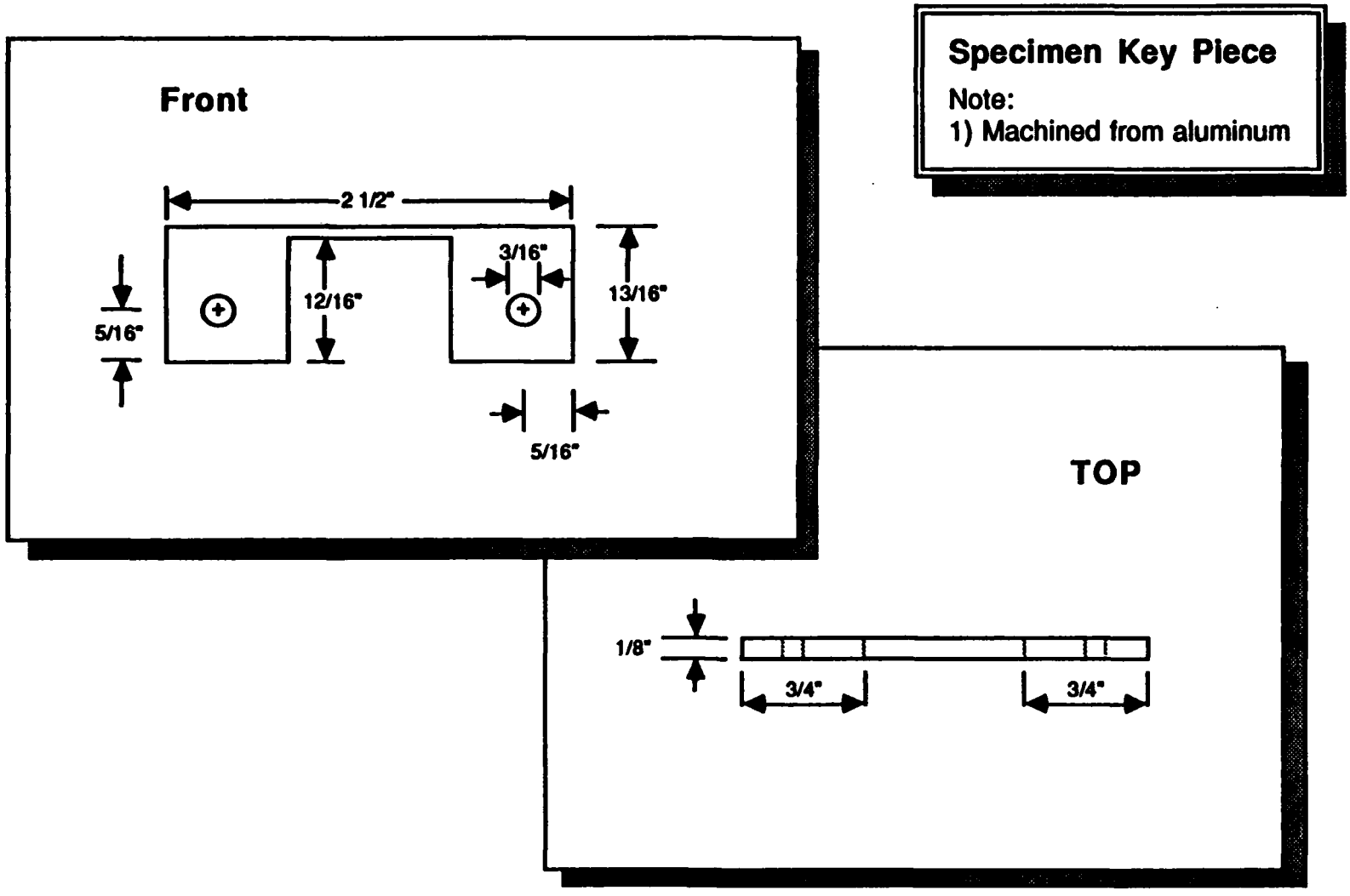
Specimen Key Piece
Note:
1) Machined from aluminum
Front
2 1/2"
3/16"
12/16"
13/16"
5/16"
5/16"
TOP
1/8"
3/4"
3/4"

Top

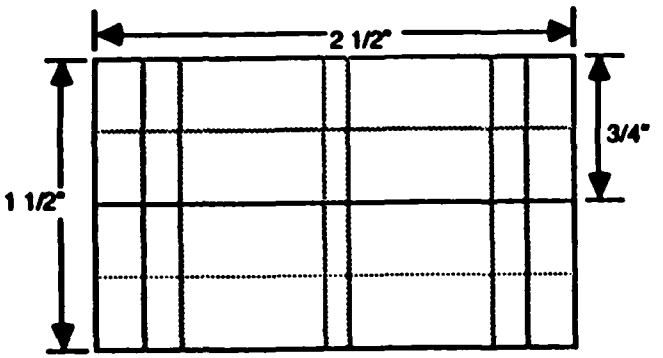

Bottom

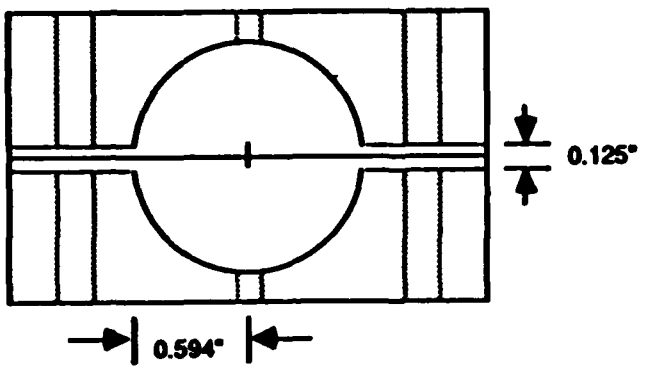

Front

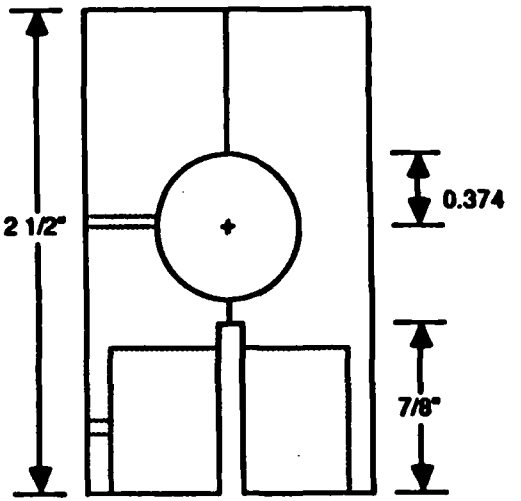

Side

(From inside, block split)

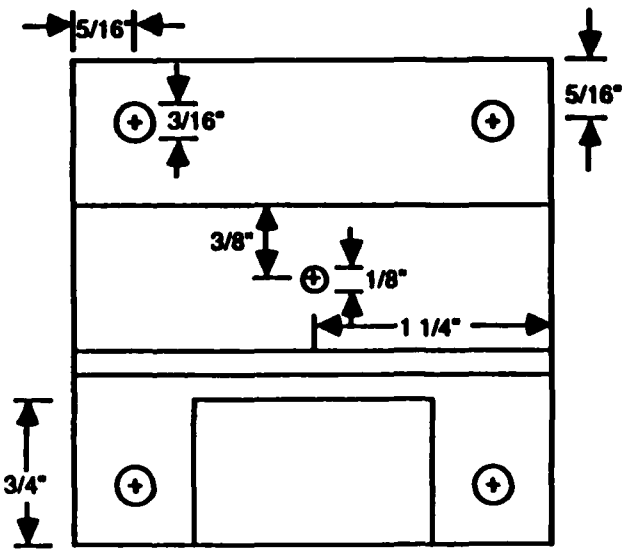

Carriage Piece

Notes:

1) Machine from solid Teflon block
2) 0.374" radius hole passes from front to back
3) 0.125 keyway passes from front to back
4) 0.594" diameter specimen holder is 1/8" below top of keyway
5) All 3/16" diameter holes are located 5/16" from the top or bottom and from the sides passing through the entire block
6) Block is split down the center from front to back
7) Drill then tap

END

10-86

DTIC